The Pennsylvania State University

The Graduate School

SCHWEINFURTHIN-MEDIATED EFFECTS ON EGFR AND AKT IN CANCER CELLS

A Thesis in

Biomedical Sciences

by

Shanika Fernando

©2019 Shanika Fernando

Submitted in Partial Fulfillment
of the Requirements
for the Degree of

Master of Science

December 2019

The thesis of Shanika Fernando was reviewed and approved* by the following:

Raymond J. Hohl
Director, Pennsylvania State Cancer Institute
Professor of Pharmacology & Medicine
Thesis Advisor

Jeffrey D. Neighbors
Assistant Professor of Pharmacology & Medicine

Nadine Hempel
Associate Professor of Pharmacology

Hong-Gang Wang
Lois High Berstler Professor
Pediatrics & Pharmacology

Ralph L. Keil
Director, Biomedical Sciences Graduate Program
Associate Professor of Biochemistry & Molecular Biology

*Signatures are on file in the Graduate School

ABSTRACT

Schweinfurthins are a class of plant-derived compounds with potential anticancer effects against a select subset of cancer cells within the NCI-60 panel. Synthetic analogs of schweinfurthins alter oncogenic signaling and homeostasis of multiple processes such as cytoskeleton and the mevalonate pathway, especially within difficult-to-treat cancers such as glioblastomas. The full schweinfurthin mechanism of action is unclear, but a combinatorial set of genetic mutations may influence sensitivity to schweinfurthins. Recently published work extends our knowledge into schweinfurthins with reports that these analogs bind to the cholesterol binding site of oxysterol binding proteins to impair intracellular cholesterol transport. This result is associated with decreased glycosylation of EGFR and decreased PI3K-AKT-mTOR signaling. Problematically, these changes were reported to occur in treated schweinfurthin-sensitive *and* –resistant cells, which fail to account for differential toxicity of schweinfurthins. The current need for alternative, novel therapeutics to circumvent non-specific and, sometimes, toxic effects of compounds, such as lovastatin, is desirable. Schweinfurthins are an intriguing alternative, although questions remain as to whether schweinfurthin-mediated effects are due to mevalonate-derived metabolites like cholesterol and dolichol. We chose to investigate effects of two schweinfurthin analogs on cancer cells that are either schweinfurthin-sensitive (SF-295 cells) or -resistant (A549 cells). MTT assays of vehicle- vs. analog-treated cells reveals that only SF-295 cells were sensitive to these compounds. I hypothesized that schweinfurthins dysregulate EGFR and AKT signaling within SF-295 cells, not A549 cells, because A549 cells have compensatory pathways to circumvent the effects of schweinfurthins. This pathway includes oncogenic activity of K-Ras, a constitutively active protein from a class of Ras isoforms that can withstand fluctuations in membrane cholesterol levels. Analyses of protein expression and phosphorylation of EGFR reveals that SF-295 cells, but not A549 cells, experience a decrease in

apparent molecular weight of EGFR and an increase in phosphorylation of EGFR at tyrosine residues 1068 (which activates AKT) and 1173 (which activates MAPK). It is important to note that much of these phosphorylations are found on lower apparent molecular weight forms of EGFR, which we suspect are immature, unmodified forms of the receptors. These suspicions are bolstered by our experiments that show tunicamycin, which inhibits glycosylation, mediates similar shifts of EGFR to lower apparent molecular weight forms in SF-295 cells. Furthermore, schweinfurthin analog TTI-3066 reduces EGF-induced levels of phospho-EGFR(Y1068) and phospho-AKT(S473). It is important to acknowledge that schweinfurthin effects on EGFR phosphorylation appeared as trends, but were not statistically significant. Nevertheless, these trends support de-coupling of phospho-EGFR from its effectors. While investigations into EGFR-MAPK signaling revealed a lack of an effect by schweinfurthins, we found that treatments with schweinfurthins on their own induce significant decreases in phospho-AKT levels in SF-295 cells, not A549 cells. Taken together, our results suggest that schweinfurthin may exert its antitumor activity by de-coupling the EGFR-AKT signaling through impairment of EGFR glycosylation.

TABLE OF CONTENTS

LIST OF FIGURES

LIST OF TABLES

ABBREVIATIONS

ABCA1 – ATP Binding Cassette Transporter, Subfamily A Member 1

ABCG1– ATP Binding Cassette Transporter, Subfamily G Member 1

AKT– Protein Kinase B

c-Cbl– Cytoplasmic Cbl E3 Ubiquitin Ligase

c-Src– SRC, Nonreceptor Tyrosine Kinase, Rous Sarcoma

DMSO– Dimethyl Sulfoxide

eIF2*α*– Eukaryotic Initiation Factor 2 Alpha

EGF– Epidermal Growth Factor

EGFR– Epidermal Growth Factor Receptor

Epo– Erythropoietin

EpoR– Erythropoietin Receptor

ERK1/2– Extracellular Signal Regulated Kinase 1/2

FPP– Farnesyl Pyrophosphate

FPTase– Farnesyl Pyrophosphate Transferase

FTI– Farnesyl Pyrophosphate Transferase Inhibitor

GAP– GTPase Activating Protein

GEF– Guanine Nucleotide Exchange Factor

GGPP– Geranylgeranyl Pyrophosphate

GGTI– Geranylgeranyl Transferase Inhibitor

GPTase I– Geranylgeranyl Transferase I

Grb2/Gab1– Growth Factor Receptor Bound Protein 2/ Grb2 Associated Binding Protein 1

LXR– Liver X Receptor

IGF1R– Insulin Growth Factor 1 Receptor

HMG-CoA– Beta-Hydroxy-Beta-Methylglutaryl Coenzyme A

MAPK– Mitogen Activated Protein Kinase

MEK– Mitogen Activated Protein Kinase

GRP78– 78 kDa Glucose-Regulated Protein

GTP– Guanosine-5'-Triphosphate

GTPase– Guanosine Triphosphatase

MLC– Myosin Light Chain

mTOR– Mammalian Target of Rapamycin

NSCLC– Non-Small Cell Lung Cancer

OSBPs/ORPs– Oxysterol Binding Proteins/OSBP Related Proteins

PARP– Poly ADP Ribose Polymerase

PDK– Phosphoinositide-Dependent Kinase

PI3K– Phosphoinositide-3-Kinase

PKM2– Pyruvate Kinase Isozyme M2

PNGase F– Peptide:N-Glycosidase F

PTB– Phosphotyrosine Binding Domain

PTEN– Phosphatase &Tensin Homolog

Raf– Rapidly Accelerated Fibrosarcoma

SDS-PAGE– Sodium Dodecyl Sulfate Polyacrylamide Gel Electrophoresis

SH2 –Src Homology 2 domain

Shc– Src Homology & Collagen Kinase

SNP-ChIP – Single Nucleotide Polymorphism Chromatin Immunoprecipitation

SRE– Sterol Response Element

Y1068– Tyrosine 1068

Y1173– Tyrosine 1173

ACKNOWLEDGEMENTS

I would like to extend my appreciation to the community of Penn State, College of Medicine for this unique opportunity to pursue cancer biology in the setting of translational research. It has been an exciting moment to immerse myself, to fulfill not just my inner curiosities about what it must be like to conduct cancer biology research, but also have a sense that one day, this work will be useful to other graduate students. Which will then be up to those higher above and beyond to turn this work into a better treatment for the clinic and patients.

I would like to especially thank Dr. Hohl, Dr. Lill, and Dr. Neighbors for their mentorship and guidance. Dr. Lill, you took me under your wing in a time when I knew nothing about cancer biology, let alone how to work with cancer cells. Your training gave me a foundation on technical execution, with a broad overview about glycoproteins and surface receptors. To Dr. Hohl, I found your intuition and background in this field to be rewarding and meaningful as I started to branch off from technical training to more independent thinking. Dr. Neighbors, thanks for your input and additional advice on my experiments and thesis writing. To present and past members of the Hohl lab, I learned a lot from you and I appreciate it. I want to mentioned Dr. Yun, Dr. Wang, Dr. Hempel, and Dr. Keil for their thoughtful advice and assistance throughout my trajectory in this work. Kathy Shuey, and the Office of Theses and Dissertation, you all were invaluable life-savers in de-mystifying graduation requirements and procedures. Thank you all so much.

I also would like to thank Dr. Thomas E. Wilson for his time, mentorship, and advice before graduate school. Finally, I want to thank my mother and father for their love and support. They always kept me smiling. They always believed the best in me and encouraged me to see the best in everything. I love you two very much.

Chapter 1

INTRODUCTION:

Schweinfurthins as Anti-Cancer Therapeutics

The late 1980s marks a time when the U.S. Developmental Therapeutics Program (NCI) began to amass plant, microbial, and marine samples for drug discovery [1]. Schweinfurthins were among those identified, first extracted from the leaves of the Western Cameroonian plant, *Macaranga schweinfurthii* [2,3,4]. Schweinfurthins act as anti-proliferative agents with GI_{50} (50% Inhibition of Growth) values ranging from tens to hundreds of nanomolar within certain cancer cell lines out of a total of sixty (NCI-60 panel) [1,3,4]. Glioblastomas, triple negative breast cancers, melanomas, leukemias, and renal cancer cell lines are sensitive to the effects of schweinfurthins, whereas non-small cell lung cancers (NSCLCs) and ovarian cancer cell lines are resistant [4]. Our group has synthesized over ninety analogs of schweinfurthins to circumvent the difficulties in obtaining the natural compounds. We are currently investigating the effects of compounds, TTI-3066 and TTI-4242, used in these experiments. Backbone structures of TTI-3066 and TTI-4242 resemble Schweinfurthin G (see Fig. 1) [5].

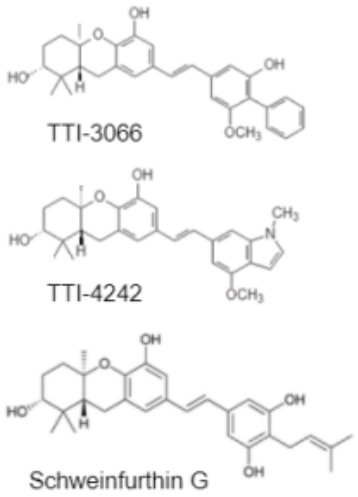

Figure 1: Backbone structures of synthetic analogs and natural schweinfurthin G. TTI-3066 & TTI-4242 are schweinfurthin analogs that have structural similarities to the natural compound, schweinfurthin G. Note that the left-half of the molecule, known to be important for differential biological activity, is intact while the right half of the molecule is chemically modified for our analogs. Both TTI-3066 and TTI-4242 are used for the purposes of these experiments.
Images obtained from Hohl Lab.

The self-organizing map of natural compounds tested on the NCI-60 panel reveals that schweinfurthins have a unique target as compared to most traditional chemotherapy agents, and have overlapping patterns of cytotoxicities with that of cephalostatins, ritterazine B, and OSW-1 [1,2,6]. A class of lipid transport proteins known as oxysterol binding proteins (OSBPs/ORPs) have been implicated as potential targets for schweinfurthins [6,7,8,9]. However, other targets which can impact cholesterol at the stages of import, export, storage, or *de novo* synthesis may exist. These include transcription factors, cytoskeleton-related factors and G proteins, regulators of AKT (PLEKHO1/THEM4), and PKM2 [8,9,10]. Our overarching goal is to identify mechanisms of action for our analogs, by investigating their pleiotropic effects on the cytoskeleton, the mevalonate pathway, small GTPases, and pro-survival signaling [4,8].

Schweinfurthin Effects on Isoprenoids & Pro-Survival Signaling

Schweinfurthins, like cephalostatins, ritterazine B, and OSW-1, promote endoplasmic reticulum stress and programmed cell death, as seen by increases in levels of eIF2α, GRP78, cleaved PARP and Caspase 9 in SF-295 glioblastoma cells [2,4,6,11]. Given that schweinfurthin structure mimics sterol chemistry, sharing in common isoprene units, our group has published how schweinfurthins negatively feedback on the mevalonate pathway to promote such effects [8]. Among various mevalonate pathway inhibitors (some listed in Fig. 2), schweinfurthins display synergy with lovastatin and can reduce various isoprenoid substrates within the mevalonate pathway [8]. Cytotoxic effects of schweinfurthins, within multiple myeloma, SF-295 glioblastoma, and A549 NSCLC cells, are accentuated if cells are made mevalonate-deplete with lovastatin or grown in lipid- depleted media [8,12].

Schweinfurthin-mediated effects on the mevalonate pathway include decreases in cholesterol, farnesyl pyrophosphate (FPP), and geranylgeranyl pyrophosphate (GGPP) levels within multiple myeloma, SF-295, and A549 cells [8,12]. Disruptions in cholesterol homeostasis are observed at the transcriptional levels for SRE and LXR-related transcripts [8,12]. ABCA1 and ABCG1 mRNA levels, for instance, decrease within SF-295 and A549 cells [8,12]. Holstein et. al. 2011 reported that, between schweinfurthin only treatments and schweinfurthin/lovastatin treatments, the combination reduces the apparent molecular weights of Ras, Rap1a, and Rab6. Addbacks of mevalonate restore the molecular weight of these proteins. FPP and GGPP are two lipid substrates (with varying number of prenyl units) used to post translationally modify small G proteins. Inquiry into the effects of addbacks of FPP and GGPP on the molecular weights of proteins like Ras and Rap1a are shown to be effective in certain combinations/conditions, not others [8, 13].

Future experiments will be performed to further characterize whether FPP and GGPP depletion reflects a schweinfurthin-mediated reduction in synthesis of more downstream intermediates (such as dolichol) or a decrease in prenylation of other small G proteins.

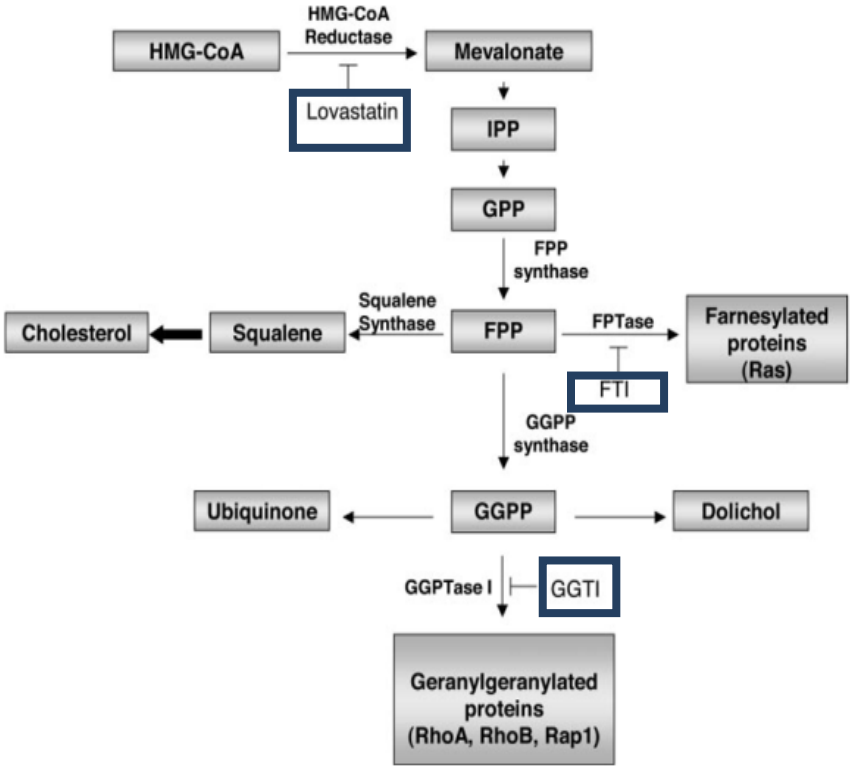

Figure 2: Schematic of the Mevalonate Pathway. Briefly, HMG-CoA is a derivative of Acetyl-CoA from the Krebs Cycle that enters into the pathway. The rate-limiting step is reduction of HMG-CoA to mevalonate. Units of five-carbon chains, known as isoprenes, are combined, of which FPP is considered the center of the pathway. FPP can be used to directly modify proteins and form larger structures such as GGPP and dolichol. Both contribute to protein post-translational modifications (geranylgeranylation and glycosylation, respectively). Additionally, FPP acts as a precursor for cholesterol and other sterol molecules. Abbreviations: FPTase= farnesyltransferase; GPTase I= Geranylgeranyltransferase I; FTI= Farnesyltransferase inhibitor; GGTI= Geranylgeranyltransferase I inhibitor.
Adapted from Hamadmad et. al. (2006), JPET.

Growth factor receptor signaling may be dependent on exquisite control of the mevalonate pathway, especially on pools of metabolites such as cholesterol, FPP, and GGPP [15,16,17,18]. For instance, both cholesterol distribution and protein prenylation status are critical components that are known to regulate the activity of proteins (EGFR/Ras/PI3K/AKT) at signaling platforms at membranes [7,15,16,17,18,19]. Much of these mevalonate-derived metabolites are therefore in association with these platforms and contribute in the formation of unique membrane microdomains such as lipid rafts [7,14,15,16,17,18].

Lipid rafts have been linked to cytoskeletal integrity, but less is known about how schweinfurthins impact receptor-mediated signals and the receptors themselves along with their effectors. Such receptors and effectors are located within cholesterol-rich membrane domains like lipid rafts [7,14,15,17,18]. What is known is that schweinfurthins impact both cancer cell morphology and cytoskeleton [10,11]. An increase in cortical actin and a decrease in stress fibers is evident within malignant peripheral sheath nerve tumor cells lacking a Ras-GAP protein, NF1 [10]. Our analogs, detailed in Kuder et. al. 2012, also produces this same effect within SF-295 cells, not A549 cells [12].

Whether these schweinfurthin-mediated effects are related to Rho or Ras signaling is not well understood. Turbyville et. al. 2010 reports that schweinfurthins reduce levels of both EGF-induced Rho-GTP and its downstream effector, Myosin Light Chain (MLC) [10]. However, it is not clear that schweinfurthins impair Rho and not Ras signaling. Initial inclinations that Ras may be involved were quickly eliminated from further study by Turbyville et. al. 2010, based on the rationale that farnesyl transferase inhibitors (FTIs) are ineffective against malignant peripheral nerve sheath tumor (MPNST) cells [10]. Ras is commonly found modified with a farnesyl lipid anchor, which suggests that within these tumors, Ras is not involved in schweinfurthin-mediated toxicities. This is due to the observation that lack of Ras farnesylation (e.g. from FTIs) do not promote meaningful toxic effects within MPNST cells.

However, Ras can either be farnesylated or geranylgeranylated and may be sensitive to changes in prenyl pools if schweinfurthins target multiple substrates within the mevalonate pathway [18,20,21]. Additionally, elimination of Ras from further study may have been short-sighted since different tumors have different baseline values of cholesterol, FPP, and GGPP [22].

Our group has shown that A549 cells are sensitive to the effects of a Rho kinase inhibitor, but not to the effects of schweinfurthins [11]. This suggests that Rho is not the only small G protein involved in maintenance of the cytoskeleton that is impaired upon treatment with schweinfurthins [11]. Investigations into schweinfurthins and their effects on growth factor receptor signaling may provide more clarity as to whether or not schweinfurthins impact Ras signaling via depletion of mevalonate pathway metabolites within cancer cells.

Isoprenoids As A Precursor to Processing of Receptors & Effectors

Post translational modifications define both distribution and signaling output of growth factor receptors. These markers can direct receptors along the secretory pathway to different trafficking stations en route to the plasma membrane [23]. At the membrane, post translational modifications like glycosylation serve to attract ligands to the extracellular binding domain of receptors [24,25]. Enhanced activation and signal transduction from this interaction to downstream effectors affects small G proteins which are lipid anchored to membranes via mevalonate-derived substrates [17,18,19,20]. Sites on receptors that are phosphorylated serve as docking sites to recruit adaptor proteins and kinases involved in signal transduction [15,17,18,25]. When it comes to the most common post translational modification within cancer cells, glycosylation is more abundantly found on proteins than phosphorylation [26]. Mevalonate pathway-derived isoprenoids that contribute to N-linked glycosylation and protein prenylation in cancer cells may in turn influence the phosphorylation and activation of growth factor receptors.

N-linked glycosylation is extensively found on many growth factor receptors as well as other cell surface receptors. This is a process in which an asparagine residue becomes attached to carbohydrate sugars to form glycosidic linkages and branched chain oligosaccharides, hereafter referred to as glycans [27,28]. One of the mevalonate pathway metabolites, dolichol, is a lipid carrier that mediates the transfer of initial core mannose sugars to the N-X-S/T motif [28,29,30]. Two other mevalonate pathway substrates, FPP and GGPP, can influence levels of dolichol synthesis. FPP and GGPP are contributors to modifications that anchor proteins onto membranes [8,13,17,19,20,21]. FPP is a fifteen-carbon lipid molecule that directly modifies H-, N-, and K-Ras via the actions of a farnesyltransferase [19,20,21]. Alternatively, FPP undergoes further condensation to form either GGPP, a twenty-carbon lipid molecule that is covalently linked to Ras-related small G proteins, squalene, a precursor to sterols, or dolichol [8,19,20,21]. GGPP addition to proteins such as Rap1a and RhoA involves the action of geranylgeranyltransferase I, while geranylgeranyltransferase II modifies a group of Rab proteins not related to Ras at a CXCX or CCXX motif [20,31]. Both farnesyltransferase and geranylgeranyltransferase I bind to the CAAX motif of Ras-related small G proteins near the C' terminus [20,31]. This CAAX motif represents a cysteine, two aliphatic amino acids, followed by an amino acid. This motif becomes modified at the thiol group of cysteine via farnesyltransferase (where the 'X' in CAAX = serine/ methionine/ glutamine/ alanine) or geranylgeranyltransferase I (where the 'X' in CAAX = isoleucine/ leucine/ phenylalanine) [20,31]. Our group as well as others have proposed that the levels of mevalonate-related metabolites may be integral to growth factor receptor signaling and proper activity for effector proteins like Ras [8,15,18,19,21,33].

Isoprenoid Inhibitors Affect Growth Factor Receptors & Small G Proteins

A recent study examined how schweinfurthins decreased Ras/AKT signaling by reducing the extent of N-linked glycosylation on growth factor receptors and other receptor tyrosine kinases [7]. More investigations are necessary to elucidate the mechanism for this change. Schweinfurthin-mediated effects on the mevalonate pathway, for instance, could be responsible for reducing substrates required for N-linked glycosylation and protein prenylation. Insight into this possibility arises from studies using lovastatin treatments on cancer cells to monitor small G proteins as well as growth factor and "growth factor like" receptors. Reductions in receptor glycosylation and cell surface receptor levels, protein prenylation and expression levels, plus signaling have been described in the case of Ras-related small G proteins, Erythropoietin receptor (EpoR), and Insulin Growth Factor 1 receptor (IGF1R) [19,32,34,35,36].

Both Holstein et. al. (2002) and Ownby et. al. (2003) report that treatments with lovastatin can induce higher expression levels of Ras-related small G proteins as a consequence of isoprenoid depletion and less prenylated Ras-related proteins [13,31]. A 24-hour timecourse of lovastatin treatment indicates an increase in protein levels of Ras, RhoA, and Rap1a early within the timecourse while protein levels of RhoB increase much later [31]. Not only do addbacks of mevalonate reverse this lovastatin-mediated effect, but addbacks of other mevalonate-related substrates display partial to complete rescue of protein prenylation, in spite of the continuous exposure to lovastatin [31,33]. Most of these patterns reflect whether or not a protein is farnesylated or geranylgeranylated [13,31,33]. However, there are cases where precursor combinations of metabolites that form FPP or GGPP display little rescue against lovastatin-mediated depletion of prenylation levels, as was seen in lovastatin-treated NIH3T3 cells that did not recover mature Ras levels when FOH was added back [13]. In spite of such setbacks, treatments of lovastatin increase synthesis and reduces degradation of Ras, with the consequence

that much of the Ras seen in lovastatin-treated cancer cells has a lower apparent molecular weight [31,33]. Addbacks of mevalonate and FPP can rescue these defects, which also indicates that lovastatin limits farnesylation of Ras [13,31,31].

The effects of lovastatin on small G proteins may extend to affect growth factor receptors. Our group has further explored how lovastatin treatments in bone marrow derived tumor cells affects EpoR, a cytokine receptor that affects survival, differentiation, and proliferation [19,32,34]. Findings from this work overlaps with research performed in melanoma cells to characterize the effects of lovastatin on IGF1R, a receptor tyrosine kinase and growth factor receptor [35,36]. EpoR is a 66 KDa, N-linked glycosylated protein, with lower-apparent molecular weight forms at 62 and 64 kDa that are assumed to be minimally or partially glycosylated [32]. When EpoR expression is initially suppressed by Epo and then induced by Epo starvation, lovastatin treatment prevents the starvation effect and formation of the mature, fully glycosylated 66 kDa isoform of EpoR [32]. This in turn reduces EpoR signaling to downstream effectors, an effect also seen when Epo-starved cells were treated with either tunicamycin or GGTI [32]. Lovastatin also reduces levels of EpoR and IGF1R at the cell surface [32,35,36]. IGF1R has several N-linked glycans based on results from glycan trimming enzymes like PNGase F (N-Glycosidase F), which cleaves N-linked glycans on IGF1R [35]. Addbacks of mevalonate and dolichol increase the levels of [^{3}H] glucosamine-labeled EpoR and IGF1R at the cell surface after lovastatin treatment [32,35,36].

These positive results from addbacks of mevalonate and dolichol with incorporation of [^{3}H] glucosamine, a substrate for N-linked glycosylation, reveal that lovastatin impairs glycosylation of EpoR and IGF1R [32,35,36]. Levels of cell surface IGF1R are fully restored with addbacks of mevalonate and dolichol [35,36]. While levels of cell surface EpoR are fully restored with addbacks of mevalonate, addbacks of dolichol only restore levels of EpoR up to 80% of that seen in controls [32]. Addbacks of GGPP following lovastatin treatments on Epo

starved cells fully restores levels of EpoR at the cell surface [32]. Altogether these results suggest that both glycosylation of the EpoR and geranylgeranylation of small G proteins contribute to the proper cell surface levels and signaling of EpoR [32]. In contrast, glycosylation likely fully contributes to levels of IGF1R at the cell surface [35,36].

EGFR as a Prototypical Growth Factor Receptor

Lovastatin treatment across cancer cells lowers the dimerization, internalization, phosphorylation, and downstream signaling of one of the most well-studied receptor tyrosine kinases, Epidermal Growth Factor receptor (EGFR) [15,16,17]. Further analysis is warranted on whether or not mevalonate pathway inhibitors impair N-linked glycosylation on EGFR, and not just prenylation of small G proteins [15,16,17]. EGFR is commonly overexpressed in cancers, especially in brain and lung cancers [37,38]. A total of seven different ligands bind to EGFR [39]. Among these ligands, Epidermal Growth Factor (EGF) acts a full agonist [15,17,39]. Proliferation, angiogenesis, differentiation, and cellular senescence/death are all possible outcomes of EGFR signaling [15,25]. Dimerization of EGFR occurs upon ligand binding or, in some cases, when monomers are in close proximity [15,17,24,25].

Heterogeneous expression of EGFR is due to homo- or hetero- dimerization of specific monomers from the ErbB family (EGFR/ErbB1/HER1, Neu/ErbB2/HER2, ErbB3/HER3, and ErbB4/HER4) [15,16,17,25,40,41]. Autophosphorylation of the intracellular tyrosine kinase domain of EGFR activates downstream signaling pathways [25]. What specific signaling pathway gets activated depends on which tyrosine residue gets phosphorylated [25]. There are two major EGFR signaling pathways, AKT and MAPK [25]. Other pathways associated with EGFR include PLC/PKC, Jak/STAT, JNK, p38 MAPK, FAK and CaMK (see Fig. 3) [25].

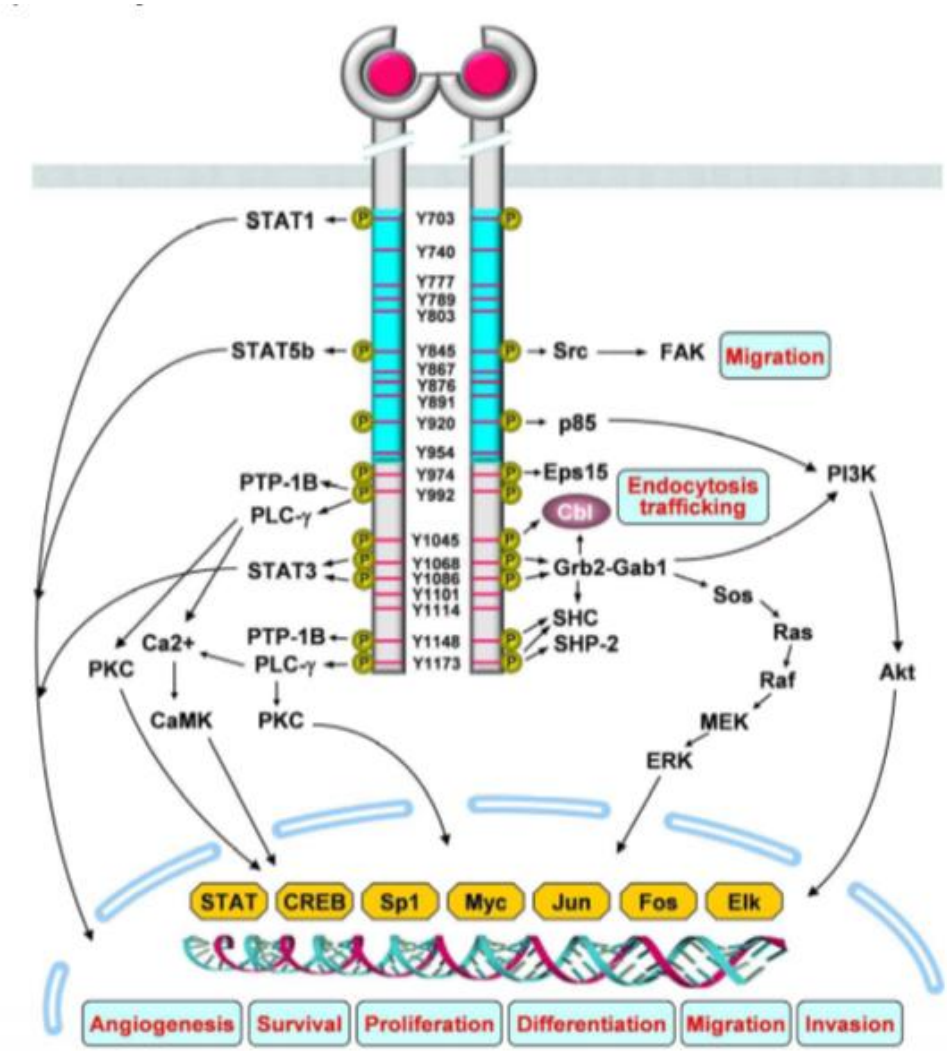

Figure 3: Signaling of EGFR Depends on Which Tyrosine in the Kinase Domain is Phosphorylated. Based on ligand identity and concentration, various pathways and transcription factors can be activated by EGFR such as AKT and MAPK. Together, this promotes growth and survival signaling, among other outcomes, according to EGFR activity.

Adapted from © 2011 Yao Huang and Yongchang Chang. Originally published in Prostate Cancer- From Bench to Bedside under CC BY 3.0license. Available from: https://doi.org/10.5772/27021

Both the Ras/AKT pathway and Ras/MAPK pathway can interact with one another [41]. Concentrations of EGF can influence the degree of activation for AKT and MAPK [41]. Downstream signaling of EGFR to the Ras/AKT pathway and Ras/MAPK pathway involves transduction activity from adaptor proteins and kinases like Shc, Grb2-Gab1, c-Src, c-Cbl, and PI3K [25,41]. Each of these proteins are able to bind to specific phospho-tyrosine residues on the intracellular tyrosine kinase domain of EGFR due to their SH2 or PTB binding domains [25,41]. Low levels of EGF are linked to activation of AKT and enhancement of MAPK activity [41]. High levels of EGF, however, are linked to increased activation of MAPK that prevents enhancement of AKT activity [41]. Within the Ras/MAPK pathway, RasGTP is formed from exchange of GDP to GTP by the protein complex, Grb2-Gab1-SOS. Grb2-Gab1-SOS activates, in turn, a cascade of serine/threonine MAP kinases, Raf-MEK-ERK1/2 [25,41,42]. Further activation of this pathway is mediated by the binding of adaptor protein, Shc, to phospho-Tyr1173, an agreed-upon marker for Ras/MAPK signaling [25,41,42].

The formation of Grb2-Gab1-SOS can be assisted by the action of PI3K, a lipid kinase that is responsible for activation of the Ras/AKT pathway [25,41]. RasGTP can also interact with PI3K and activate AKT [25,41]. Within the Ras/AKT pathway, PI3K phosphorylates and mediates conversion of phosphatidylinositol-4,5-diphosphate to phosphatidylinositol-3,4,5-triphosphate [7,25,41]. This recruits PDK proteins and AKT [25,41]. A negative regulator and phosphatase of this step in the pathway, PTEN, is sometimes deleted in cancer cells for full AKT activation [25]. Fully activated AKT is phosphorylated at Thr308 and Ser473 and signals downstream to multiple effector pathways like mTOR, which in turn increases protein translation [25]. Grb2-Gab1 binding at phospho-Tyr1068 (Y1068) and phospho-Tyr1086 (Y1086) allows for activation of both the Ras/AKT pathway and Ras/MAPK pathway [25,42]. Therefore, increases

in phospho-Y1068 levels will be used as a marker for Ras/AKT signaling. Other phosphorylation sites on Ser1046, Ser1047, and Thr654 can lower and fine tune EGFR signaling [25]. Another phosphorylation site on Tyr1045, can be recognized by E3 ubiquitin ligase, c-Cbl, which regulates EGFR degradation [25,42].

Findings reported from Dimitroulakos et. al. 2008 focuses on how treatments of lovastatin affect EGFR activity within epithelial cancer cells [15,16,17]. Administration of a statin followed by EGFR tyrosine kinase inhibitor, gefitinib, increases apoptosis within these cells [15,16]. This increase in apoptosis may be explained by MTT studies where compounds show a synergy [15]. Treatment of lovastatin on squamous cancer cells reduces dimerization and internalization of EGFR as well as EGF-induced phosphorylation of the receptor at Y1068 [15,17]. This in turn decreases phosphorylation at AKT(S473) [15]. Reductions in phosphorylations of downstream effectors of AKT, known to be connected to mTOR and protein translation, have been identified as a consequence of the effects of lovastatin on EGFR [17]. Addbacks of FPP, GGPP, and mevalonate, but not dolichol, rescues cells from lovastatin-mediated reductions in these EGF-induced phosphorylation sites [17]. Lovastatin-mediated decreases in internalization and dimerization of EGFR is reversed when addbacks of mevalonate and GGPP are added to cells [17]. No further information is available on the effects of addbacks of FPP and dolichol on internalization and dimerization of EGFR in cells treated with lovastatin [17].

The mitigating effects of mevalonate and GGPP on lovastatin-mediated dysregulation of EGFR suggest that geranylgeranylation of small G proteins is integral to EGFR activity [17,18]. This claim is backed by observations that treatments with lovastatin promotes the accumulation of unprenylated Cdc42 and RhoA in cancer cells, two geranylgeranylated proteins [17]. Treatments with Y27632, an inhibitor of the family of ROCK proteins responsible for RhoA signaling, was noted to decrease EGF-induced signaling and dimerization of EGFR [17].

Because this effect is similar to the effects seen in treatments with lovastatin with regards to the cytoskeleton and EGFR dynamics, Dimitroulakos et. al. 2010 concludes that EGFR activity is dependent on the levels of RhoA and Cdc42 in their geranylgeranylated forms [17].

It is important to note, however, that this study is complicated by results in which addbacks of mevalonate and GGPP do not reverse the signaling defects of EGFR when cells were treated with Y27632, despite rescue of EGFR dimerization seen with this treatment [17]. This suggests that potential rescue of protein geranylgeranylation with GGPP, or a precursor to it, is not sufficient enough to fully restore EGFR activity and that impairment of RhoA/Cdc42 activity requires something more to overcome the effects of Y273632 on these small G proteins. Moreover, this treatment may be limited in its scope and not be an accurate example of the effects that lovastatin can have on EGFR. For instance, dysregulation of N-linked glycosylation has been shown to block cell surface presentation of EGFR as well as signaling, in the case of disrupting oligosaccharyltransferase function in yeast [43]. It may be that lovastatin may impair N-linked glycosylation of EGFR more promiscuously and that dolichol addbacks should be re-investigated. Such findings warrant further examinations into the effects of lovastatin on EGFR, given that addbacks of dolichol are able to overcome lovastatin-mediated effects on EpoR and IGF1R activity in cancer cells [32,36].

EGFR as an N-linked Glycosylated Receptor

Schweinfurthin- or lovastatin-mediated defects on glycosylation and downstream signaling of EGFR could be related to specific sites of glycosylation shared on growth factor receptors within several cancers. Fully glycosylated EGFR is located on the plasma membrane of cells and has a structure which consists of an extracellular, a transmembrane, and an intracellular tyrosine kinase domain [24,25]. Within the extracellular domain of EGFR, a total of 12 N-linked glycosylation sites are thought to exist within four separate subdomains [24,28,29,44,45]. Subdomains I and III form the ligand binding site for EGFR, with the assistance of subdomains II and IV [28,29,44,45]. Subdomain II acts as an "arm" to promote EGFR dimerization [28,29,45]. Subdomain IV regulates the extension of EGFR needed to promote a sequential binding of EGF to monomers of EGFR, one monomer at a time [28,29,45] (see Fig. 3). Each N-linked glycan from these four subdomains form interactions to decrease the size of the ligand binding site and lower the binding energy of EGF to EGFR [24]. N-linked glycans on N^{151} and N^{156} from subdomain I plus N^{328} and N^{333} from subdomain III can regulate EGF binding to EGFR/ErbB4 receptors [29]. N-linked glycan N^{350} was found to be important for EGF-EGFR interactions as well [24]. Another set of N-linked glycans on N^{418} from subdomain III of EGFR, on N^{420} from subdomain III of ErB3, and on N^{579} from subdomain IV can mediate dimerization of EGFR [28,29,44,45]. N-linked glycans on N^{544} from subdomain IV can influence the protein folding of subdomain III and can, therefore, control EGFR structure [28].Other N-linked glycans found on N^{32}, N^{337}, and N^{389} have unknown functions, but do not influence EGF-EGFR binding [28].

To date, not much is known about which sites of glycosylation are disrupted after treatments with schweinfurthins or lovastatin.

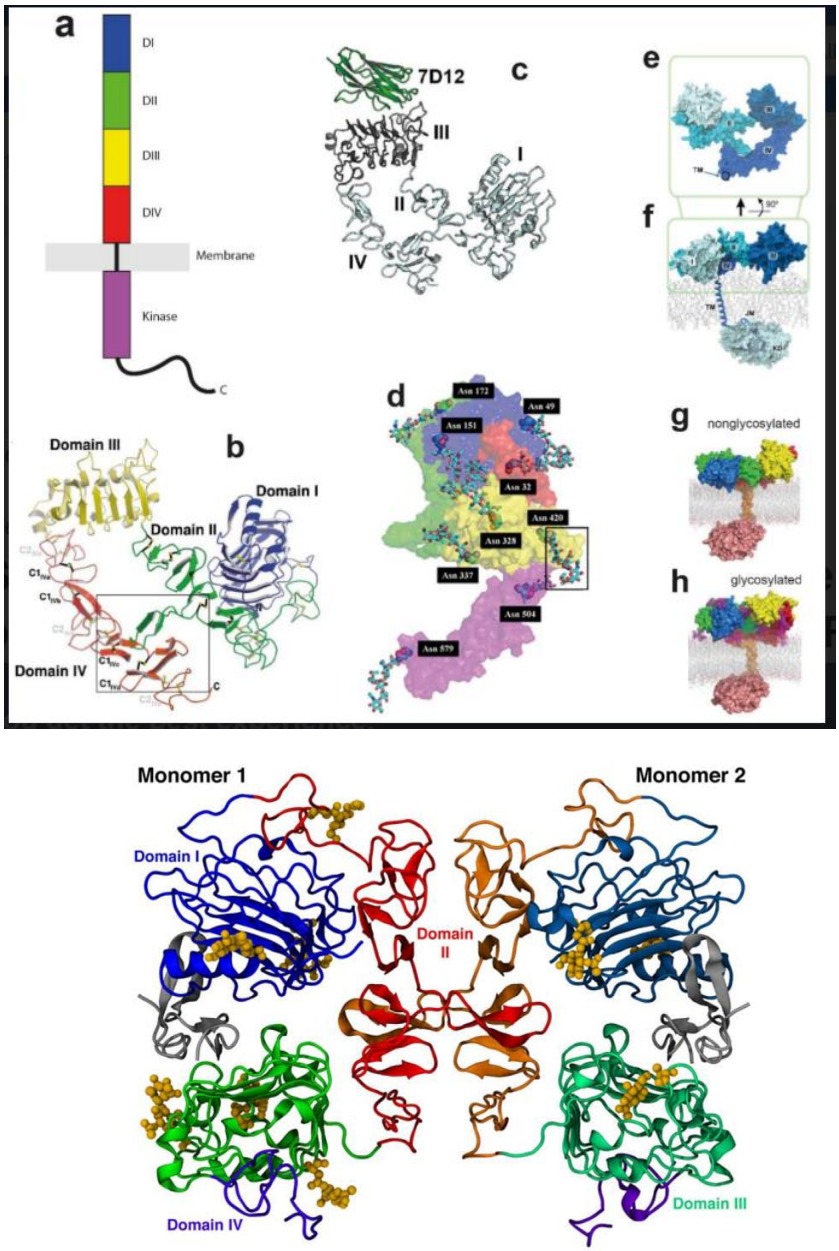

Figure 4: Depiction of the Four Different Subdomains of EGFR. A) Schematic and 3D topological structures of an EGFR monomer is shown above. Note structures of the soluble form of EGFR (see b-d) are found in Protein Database Bank (PDB) as well as other papers. Observe in b) the interaction between the dimerization arm (Subdomain II) and Subdomain IV. Note in d) all asparagine residues that are N-linked glycosylated in d. **B)** MD simulations of EGFR shows that N-linked glycans are integral for EGFR stability when it comes to EGFR dimerization and EGF binding. N-linked glycans partly enhance EGFR stability by interacting with the cell surface membrane. Glycans are shown in yellow. Loss of N-linked glycans leads to a destabilization of domains III & IV from both monomers. N^{350} was found to be integral for EGF-EGFR interactions.

Adapted from Martin-Fernandez et. al. (2019) & Lower et. al. (2017)

The assortment of N-linked glycans that can be found on EGFR can also be considered to influence EGFR activity as well. Multiple mannose residues to complex or hybrid types of glycans are found at various sites of glycosylation within EGFR [24,27,28,45,46]. This arrangement of glycans added or modified onto EGFR depends on how this receptor is trafficked within the secretory pathway [27,46,48,49,50]. Briefly, the first step of N-linked glycosylation for any glycoprotein occurs within the endoplasmic reticulum [27,46,48,49,50]. This is where fourteen different glycans (2 N-acetylglucosamine, 9 mannoses, and 3 glucoses) are transferred from dolichol to an N-X-S/T protein motif [27,46,48,49,50]. Further modifications then proceed within the Golgi through the actions of glycosyltransferases, mannosidases, and glycosidases before being transported either to the plasma membrane or secreted via exosomes [27,46].

Studies to investigate proximal or terminal glycans and their influence to EGF-EGFR binding have produced mixed results. Current findings indicate that both terminal sialylated and fucosylated glycans interact with EGF to modulate EGF-EGFR binding [44,45]. However, changes to N-acetylglucosaminyltransferase III activity which adds on more proximal glycans to EGFR also reduces EGF-EGFR binding within A431 cells [43]. Although treatments of lovastatin and its effect on specific glycans has been understudied, recent findings have started to uncover the types of glycans that are affected by treatments with schweinfurthins, narrowing it down to a lack of terminal sialylation.

Glycosylation Inhibitors Affect EGFR Activity

The effects of schweinfurthins include depletions in glycans for EGFR, similar to results from various growth factor receptors after treatments with lovastatin or glycosylation inhibitors [7]. EGFR is composed of three to four different isoforms that are either fully glycosylated or partially glycosylated [27,46,48,49,51]. The molecular mass of EGFR can be calculated as 134 kDa according to its primary structure which has 1186 amino acids [49]. Yet, mature, fully glycosylated EGFR runs at an apparent molecular weight of 165 to 175 KDa on SDS-PAGE [27,46,48,49,51]. The varying apparent molecular weights of fully glycosylated EGFR accounts for both ligand-bound and unbound receptors. Tunicamycin, monensin, swainsonine, and 2-deoxyglucose are a group of inhibitors that disrupt N-linked glycosylation [27,48,49,51]. These inhibitors have been used in experiments to glean more insight into how N-linked glycans affect the ligand binding activity and signaling of EGFR.

Tunicamycin inhibits the transfer of core glycans to asparagine sites of glycoproteins within the endoplasmic reticulum [27,49]. Treatments with tunicamycin and tyrosine kinase inhibitors reveal that EGFR can be found in multiple glycosylation states [27,46,48,49,51]. This has been identified in A431 cells and in cancer cells like glioma and lung [27,46,48,49,51]. Treatment with tunicamycin decreases the apparent molecular weight of EGFR to form two minor glycoforms. Both glycoforms, one at 130 to 138 KDa and another at 68 to 77 KDa, have been shown to accumulate within cells, with some EGFR proteins trapped inside the endoplasmic reticulum [49,52]. ^{25}I-EGF binding timecourse experiments and *in vitro* phosphorylation assays indicate that these glycoforms of EGFR share little to no binding affinity to ^{25}I-EGF, with diminished/absent levels of autophosphorylation [27,48]. Monensin, swainsonine and 2-deoxyglucose impair later steps of N-linked glycosylation which involve glycan elongation at the Golgi [27,46,48,49,51]. Treatments with these compounds in A431 cells reduce the apparent

molecular weight of EGFR by as much as 30-40 KDa, but there is also a 160 KDa isoform of EGFR that is also produced [27,46,48,49,51]. Autophosphorylation, cell surface levels, and EGF binding affinity of EGFR are unchanged by the decreased apparent molecular weight brought about by these compounds [27,46,48,49,51].

Although much has been uncovered on the effects of glycosylation inhibitors on EGFR, the need for more specific, less toxic effects from such inhibitors makes schweinfurthins an attractive alternative to deplete fully glycosylated EGFR.

Schweinfurthins Effects on Oncogenic Ras Activity

Much of the research that surrounds the actions of schweinfurthins covers two disparate outcomes that may be part of the same network targeted by schweinfurthins. These schweinfurthin-mediated effects on Ras-related small G proteins and growth factor receptors could serve as a paradigm for further investigations into differential, anticancer effects of schweinfurthins. The premise for our investigations arises from our interest in EGFR and genetic differences between SF-295 cells and A549 cells, which are sensitive and insensitive to the effects of schweinfurthins, respectively (Table 1).

	SF-295	A549
	Sensitive	Resistant
# of EGFR reads	> 4 copies	normal 1 or 2
PI3K/AKT	No known mutations	
PTEN	Loss of Function	Wild Type
K-RAS	Wild Type	Gain of Function

Table 1: Summary of genetic mutations within SF-295 and A549 cells in the context of EGFR and its effectors, PTEN and K-Ras. Oncogenic K-Ras is present within schweinfurthin-insensitive A549 cells and may be involved in a compensatory mechanism to alleviate schweinfurthin-mediated effects on EGFR signaling. See text for information.

Although real time PCR and high-density SNP-ChIP indicate that SF-295 cells have a copy number amplification of EGFR, this amplification lacks correlation with EGFR protein expression [53]. Similar protein levels of EGFR between SF-295 cells and A549 cells can also be verified within the NCI-60 cancer cell panel database. We next considered genetic differences into the mutational statuses of effector proteins downstream of EGFR. In this context, SF-295 cells contain a loss of function in PTEN, which has been reported to be a marker indicative of schweinfurthin sensitivity [7,9]. A panel of large diffuse B-cell lymphomas, however, only showed this pattern of sensitivity to schweinfurthins under shorter treatment times [7]. Prolonged schweinfurthin treatments, on the other hand, showed that inhibitory-concentration 50 values were similar amongst the cells [7]. This was irrespective of PTEN statuses within these B-cell lymphoma lines [7]. Additionally, within a panel of cancer cell lines with various B-Raf and PTEN expressions, those cancers with a loss of PTEN expression showed a slower decrease in AKT activation than those cancers with wild type expression of PTEN when treated with schweinfurthins [7]. Thus, PTEN may not be the sole predictor of schweinfurthin sensitivity.

On the other hand, A549 cells express oncogenic K-Ras (G12V). Oncogenic Ras proteins signal to downstream effectors of AKT and MAPK pathways, irrespective of the active state of growth factor receptors. Our belief is that such a mutation may yield insight into a compensatory pathway that circumvents the actions of schweinfurthins. It is important to note, however, that this compensation is unlikely to be directly related to K-Ras itself as both schweinfurthin-sensitive and -insensitive cancers from the NCI-60 cancer cell panel express similar oncogenic mutations within K-Ras [55].

Effects of Isoprenoid Levels on Oncogenic Ras Activity

Members of Ras and Ras-related small G proteins relay a gradient of signals that regulates vesicular trafficking, differentiation, cell cycle, and cytoskeletal dynamics [33,55]. Ras-mediated signals are dialed up or down based on the activity from receptors and adaptor proteins [55]. Association and dissociation of GTP and GDP during the GTPase cycle for Ras-related proteins leads to signal transduction while various GEFs and GAPs assist to increase binding and intrinsic hydrolysis of GTP [55]. Ras-related small G proteins are anchored to membranes via 1) a sequence of Lys or Arg residues and/or 2) one or more lipids from myristoylation, palmitoylation, or prenylation. K-Ras is most commonly mutated across cancers out of the three Ras isoforms (H-Ras, N-Ras, and K-Ras), with the highest mutational frequencies in pancreatic, colon, and lung cancers [33,55]. Much of these mutations, like those at codons 12, 13, and 61, are located near the nucleotide binding site of Ras [55]. Ras proteins, both wild type and mutant, as previously mentioned, require a farnesyl lipid anchor to be localized to membranes, though cross-prenylation with a geranylgeranyl can occur if farnesyl is unavailable [21,33,55].

About 10 to 45 mole percent of total lipids in the plasma membrane is composed of cholesterol [56]. Interactions of lipid anchors with cholesterol modulates both localization and activity of H-Ras, N-Ras, and K-Ras [57,58]. Each of these proteins differ in overall lipid anchor composition. H-Ras and N- Ras are modified with palmitates that interact with cholesterol deep within membranes [57]. Certain K-Ras isoforms lack this modification since it has, instead, a sequence of Lys residues which binds to the surface of membranes via electrostatic interactions with lipids like phosphatidylserines and phosphatidylinositols [57,58,59,60,61,62]. Cancers that express oncogenic K-Ras likely can circumvent treatments that target cholesterol and farnesyl pools [21,33,55,57,58,59,60,61,62]. However, this comes under certain conditions.

Indeed, within our work, a comparison between two multiple myeloma cell lines that differ in sensitivities to schweinfurthins reveals that co-treatment with lovastatin and schweinfurthins exhibits slower increases of unmodified Ras within RPMI-8226 cells. One potential reason for this is that RPMI-8226 cells display an oncogenic mutation in K-Ras, a Ras form that is likely able to localize to membranes via electrostatic interactions, even in the face of isoprenoid/cholesterol depletions. This schweinfurthin-mediated loss of mature Ras is more potent in U266 cells, another multiple myeloma cancer cell line [8,22]. Increases in immature Ras in RPMI-8226 cells, not U266 cells, is similar to that seen when both cancer cell lines are treated with lovastatin by itself [8,22]. However, the cytotoxic profiles of these multiple myeloma cancer cell lines suggests that, despite a mutation in K-Ras, RPMI-8226 cells are sensitive to the effects of schweinfurthins and lovastatin when compared to U266 cells [8,22]. One reason for this may be due to the lower total levels of FPP/GGPP pools within RPMI-8226 cells, not seen in U266 cells [22]. This led to questions about whether there are cancer lines with an oncogenic K-Ras mutation that would still be sensitive to schweinfurthins, should basal levels of FPP/GGPP pools be higher. The slow accumulation of unprenylated K-Ras in K-Ras mutated cancer cells upon schweinfurthin treatment may be even more apparent and, perhaps, biologically significant in this case.

Effects of Schweinfurthins on Glycosylation and Signaling from EGFR

The selectivity of schweinfurthins and their cytotoxic effects against certain cancer cells links to depletions of substrates within the mevalonate pathway [8,12]. This in turn translates to less pro-survival signaling from receptor tyrosine kinases as well as growth factor receptors like EGFR [7]. While much of the research done on schweinfurthins has focused on small G proteins and depletions of FPP and GGPP in receptor signaling pathways, further work is

necessary to determine whether schweinfurthins affect receptor signaling and small G protein activity via distorting other compounds such as dolichol and cholesterol. Reductions in dolichol inhibit N-linked glycosylation of proteins [32,35]. Losses in intracellular cholesterol disrupt receptor-mediated signals and small G protein distribution within cholesterol-rich membrane domains such as lipid rafts [7,8,14,15,16,17,18,19,21,33]. Work from Bao et. al. 2015 claims that schweinfurthins disrupt glycosylation and lipid raft integrity, which in turn, dampens signals from receptors like EGFR [7].

Bao et. al. 2015 proposes that a limited, 6-hour treatment of schweinfurthins reduces levels of sphingolipids and cholesterol within the Golgi, irrespective of cancer type. An enhanced interaction between schweinfurthins and ER- or Golgi-related OSBPs is thought to contribute to disruptions in lipid raft composition seen at the Golgi [6,7,8,9]. Consequentially, a lack of proper distribution of various glycoproteins and their downstream effectors, including mTOR, is seen from treatments with schweinfurthins [7]. Bao et. al. 2015 reported that treatment with schweinfurthins decreases the apparent molecular weight of EGFR as well as reduces phosphorylation of AKT, likely as a consequence of above effects [7]. Bao et. al. 2015 suggests that treatment with schweinfurthins decreases sialylation of receptor tyrosine kinases based on detection using various glycan binding proteins called lectins. Yet, the connection that schweinfurthins specifically inhibit signal transduction from EGFR to AKT is not established.

Chapter 2

Specific Aims & Hypothesis

Our long-term goal is to elucidate the mechanisms by which schweinfurthins mediate cytotoxicities in a differential manner within cancer cells. Schweinfurthin analogs demonstrate pleiotropic effects on the mevalonate pathway, cytoskeleton, and small G proteins, among other cellular anti-cancer effects [4,8]. Our work prominently focuses on similarities and differences between lovastatin and schweinfurthins, which in combination with lovastatin, depletes essential metabolites like FPP and GGPP and impairs *de novo* cholesterol synthesis [8,12]. A subset of this research shows that this effect reduces prenylations of small G proteins, specifically Ras [8]. Published work by Bao et. al. 2015 recently demonstrated that schweinfurthins bring about Golgi disruption and trafficking impairment that reduces the levels of glycosylation seen at growth factor receptors. The appearance of receptors with lower apparent molecular weights corresponds with lower AKT/mTOR signaling seen after schweinfurthin treatment [7]. Whether or not the effects of schweinfurthins on EGFR glycosylation and Ras signaling occurs in certain cancers as a consequence of known differential effects of the compound requires further investigations into EGFR/Ras signaling.

Previous studies from Bao et. al. 2015 have already implicated loss of PTEN while other bioinformatic analyses have suggested that regulators of AKT are correlated with schweinfurthin sensitivity [7]. However, our group believes a more complex combination of mutations influence schweinfurthin sensitivity, partly supported by findings that seem to contradict conclusions within Bao et. al. 2015. A comparison of cancers with and without PTEN expression showed that schweinfurthin treatment reduces activation of AKT within the entire panel, yet cancers lacking PTEN expression showed slower rates of decrease for phospho-AKT when treated with schweinfurthins [7].

We narrowed our focus to a schweinfurthin-sensitive cancer (SF-295 glioblastoma) and a schweinfurthin-insensitive cancer (A549 NSCLC) to interrogate additional markers of schweinfurthin sensitivity in the context of EGFR signaling. A549 cells expressed an oncogenic mutation for K-Ras, a small G protein that is farnesylated but lacks multiple palmitates found on H- and N-Ras for deeper anchorage with cholesterol within cellular membranes [57]. It is believed, hence, that perhaps K-Ras is not reliant on membrane cholesterol as much as other Ras isoforms [57,58,59,60]. However, the important assumption with this hypothesis is that K-Ras may still be reliant on total FPP/GGPP pools to be in abundance in cancer cells before any treatments [22]. Hence, we hypothesize that schweinfurthins impair EGFR/Ras signaling in SF-295 cells while A549 cells have other pathways to compensate for the dysregulation of EGFR signals when treated with schweinfurthins. Such mechanisms of compensation within A549 cells are partly related to the presence of oncogenic K-Ras, a protein that not only has more flexible requirements for localization, but also partakes in EGFR-independent signaling as a mutant.

Aim I. Determine the mechanism for the apparent shift in apparent molecular weight of EGFR in SF-295 cells and whether this is directly coupled to decreases in phospho-AKT signaling in SF-295 cells, not A549 cells. A549 cells could potentially rely on MAPK activity for interactions with AKT instead.

A. Re-validate previous findings from our group as well as Bao. et. al. (2015) that treatments with schweinfurthins can reduce the apparent molecular weight of EGFR and AKT signaling [7]. Schweinfurthin analogs, TTI-3066 and TTI-4242, were tested in SF-295 and A549 cells using MTT assay to derive a dose response curve and effective concentration-50. Both cancer cell lines were treated over a 24-hour time-course with schweinfurthin analogs, TTI-3066 and TTI-4242, with antibody detection against EGFR, phospho-EGFR(Y1068), phospho-EGFR(Y1173), AKT, phospho-AKT(S473), phospho-MAPK (Thr202/Tyr204), MAPK, and γ-tubulin proteins.
   Protein analyses were perform using Western blots.

B. Determine whether or not pre-conditioning of SF-295 cells and A549 cells with EGF would buffer SF-295 cells from the effects of schweinfurthins or would reveal a direct impact of schweinfurthins on AKT and/or MAPK signaling via actions on EGFR itself. Our findings suggest that schweinfurthins reduce the apparent molecular weight of EGFR while increasing phospho-EGFR(Y1068) and phospho-EGFR(Y1173) levels on partially modified forms of the receptor. Experiments were done to test the effect of an acute vs. continuous stimulation of EGF on EGFR to see if schweinfurthin effects would be the same and if A549 cells would demonstrate a selective advantage in survival in terms of either EGFR/Ras/AKT or EGFR/Ras/MAPK signaling. We predict that levels of either phospho-AKT or phospho-MAPK would increase in A549 cells under these conditions.

Aim II. Determine the mechanism for the apparent shift in apparent molecular weight of EGFR in SF-295 cells and whether the loss in apparent molecular weight of EGFR is limited to loss of terminal sialylation from the trans-Golgi/trans-Golgi network.

C. Identify appropriate glycosylation inhibitors and/or glycan trimming enzymes that would overlay the reduction in apparent molecular weight seen in EGFR upon schweinfurthin treatment in SF-295 cells. Tunicamycin, swainsonine, and PNGase F will be tested as controls within SF-295 cells in order to monitor de-glycosylation of EGFR. ER- and Golgi- specific in vivo treatments as well as in vitro treatments of cell lysates with PNGase F will be compared with the effects of TTI-3066, a schweinfurthin analog, on SF-295 cells. We anticipate that tunicamycin will reduce the levels of glycans on EGFR to a greater extent than that seen with TTI-3066 treatment since this inhibitor acts at an early stage to prohibit N-linked glycosylation of the receptor.

D. Contrast the effects of some of the glycosylation inhibitors above on EGFR with another protein that undergoes N-linked glycosylation and terminal sialylation. For this experiment, LDLR was chosen for western blot analyses and tested with TTI-3066 in SF-295 cells alongside the above treatments. We expect to verify preliminary data to confirm whether schweinfurthins have no effect on LDLR. We also plan to verify contribution of N-linked glycans to the apparent molecular weight of LDLR using tunicamycin.

Summary: Successful completion of this aim will reveal whether or not future experiments should be pursued to look directly at Ras GTPase activity or Ras distribution within cancer cell lines that either express or do not express oncogenic K-Ras. Preliminary findings that confirm and extend on schweinfurthin-mediated effects on dominant oncogenic signaling pathways (AKT/MAPK) will confirm whether disruptions in apparent molecular weight of EGFR are truly related to dysregulation of these pathways. Both AKT/MAPK are central hubs for many extracellular signals. Interrogation of glycosylation of proteins not affected by schweinfurthins may also open up more directions for how the process of terminal sialylation could be compromised. This may help elucidate ways in which an oncogenic K-Ras mutation may be involved beyond canonical signaling pathways (AKT/MAPK) as part of a protective mechanism against the effects of schweinfurthins. This may also explain whether and how schweinfurthins impact oncogenic K-Ras activity within our resistant A549 cancer cell line.

Should our results fit our hypothesis, future investigations will be done in the context of EGFR signaling to explore effects of schweinfurthins on certain OSBPs like ORP8, a lipid transport protein implicated in transfer of phosphatidylserine to the plasma membrane, since lipid transport differences may explain subsequent, schweinfurthin-mediated effects on EGFR and Ras/AKT activity. Additionally, Ras may be explored to see if potential differences are seen in Ras activity between SF-295 and A549 cells. Indeed, others in our group have seen that schweinfurthins affect ORP8 levels within cancers (unpublished results of Craig Kuder), but little is known about feedback between OSBPs and growth factor receptor signaling pathways.

Chapter 3

Materials & Methods

Chemical compounds:

Schweinfurthin analogs TTI-3066 and TTI-4242 were generously provided by Terpenoid Therapeutics Incorporated (TTI). Tunicamycin and EGF was obtained from Sigma Aldrich. PNGase F and associated reagents were acquired from New England Biolabs.

Cell culture:

SF-295 glioblastoma and A549 non-small cell lung cancer cell lines were conditioned in RPMI-1640 media supplemented with 10% FBS and 4 mM of L-Glutamine for time-course treatments. The use of conditioned media is appropriately applied in large-scale screening of multiple cell lines as described in *Kirsch et. al. 2003* [63]. Later experiments were narrowed down to two timepoints alongside controls to confirm prior findings. These experiments were conducted with SF-295 and A549 lines cultured in RPMI-1640 and Ham's F-12 media, respectively. Both medias were supplemented with 10% FBS, Penicillin, Streptomycin, and 2 mM L-Glutamine as recommended by ATCC. Both SF-295 cells and A549 cells were incubated at 37 °C and 5% CO_2.

MTT assay:

Metabolic activity within SF-295 cells and A549 cells was assessed under TTI-3066 and TTI-4242 treatments. Briefly, 4000 cells/well (for SF-295) and 6000 cells/well (for A549) were seeded in a 96-well plate in a volume of 100 μL cell suspension/well for 24 hrs to achieve 70-80% confluency. A logarithmic range of concentrations of each TTI compound was tested for 48 hours and incubated at 37°C and 5% CO_2. Four hours before the end of the experiment, 10 μL of 5 mg/mL of MTT solution was spiked into each well as a readout for mitochondrial reductase

activity for surviving cancer cells. At the end of 48 hours, media containing MTT solution was removed and 100% DMSO was added into the wells to dissolve formazan crystals produced from the MTT reaction. Plates were read on Spectramax i3 (Molecular Devices) at wavelengths of 570 and 690 nm.

Western Blot:

Timecourse experiments on SF-295 and A549 cells with either TTI-3066 or TTI-4242 treatments were conducted as follows. Cells were plated in 100 mm dishes and treated with TTI compounds or DMSO vehicle. After 24 hours, cells were washed in cold PBS and lysed with Triton-X-100 buffer supplemented with appropriate protease and phosphatase inhibitors (sodium vanadate, sodium fluoride, leucine, and PMSF). Protein quantification was assessed using the Bradford-Lowry method with Pierce Thermofisher BCA standards and 100 μg of each sample was made up in Laemmli Buffer to be loaded onto gels. 8% Bis-acrylamide, Tris pH 6.8/8.8 stacking and separating gels were casted before loading samples in each well in a discontinuous buffer system (Hoefer SE400). Samples ran through the stacking gel at 110 V which was increased to 150 V once samples reached the separating gel. Transfer occurred overnight at 25 V and membranes were blocked for 2 hours in 2% fish gelatin supplemented with sodium azide and dissolved in TBST. Membranes were then probed with the first set of primary antibodies. All primaries were prepared in TBST with 0.5% Sodium azide. Either Protein A HRP or mouse HRP prepared in TBST was used as secondary detection antibody. Membranes were subsequently stripped with Harsh Stripping Buffer containing 2% SDS at 56°C for 30 minutes before probing with subsequent antibodies. Membranes were stripped to look at different proteins with different primary antibodies for up to three times for results.

Later experiments that focused on a one- or two-timepoint treatment with TTI-3066 and TTI-4242 were conducted as before with the following modifications. First, cells were plated in 60 mm dishes before harvesting with RIPA lysis buffer supplemented with protease and phosphatase inhibitors 1, 2 and 3 from Sigma Aldrich. Between 10 to 20 μg of lysate was prepared in Laemmli Sample Buffer and was loaded onto Bis-Tris NuPAGE 4-12% gradient precast mini gels from Thermofisher Scientific under a discontinuous buffer system (MOPS buffer, 175 V run). Protein transfer was approximately 2 hours at 25 V. Membranes were blocked in ScanLater buffer and probed with fluorescent, Europium labeled secondary detection antibody after applying primary antibodies. Blots were scanned using Spectramax i3 (Molecular Devices) to obtain results. Membranes were stripped as above and this procedure was repeated to look at the phosphorylated forms of the proteins. Note that some lysates from the previous experiments were analyzed with different primary antibodies using this system, with the methods listed above.

All samples were normalized to γ-tubulin in the timecourse experiments. For experiments focused on one- or two-timepoints of TTI treatment, all samples were normalized to GAPDH. Statistical significance was assessed using one-way ANOVA (with Dunnet's Post Hoc) on GraphPad Prism.

Chapter 4

Results

Experiments were performed within SF-295 cells and A549 cells, two different cancer cell lines known to be sensitive and insensitive to the effects of schweinfurthins, respectively. MTT assays, were conducted to assess the effects of two different schweinfurthin analogs, TTI-3066 or TTI-4242, on the metabolic activity of these cancer cells (Fig. 5). Addition of MTT four hours before the end of the 48-hour treatment with a schweinfurthin analog revealed that SF-295 cells were sensitive to the effects of both TTI-3066 and TTI-4242 over higher log concentrations of each compound (Fig. 5). This was visibly evident in our assay as less MTT was converted to a purple formazan product at the higher concentrations of TTI-3066 and TTI-4242 (Fig. 5). Effective Concentration-50 (EC_{50}) for each compound was different in spite of similar, sub-confluent cell densities throughout treatment and treatments using serial dilutions of the compounds (Fig. 5). Aside from chemical structure differences between TTI-3066 and TTI-4242, later experiments revealed compound degradation in TTI-4242 (not shown) (Fig. 5). This explains a difference in response within A549 cells when treated with both schweinfurthin analogs (Fig. 5). A549 cells subjected to log concentrations of TTI-3066 continued to exhibit mitochondrial activity comparable to control treated cells. In contrast, A549 cells treated with log concentrations of TTI-4242 continued to convert MTT to formazan, but at a higher level when treated with higher concentrations of TTI-4242. 100 nM of each compound was chosen for Western blot experiments since it reflected approximate EC_{50} of TTI-3066 in SF-295 cells.

5A

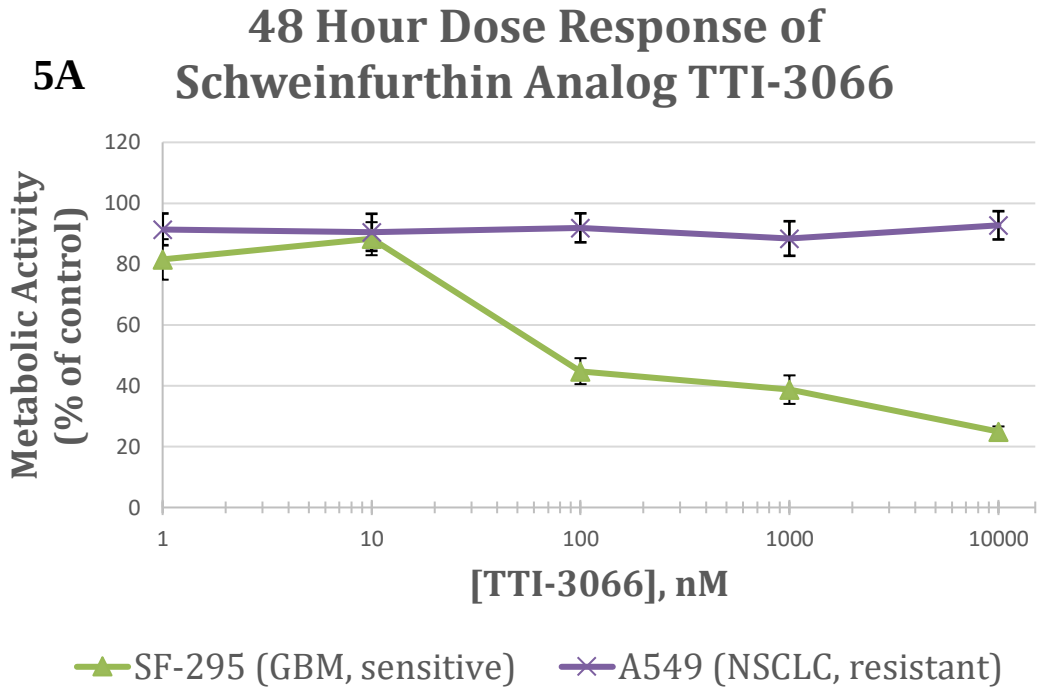
48 Hour Dose Response of Schweinfurthin Analog TTI-3066
Metabolic Activity (% of control)
120
100
80
60
40
20
0
1
10
100
1000
10000
[TTI-3066], nM
SF-295 (GBM, sensitive)
A549 (NSCLC, resistant)

5B

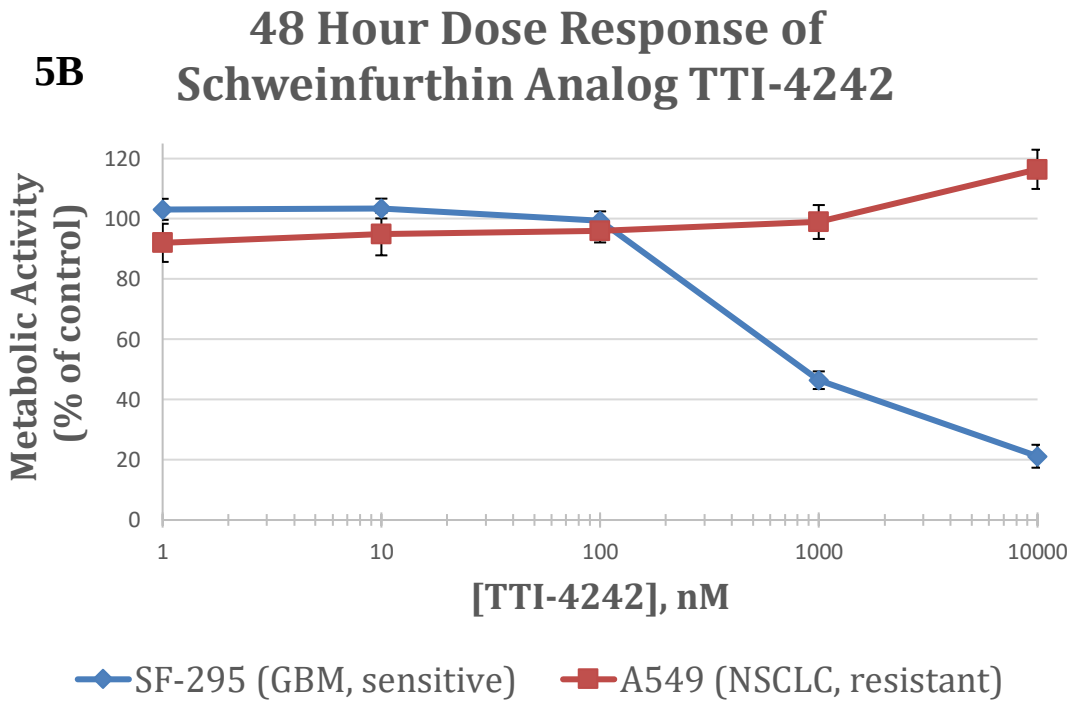
48 Hour Dose Response of Schweinfurthin Analog TTI-4242
Metabolic Activity (% of control)
120
100
80
60
40
20
0
1
10
100
1000
10000
[TTI-4242], nM
SF-295 (GBM, sensitive)
A549 (NSCLC, resistant)

Figure 5: Metabolic activity of schweinfurthin analogs reaches an EC_{50} ~ 100 nM.
A & B) SF-295 cells seeded at 4000 cells/well and A549 cells seeded 6000 cells/well were allowed to adhere to the wells of a microtiter 96-well plate for 24 hours. Cells were then treated with serial dilutions of TTI-3066 & TTI-4242 from a stock concentration at 10 mM. Logarithmic doses were tested on a series of triplicate wells for 48 hours. 44 hours into the treatment, 10 uL of 5 mg/mL MTT was spiked in cell culture media. At the end of the assay, media from each well was carefully removed before the addition of DMSO for dissolution of reduced product and readout. See results section for details about troubleshooting of TTI-4242 (a result repeated with same outcome by other researchers). Results were repeat for an N=3. Error bars represent mean ± SD.

Incubation of cells with 100 nM of schweinfurthin analog, TTI-3066, over varying intervals of time were used to explore phosphorylations of EGFR as well as shifts in apparent molecular weight of EGFR. Figure 6 shows the results of this treatment over a 24-hour time course. Detection of EGFR with an antibody at time zero for both SF-295 and A549 cells reveals at least one to three forms of EGFR in which the highest apparent molecular weight isoform(s) are believed to be fully modified, mature forms of the receptor (Fig. 6).

This is consistent with prior studies that suggest that across cancers, mature EGFR can exist in a ligand-bound or unbound state between 175-170 kDa while unmodified form(s) may also be present (Fig. 6). As the blots in Figure 6 show variable results from one experiment to another, presence of unmodified forms of EGFR may be present within both cancer types at time zero. Treatment with TTI-3066 does not affect EGFR levels in either cancer type and has no effect on apparent molecular weight of EGFR in A549 cells (Fig. 6). SF-295 cells, however, display a shift of EGFR towards lower apparent molecular weight species within 6 to 12 hours of treatment with TTI-3066 (Fig. 6). A significant loss of mature EGFR in SF-295 cells is seen within 24 hours of treatment with TTI-3066 (Fig. 6).

Phosphorylation of EGFR at Y1068 or Y1173 indicates activation of AKT or MAPK, respectively. Detection of phospho-EGFR(Y1068) and phospho-EGFR(Y1173) with different phospho-EGFR antibodies shows that there is basal levels of phosphorylation at both sites of EGFR within our cancer cells (Fig. 6). This phosphorylation is seen for the mature form of EGFR in both SF-295 and A549 cells (Fig. 6). Treatment with TTI-3066 results in a differential shift seen only in SF-295 cells where not only mature forms of EGFR are phosphorylated, but also unmodified forms of EGFR are phosphorylated (Fig. 6).

Overlay of films from EGFR and phospho-EGFR detection according to their respective antibodies reveals that this shift in phosphorylation of EGFR likely corresponds to unmodified forms of EGFR (Fig. 6). Not only does this indicate an aberrant phosphorylation of EGFR, but also an increase in the levels of EGFR phosphorylation for SF-295 cells (Fig. 6). These phosphorylation patterns of EGFR upon TTI-3066 treatment are unique and are not seen in A549 cells (Fig.6).

6A

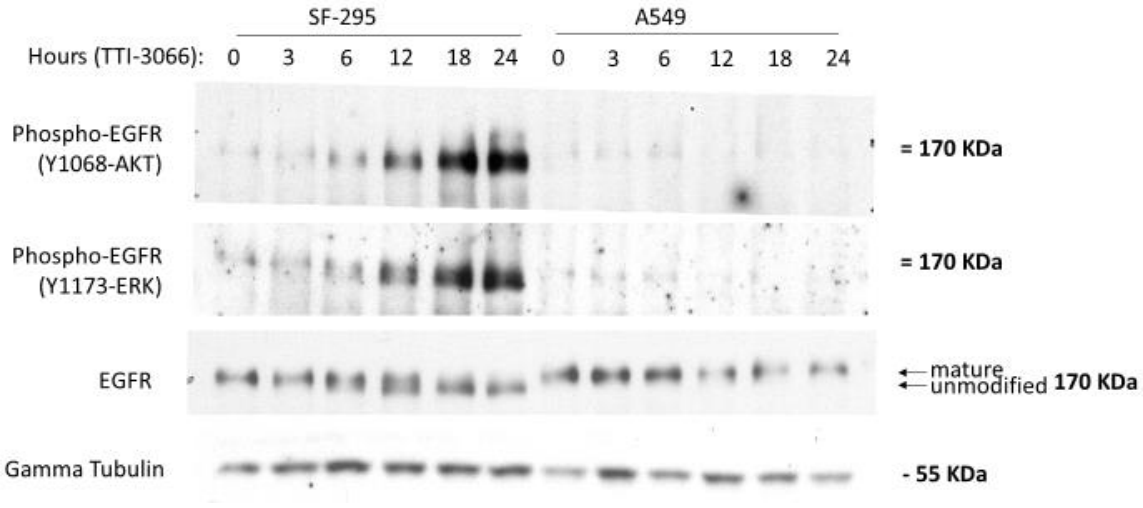
SF-295
A549
Hours (TTI-3066): 0 3 6 12 18 24 0 3 6 12 18 24
Phospho-EGFR (Y1068-AKT)
= 170 KDa
Phospho-EGFR (Y1173-ERK)
= 170 KDa
EGFR
mature
unmodified
170 KDa
Gamma Tubulin
- 55 KDa

6B

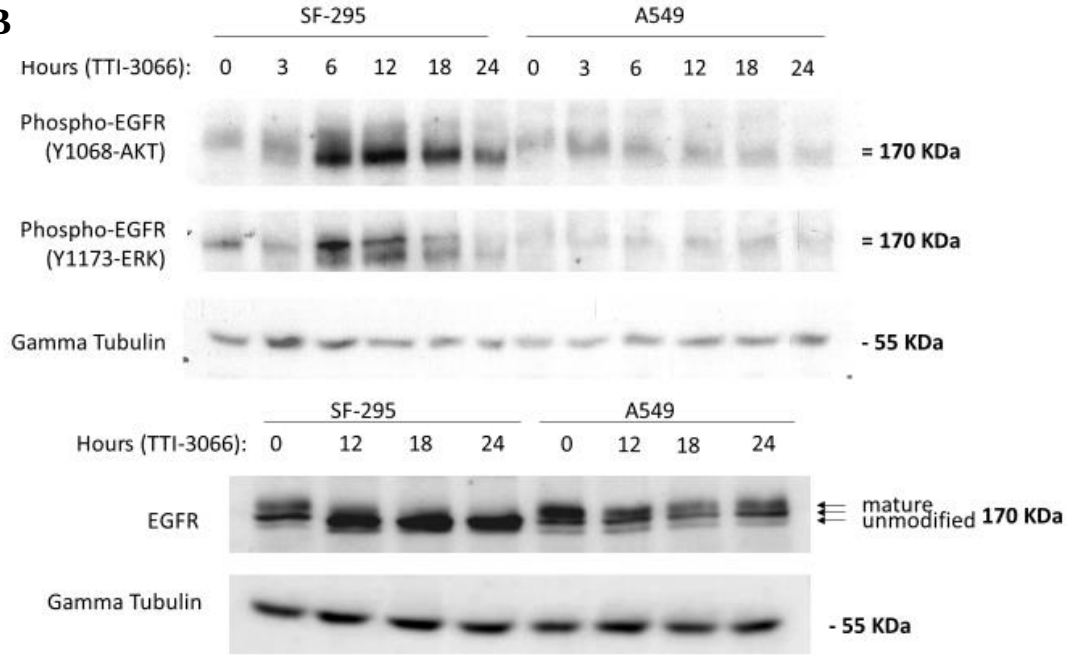
SF-295
A549
Hours (TTI-3066): 0 3 6 12 18 24 0 3 6 12 18 24
Phospho-EGFR (Y1068-AKT)
= 170 KDa
Phospho-EGFR (Y1173-ERK)
= 170 KDa
Gamma Tubulin
- 55 KDa
SF-295
A549
Hours (TTI-3066): 0 12 18 24 0 12 18 24
EGFR
mature
unmodified
170 KDa
Gamma Tubulin
- 55 KDa

6C

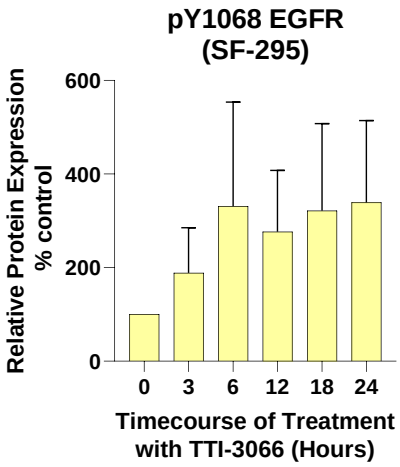
pY1068 EGFR
(SF-295)
Relative Protein Expression
% control
600
400
200
0
0 3 6 12 18 24
Timecourse of Treatment
with TTI-3066 (Hours)

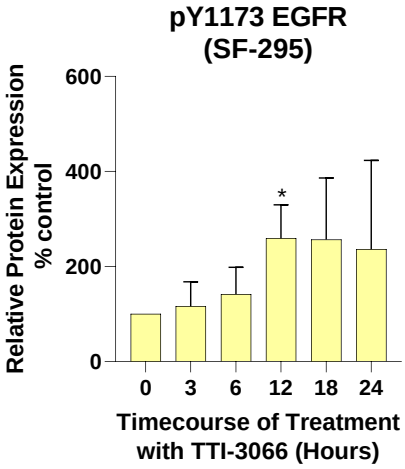
pY1173 EGFR
(SF-295)
Relative Protein Expression
% control
600
400
200
0
*
0 3 6 12 18 24
Timecourse of Treatment
with TTI-3066 (Hours)

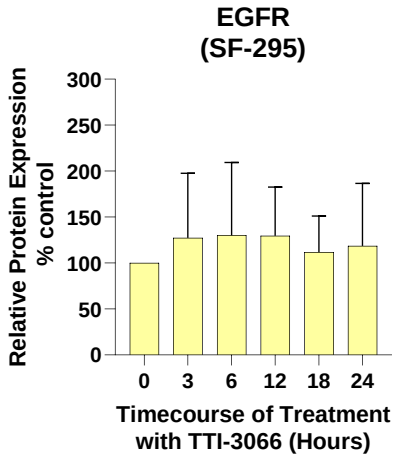
EGFR
(SF-295)
Relative Protein Expression
% control
300
250
200
150
100
50
0
0 3 6 12 18 24
Timecourse of Treatment
with TTI-3066 (Hours)

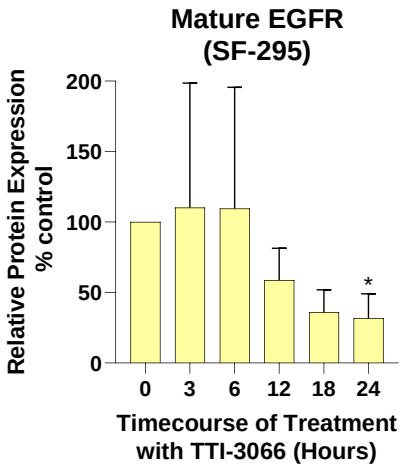
Mature EGFR
(SF-295)
Relative Protein Expression
% control
200
150
100
50
0
*
0 3 6 12 18 24
Timecourse of Treatment
with TTI-3066 (Hours)

6D

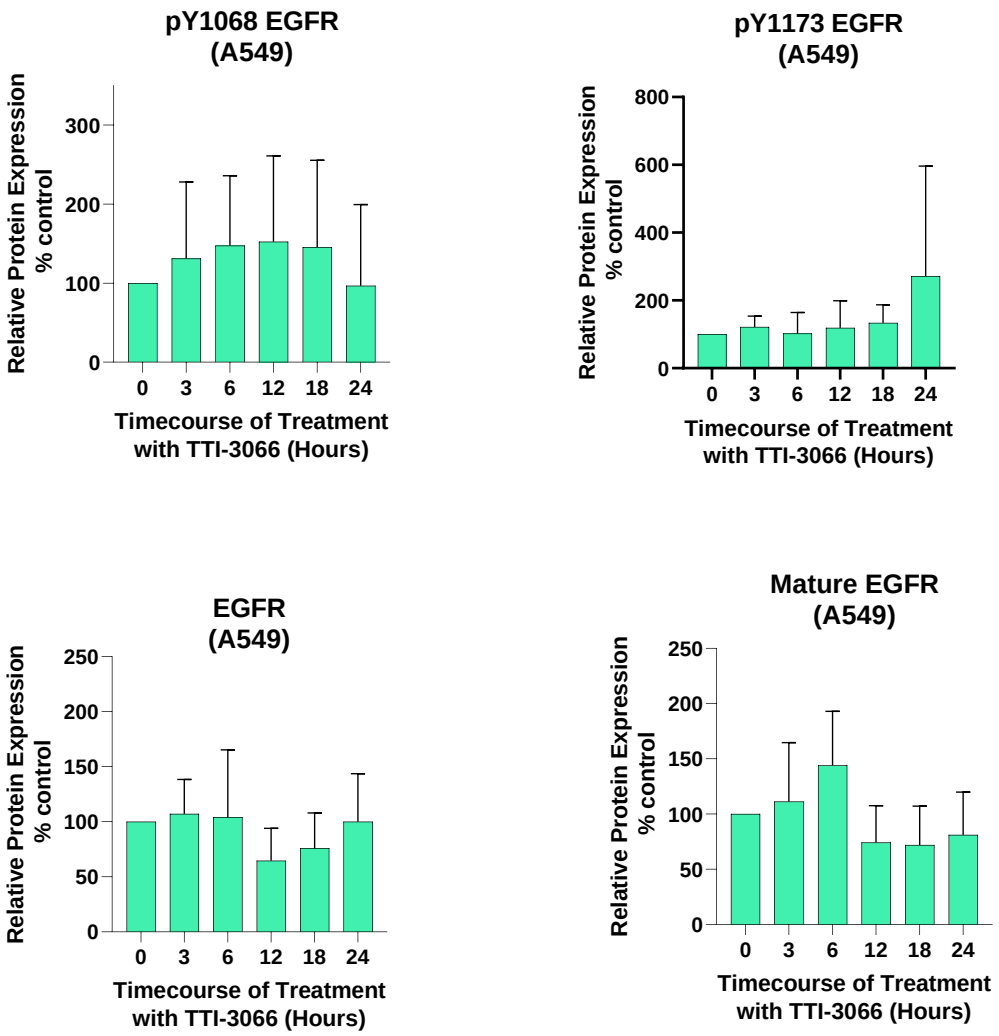

Figure 6: **TTI-3066 increases levels of phosphorylation, but lowers levels of mature EGFR in schweinfurthin sensitive SF-295 cells. A)** SF-295 cells and A549 cells were harvested after treatments with vehicle (DMSO) at time zero or schweinfurthin analog TTI-3066 at specific timepoints. Vehicle (DMSO) treated cells were harvested at the same time as 24 hour treated samples. A shift in EGFR towards lower apparent molecular weights is seen approximately 6 hours after schweinfurthin treatment in SF-295 cells as well as an increase in both phospho-EGFR(Y1068) (coupled to AKT activation) and phospho-EGFR(Y1173) (coupled to MAPK activation). Signals were captured using films; overlay of films indicate that much of this phosphorylation takes place on the lower molecular weight forms of EGFR. This was not the case for A549 cells. **B)** Representative images from antibody detection of EGFR and its phospho-sites across multiple blots. See A for description.
C & D) Quantification of phosphorylated, mature, and total levels of EGFR was performed with Image Studio and GraphPad Prism software with no statistical significance found. Phospho-EGFR(Y1068) and phospho-EGFR(Y1173) levels were normalized to EGFR.
Values represent mean (N=7) ± SD. * indicates mean values with a p-value < 0.03, as performed with one-way ANOVA (post hoc Dunnett's test).

AKT, a downstream effector of EGFR, is coupled to phosphorylation levels seen on EGFR(Y1068). Detection of AKT with an antibody reveals a top band, which is believed to be a highly phosphorylated form of AKT, and a bottom band, which is likely a non-phosphorylated form of AKT (Fig. 7). Treatment with or without TTI-3066 appears to have little to no effect on total cytoplasmic levels of AKT in both cancer types (Fig. 7). When investigating levels of phospho-AKT with a S473-specific antibody, vehicle (DMSO) treated SF-295 cells and A549 cells display basal levels of phosphorylation (Fig. 7). Overlap of films from AKT and phospho-AKT(S473) probes reveals that the phospho-signal migrates at the same position as the top band seen during AKT detection (Fig. 7). Treatment with TTI-3066 results in a significant, time-dependent decrease in levels of phospho-AKT(S473) within SF-295 cells, between 6 to 12 hours after treatment (Fig. 7). This is around the same timeframe when levels of phospho-EGFR(Y1068) accumulate on unmodified EGFR at increased levels within SF-295 cells (Fig. 7). This de-coupling and decrease in AKT phosphorylation is seen in SF-295, not A549 cells (Fig. 7).

7A

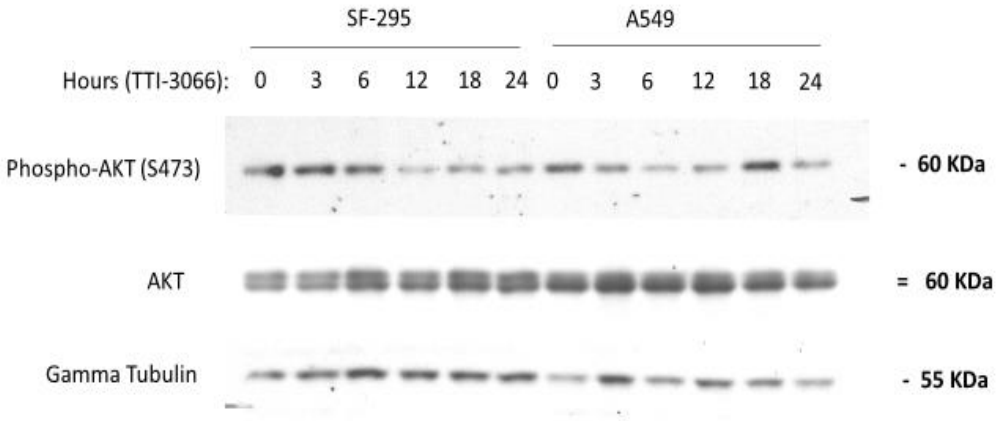
SF-295
A549
Hours (TTI-3066): 0 3 6 12 18 24 0 3 6 12 18 24
Phospho-AKT (S473)
- 60 KDa
AKT
= 60 KDa
Gamma Tubulin
- 55 KDa

7B

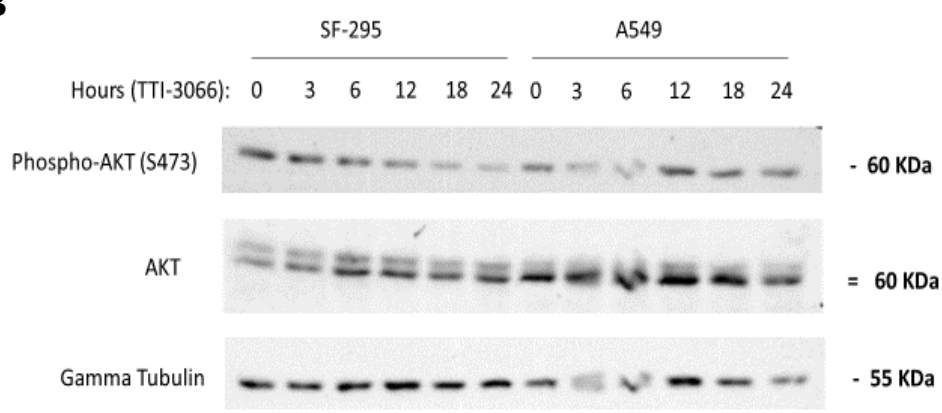
SF-295
A549
Hours (TTI-3066): 0 3 6 12 18 24 0 3 6 12 18 24
Phospho-AKT (S473)
- 60 KDa
AKT
= 60 KDa
Gamma Tubulin
- 55 KDa

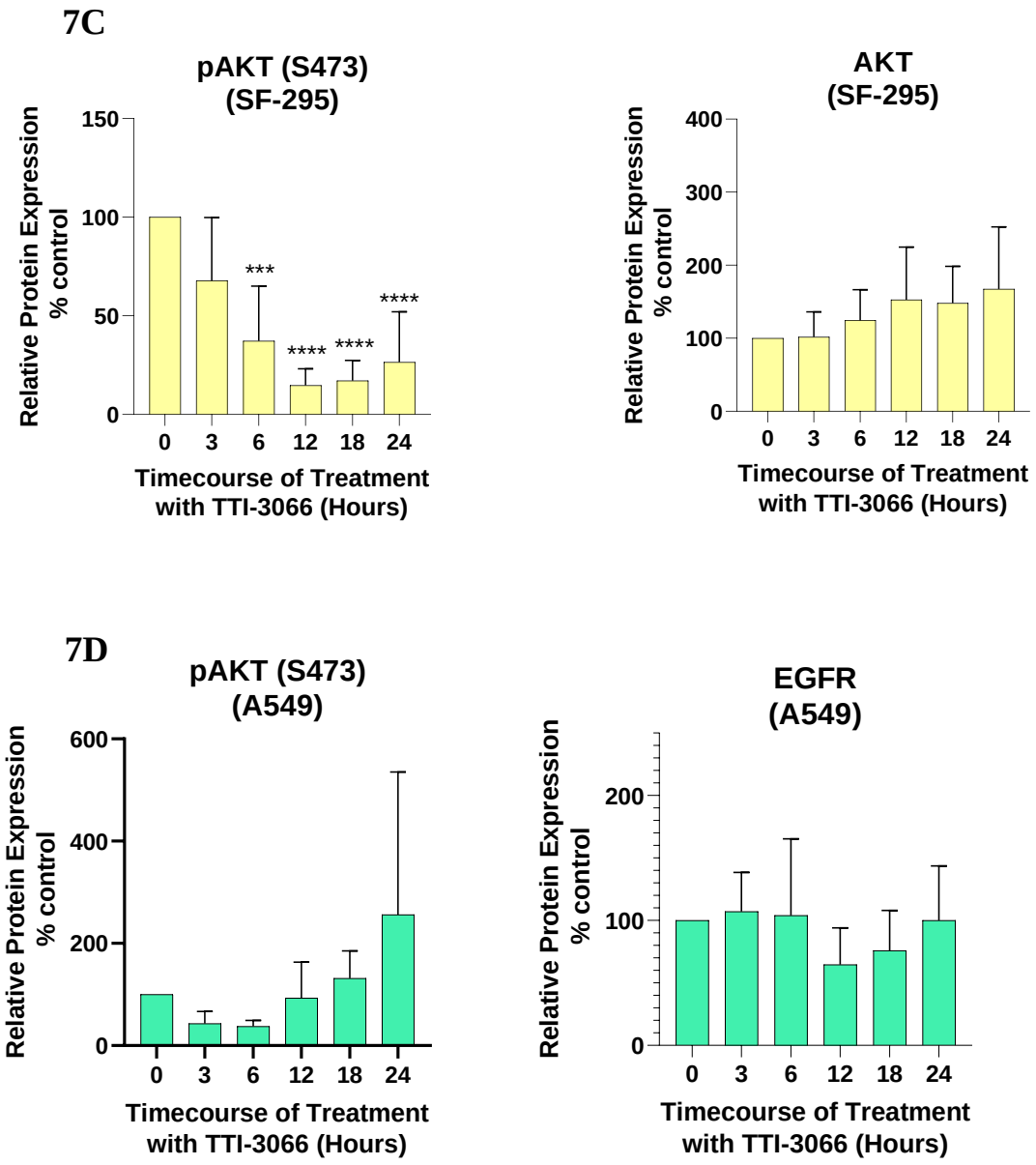

Figure 7: **TTI-3066 decreases phosphorylation of AKT at S473 in schweinfurthin sensitive SF-295 cells. A)** Shown are representative western blots in which lysates were processed as described alongside blots from Figure 4 as part of the same experiment. Treatment with TTI-3066 induces a selective decrease in phosphorylation of AKT(S473) after 6 hours of schweinfurthin treatment for SF-295 cells. This effect was not evident in A549 cells. **B)** Representative images from antibody detection of AKT and phospho-AKT across multiple blots. See A for description. **C & D)** Quantification of phosphorylated and total levels of AKT was performed with Image Studio and GraphPad Prism software. Phospho-AKT(S473) was normalized to AKT. Values represent mean (N=7) ± SD and *** and **** indicates mean values with a p-value <0.0002 or <0.0001, respectively, as performed with one-way ANOVA (post hoc Dunnett's test). Note that above the images not may reflect exact trends seen on graphs.

SF-295 cells and A549 cells were next incubated with 100 nM of another schweinfurthin analog, TTI-4242, to see if the effects of schweinfurthins on EGFR and AKT are not limited to just one analog. Figure 8 shows these results over varying time intervals in a 24-hour time course. Much of these results are very similar to that found on blots where lysates were treated with TTI-3066 (Fig.6). Detection of EGFR using an antibody reveals that at time zero, SF-295 cells and A549 cells express up to three different isoforms of EGFR, in which the two bands with highest apparent molecular weights are believed to be ligand-bound and -unbound receptors (Fig. 8). A faint lower band below these two isoforms indicates that an unmodified form of EGFR is present as well within both cancer types (Fig. 8). For SF-295 cells, treatments with TTI-4242 leads to a time-dependent shift in mature EGFR towards an intermediate, less modified form of EGFR not seen in either cancer before (Fig. 8).

This observation is apparent in Figure 8, but it is important to note that variability is present between blots across multiple experiments. Loss of mature EGFR upon treatment with TTI-4242 shows significance at the 24-hour timepoint in SF-295 cells, when compared to vehicle (DMSO)-treated SF-295 cells (Fig. 8).

Detection of phospho-EGFR(Y1068) and phospho-EGFR(Y1173) with their respective antibodies indicates that both SF-295 cells and A549 cells display basal levels of phosphorylation (Fig. 8). Treatment with TTI-4242 induces phosphorylation of EGFR at both sites, according to antibody detection in SF-295 cells (Fig. 8). Overlap of films that display signals from EGFR and phosphorylated EGFR, however, reveals that phosphorylation occurs on the unmodified form(s) of EGFR (Fig. 8). While increases in levels of unmodified EGFR and phosphorylation of EGFR is evident within SF-295 cells, TTI-4242 treatment does not affect EGFR in these ways in A549 cells (Fig. 8). A trend of phosphorylation induction in SF-295 cells is apparent between 6 to 12 hours of treatment with TTI-4242 (Fig.8).

8A

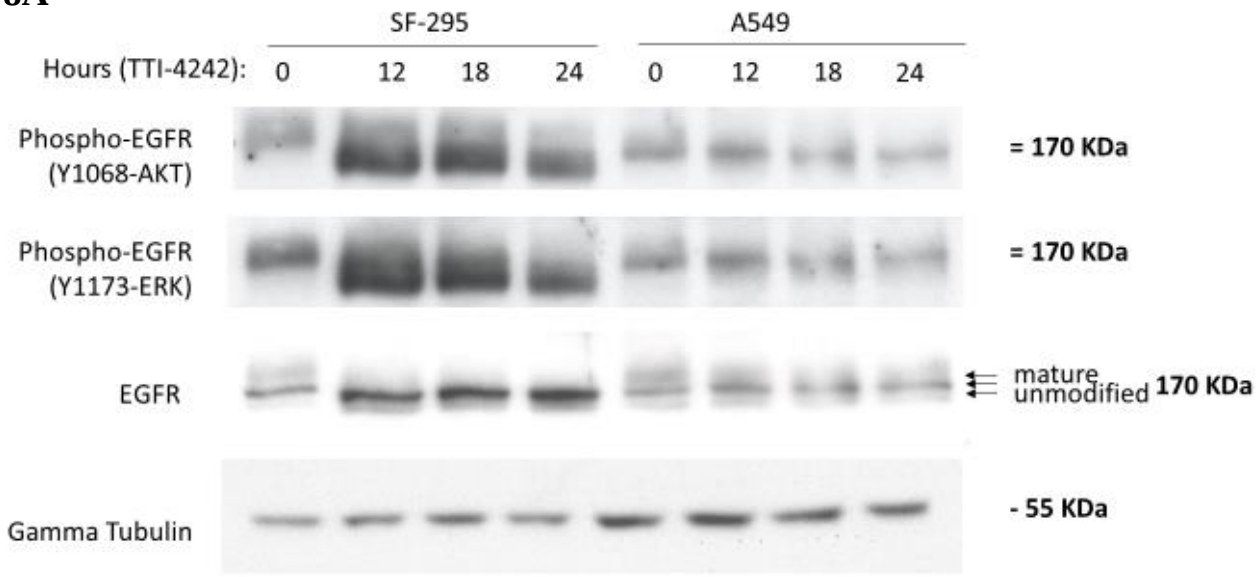
SF-295
A549
Hours (TTI-4242):
0
12
18
24
0
12
18
24
Phospho-EGFR (Y1068-AKT)
= 170 KDa
Phospho-EGFR (Y1173-ERK)
= 170 KDa
EGFR
mature
unmodified
170 KDa
Gamma Tubulin
- 55 KDa

8B

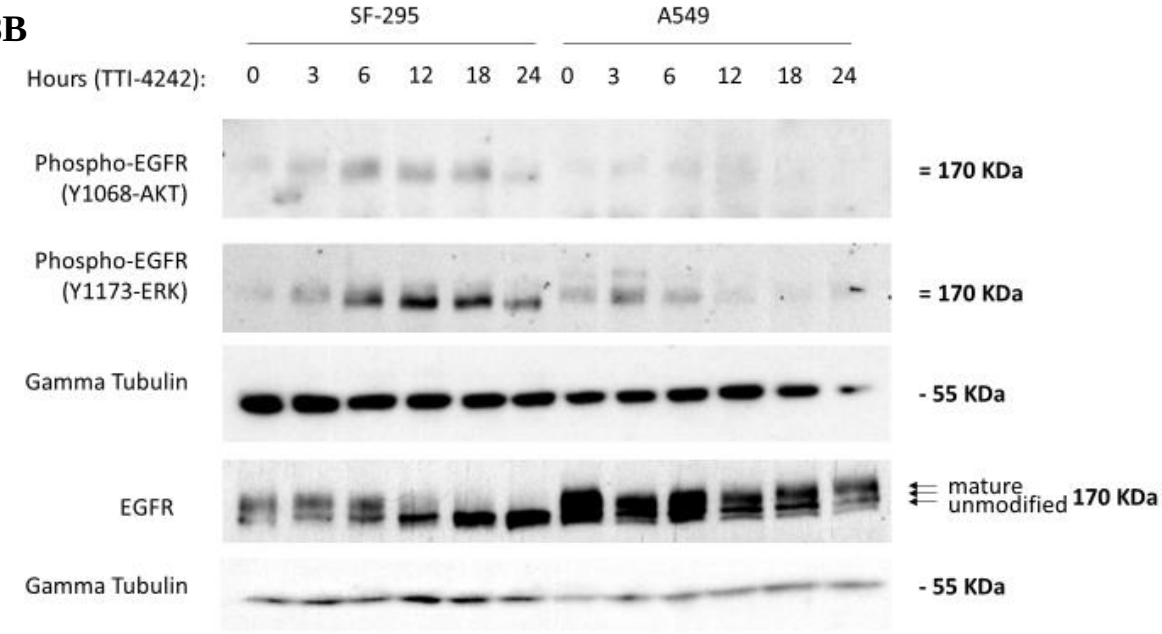
SF-295
A549
Hours (TTI-4242):
0
3
6
12
18
24
0
3
6
12
18
24
Phospho-EGFR (Y1068-AKT)
= 170 KDa
Phospho-EGFR (Y1173-ERK)
= 170 KDa
Gamma Tubulin
- 55 KDa
EGFR
mature
unmodified
170 KDa
Gamma Tubulin
- 55 KDa

8C

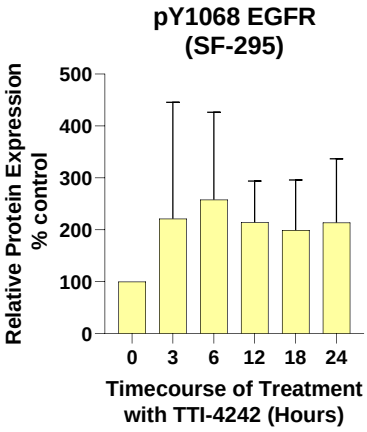
pY1068 EGFR
(SF-295)
Relative Protein Expression
% control
500
400
300
200
100
0
0 3 6 12 18 24
Timecourse of Treatment
with TTI-4242 (Hours)

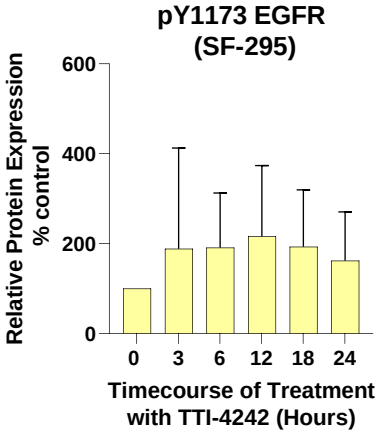
pY1173 EGFR
(SF-295)
Relative Protein Expression
% control
600
400
200
0
0 3 6 12 18 24
Timecourse of Treatment
with TTI-4242 (Hours)

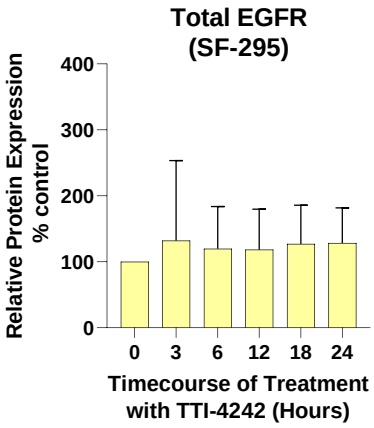
Total EGFR
(SF-295)
Relative Protein Expression
% control
400
300
200
100
0
0 3 6 12 18 24
Timecourse of Treatment
with TTI-4242 (Hours)

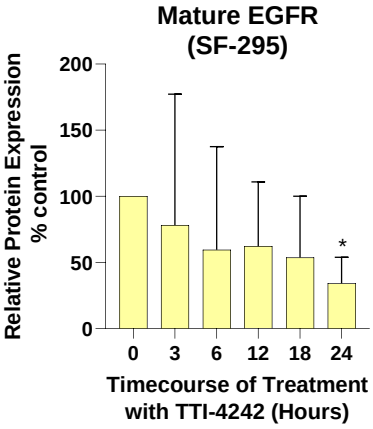
Mature EGFR
(SF-295)
Relative Protein Expression
% control
200
150
100
50
0
*
0 3 6 12 18 24
Timecourse of Treatment
with TTI-4242 (Hours)

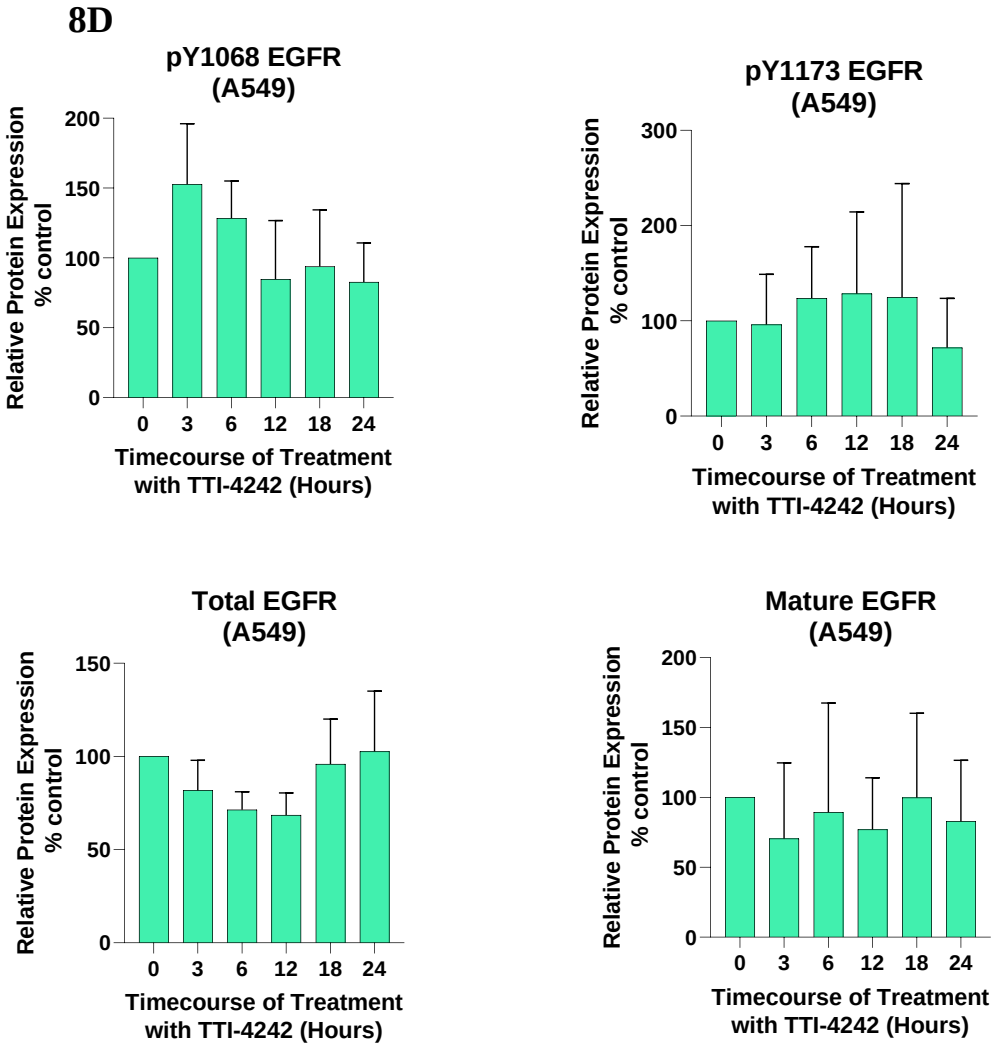

Figure 8: TTI-4242, another schweinfurthin analog, reduces phosphorylations and mature EGFR levels within schweinfurthin sensitive SF-295 cells. A) SF-295 cells and A549 cells were treated over a 24-hour time course with TTI-4242 or were incubated with vehicle (DMSO) under continuous exposure. A shift in the apparent molecular weight of EGFR towards unmodified forms of the receptor, and increased phosphorylations of EGFR at Y1068 and Y1173, appears within SF-295 cells and not A549 cells. Signals were captured using films and overlap of films indicates that most of the phosphorylation seen on EGFR is found on lower apparent molecular weight, unmodified forms of EGFR. **B)** Representative images from antibody detection of EGFR and its phospho-sites across multiple blots. See A for description. **C & D)** Analyses were performed with Image Studio and GraphPad Prism software with no statistical significance found. Phospho-EGFR(Y1068) and phospho-EGFR(Y1173) levels were normalized to EGFR. Values on graph represent mean (N=7) ± SD.

Transduction of phospho-signals from EGFR was inferred as before from western blot analyses of AKT in SF-295 cells and A549 cells upon treatment with TTI-4242. Incubation of an AKT antibody for these blots reveals that lysates harvested from SF-295 cells and A549 cells treated with TTI-4242 display no changes in overall, cytoplasmic levels of AKT (Fig. 9). Although variation exists between AKT and phospho-AKT signals between different experiments, we suspect that one or two bands of AKT exists, one phosphorylated form of AKT that migrates as a higher band and, on occasion, a second, non-phosphorylated form of AKT that migrates as a lower band on SDS-PAGE (Fig. 9). We infer this conclusion based on overlap of films detected with antibodies against AKT and phospho-AKT(S473) which shows that phospho-AKT(S473) signal is at the same position as the top band of AKT (Fig. 9). Detection of phospho-AKT(S473) with an antibody, however, indicates that treatment with TTI-4242 inhibits phosphorylation of AKT at this site significantly within SF-295 cells (Fig. 9). This effect takes place within 6 to 12 hours, but lasts till the end of the time course of treatment (Fig. 9). In contrast, A549 cells seem to be resistant to effects of TTI-4242 on phospho-AKT since AKT phosphorylation at S473 increases at 12 to 18 hours into TTI-4242 treatment (Fig. 9). This increase is transient as phospho-AKT(S473) levels return close to that seen in vehicle (DMSO)-treated A549 cells at the end of time course (Fig. 9).

9A

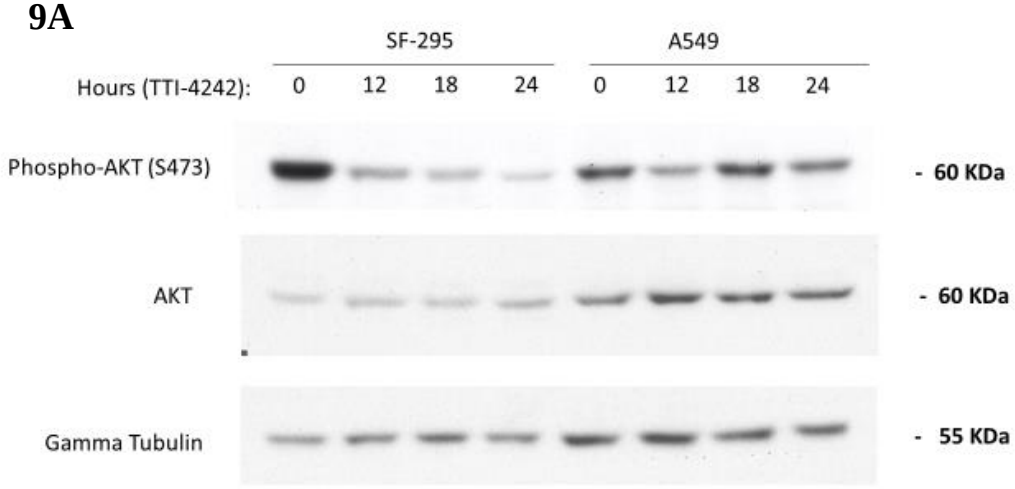
SF-295
A549
Hours (TTI-4242):
0
12
18
24
0
12
18
24
Phospho-AKT (S473)
- 60 KDa
AKT
- 60 KDa
Gamma Tubulin
- 55 KDa

9B

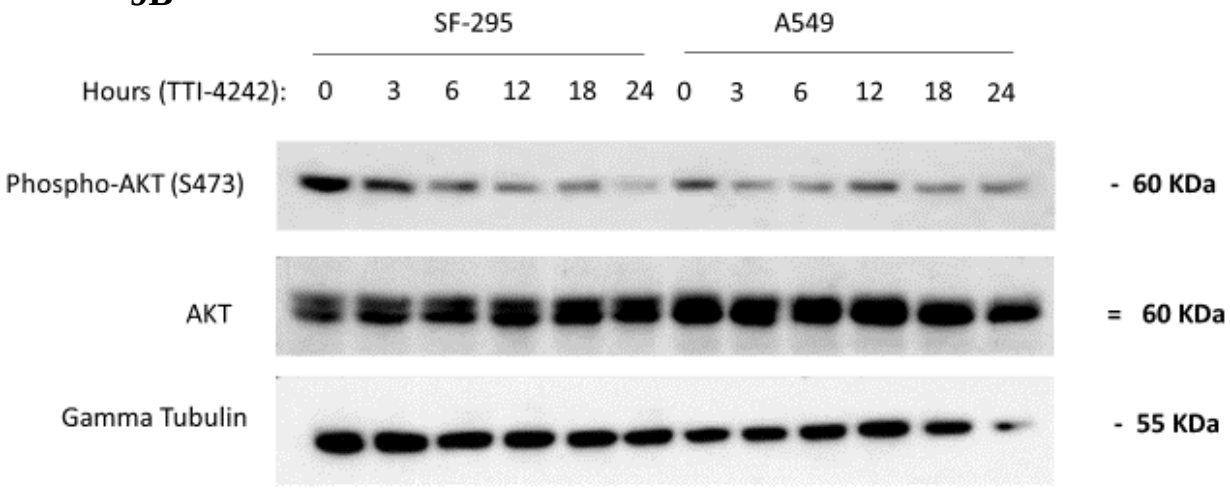
SF-295
A549
Hours (TTI-4242):
0
3
6
12
18
24
0
3
6
12
18
24
Phospho-AKT (S473)
- 60 KDa
AKT
= 60 KDa
Gamma Tubulin
- 55 KDa

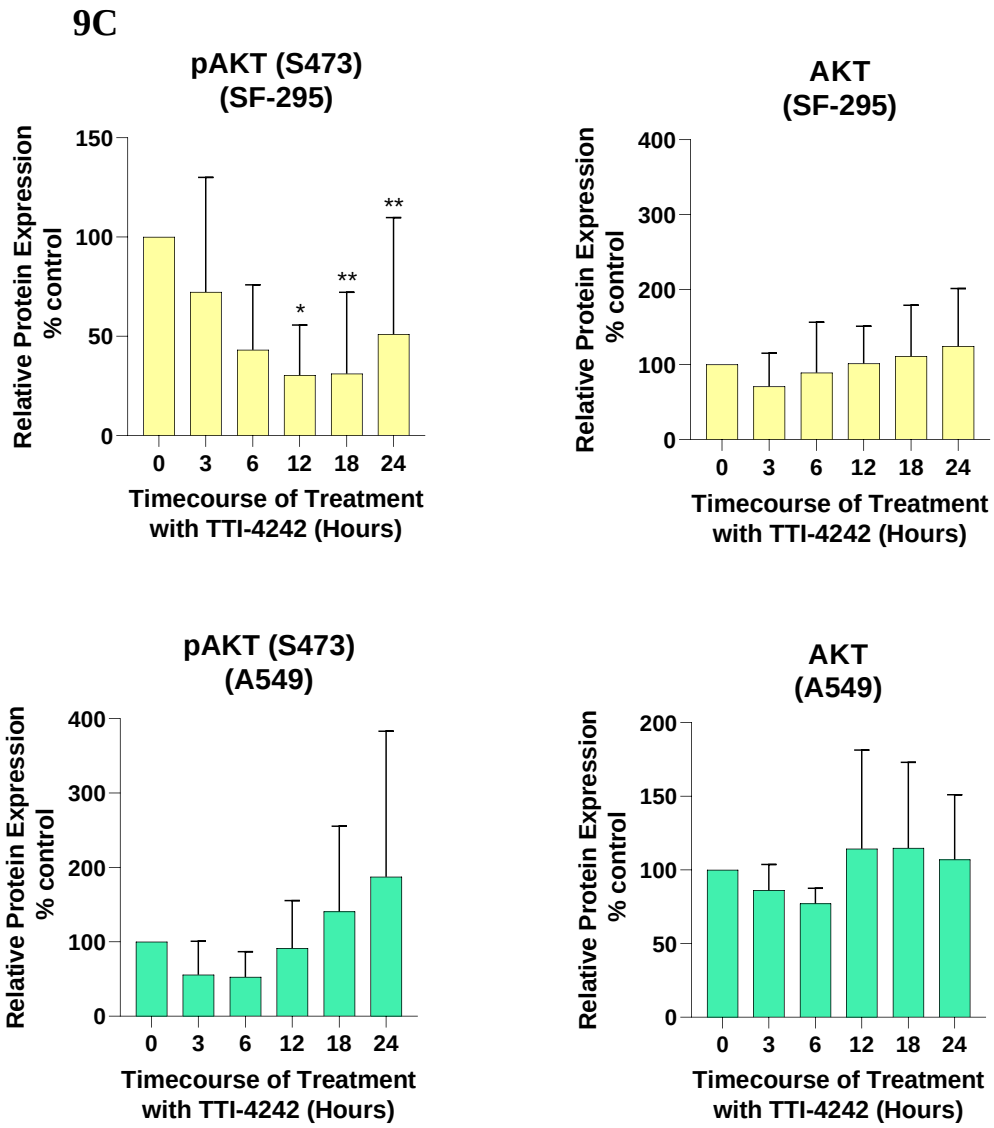

Figure 9: **TTI-4242 leads to a time-dependent decrease in phospho-AKT(S473) levels within schweinfurthin sensitive SF-295 cells. A)** Representative blots above are from the same experiments performed in Figure 3 and all lysates were harvested as described in Figure 3. Phospho-AKT(S473) levels decrease within SF-295 cells upon treatment with TTI-4242. This effect was not seen in A549 cells. **B)** Representative images from antibody detection of AKT and phospho-AKT across multiple blots. See A for description. **C)** Quantification of phospho-AKT and AKT was performed with Image Studio and GraphPad Prism software. Phospho-AKT(S473) was normalized to AKT. Values represent mean (N=7) ± SD.
* and ** indicates mean values with a p-value <0.03 or p-value <0.002, respectively, as performed with one-way ANOVA (post hoc Dunnett's test). Note that above images not may reflect the exact trends seen on graphs.

MAPK, another downstream effector of EGFR, is coupled to phosphorylation levels seen in EGFR(Y1173). Detection of MAPK with an antibody reveals two bands, both of which are believed to be different forms of MAPK (ERK1 and ERK2) (Fig. 10). Treatment with schweinfurthin analog TTI-3066 over a period of 12 to 24 hours reveals a fluctuating pattern of MAPK expression in SF-295 cells and A549 cells (Fig. 10). Detection of MAPK using an antibody indicates increased levels of the protein compared to vehicle (DMSO) treated cells within 12 hours of TTI-3066 treatment (Fig. 10). This increase is reversed after 18 hours of TTI-3066 treatment in which levels return back to baseline seen in vehicle (DMSO) treated SF-295 cells (Fig. 10). 24 hours into TTI-3066 treatment, levels of MAPK spike, about four-fold more than that seen in vehicle (DMSO) treated SF-295 cells (Fig. 10). Phosphorylation of MAPK at Thr202/Tyr204 was investigated as a readout for Ras induced MAPK activation. Although detection of phospho-ERK1/2 shows variable results across blots, normalization of the bands reveals a time dependent decrease in phospho-ERK1/2 levels (Fig. 10). Investigations into the effects of TTI-3066 on MAPK levels in A549 cells show a response to schweinfurthin that is variable across timepoints of schweinfurthin treatment as well (Fig. 10). Detection of MAPK with an antibody indicates an increase in MAPK levels after 12 hours of TTI-3066 treatment (Fig. 10). This increase appears to minimally decrease after 18 hours of TTI-3066 treatment only to decrease further at 24 hours to levels that are near or lower than baseline (Fig. 10). Phospho-ERK1/2 levels either mirrored that of MAPK or stay relatively unchanged compared to vehicle (DMSO) treated control cells throughout treatment (Fig. 10).

10A

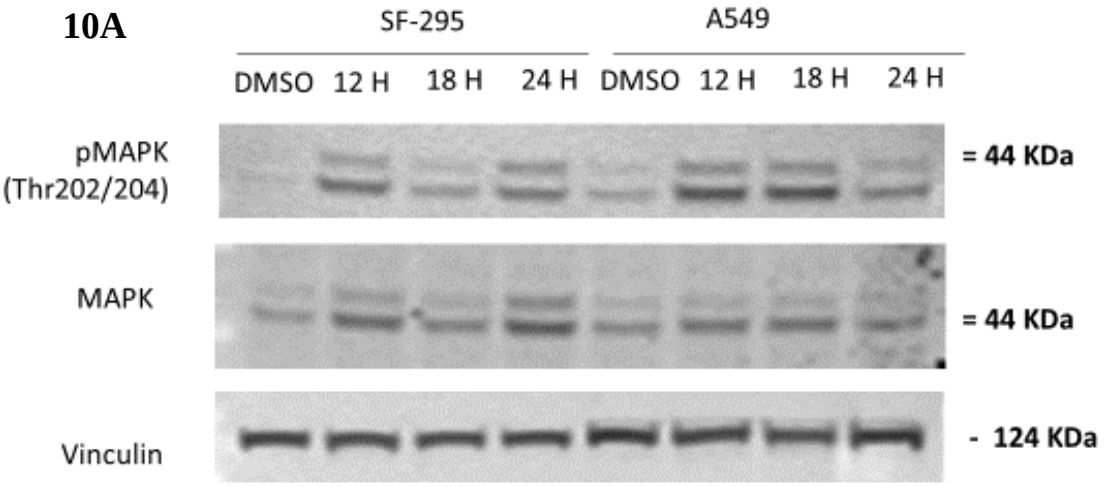
SF-295
A549
DMSO 12 H 18 H 24 H DMSO 12 H 18 H 24 H
pMAPK (Thr202/204)
= 44 KDa
MAPK
= 44 KDa
Vinculin
- 124 KDa

10B

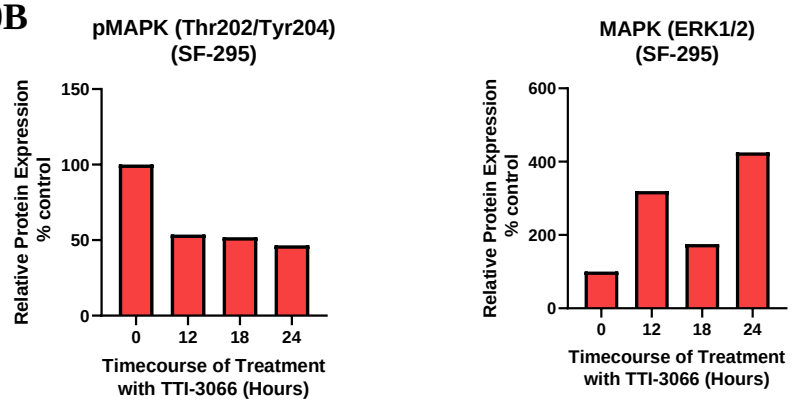
pMAPK (Thr202/Tyr204) (SF-295)
Relative Protein Expression % control
150
100
50
0
0 12 18 24
Timecourse of Treatment with TTI-3066 (Hours)
MAPK (ERK1/2) (SF-295)
Relative Protein Expression % control
600
400
200
0
0 12 18 24
Timecourse of Treatment with TTI-3066 (Hours)

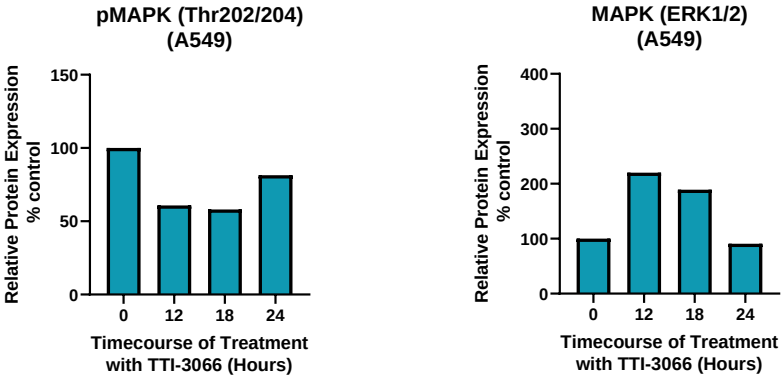
pMAPK (Thr202/204) (A549)
Relative Protein Expression % control
150
100
50
0
0 12 18 24
Timecourse of Treatment with TTI-3066 (Hours)
MAPK (ERK1/2) (A549)
Relative Protein Expression % control
400
300
200
100
0
0 12 18 24
Timecourse of Treatment with TTI-3066 (Hours)

Figure 10: TTI-3066 treatment induces fluctuations and a reducing trend, but no significant decrease in Ras-mediated phospho-MAPK levels in SF-295 cells.
A) Representative blots above from SF-295 and A549 cell lysates represents fluctuations in MAPK levels upon treatment with 100 nM TTI-3066 as detected by a MAPK antibody. **B)** Quantification of phospho-MAPK (Thr202/Tyr204) was performed with Image Studio. Phospho-MAPK (Thr202/Tyr204) was normalized to MAPK. Values represent mean N=2.

Schweinfurthins have been implicated to deplete glycans from EGFR as well as impair signal transduction between EGFR and AKT [7]. Study of various treatments that disrupt glycosylation and either increase or decrease activation of AKT and MAPK were tested on SF-295 cells as a set of controls for schweinfurthin treated cells. PNGase F, an enzyme that cleaves N-linked glycan residues, was added to a small fraction of whole cell lysate collected during harvest for qualitative assessment and was not quantified with the rest of the samples (see Materials and Methods). Two bands appear of lower apparent molecular weight than fully modified, mature EGFR (Fig. 11). These lower molecular weight bands have an apparent molecular weight lower than 170 kDa, but higher than 130 kDa. Treatment of SF-295 cells with tunicamycin reveals a downshift in apparent molecular weight of EGFR similar to that of PNGase F with two lower apparent molecular weight bands in addition to fully modified EGFR. Both treatments can decrease the apparent molecular weight of EGFR to the same extent as that seen when SF-295 cells are treated for 24 hours with TTI-3066. Quantification of bands from SF-295 cells treated with tunicamycin or TTI-3066 shows a reduced level of EGFR expression compared to vehicle (DMSO) treated cells (Fig. 11).

SF-295 cells were pretreated with an acute, 10 ng/mL concentration of EGF after serum starvation as a way to test whether TTI-3066 disrupts transmission of signals from EGFR to AKT (Fig. 11). Though serum starvation followed by EGF treatment impacts EGFR levels, addition of TTI-3066 to this initial conditioning of SF-295 cells creates a noticeable downshift in the apparent molecular weight of EGFR. This downshift is similar to that seen in unconditioned SF-295 cells treated with TTI-3066. Potential activation of AKT and MAPK were analyzed through detection of phospho-Y1068 EGFR and phospho-Y1173 EGFR expression.

Overlay of films from EGFR and phospho-EGFR probes indicates that mostly, if not all, of the phospho-EGFR species present vehicle (DMSO) treated SF-295 cells are from mature EGFR species. However, this phosphorylation shifted to more unmodified forms of the receptor under certain treatments (Fig. 11).

Detection of phospho-EGFR(Y1068) levels with an antibody indicates that SF-295 cells treated with EGF displayed high levels of phosphorylation while cells treated with tunicamycin or TTI-3066 showed an increase in phosphorylation for mostly unmodified forms of EGFR (Fig. 11). SF-295 cells treated with EGF/TTI-3066 display substantial decreases in phospho-EGFR(Y1068) expression compared to EGF treated SF-295 cells, with levels comparable/slightly higher than vehicle (DMSO) treated SF-295 cells. Much of this phosphorylation is evident within unmodified EGFR species. Detection of phospho-EGFR(Y1173) levels with an antibody mirrors trends seen with phospho-EGFR(Y1068) levels, with the emphasis that both EGF stimulated and unstimulated SF-295 cells treated with TTI-3066 show an induction in phosphorylation for mostly unmodified forms of EGFR. SF-295 cells treated with perifosine, an AKT inhibitor, also showed substantial decreases in phospho-EGFR(Y1068) levels, but for the fully modified form of the receptor. Phospho-EGFR(Y1173) expression in SF-295 cells treated with perifosine is also reduced, consistent with reports that this inhibitor also indirectly lowers activation of MAPK (Fig. 11).

11A

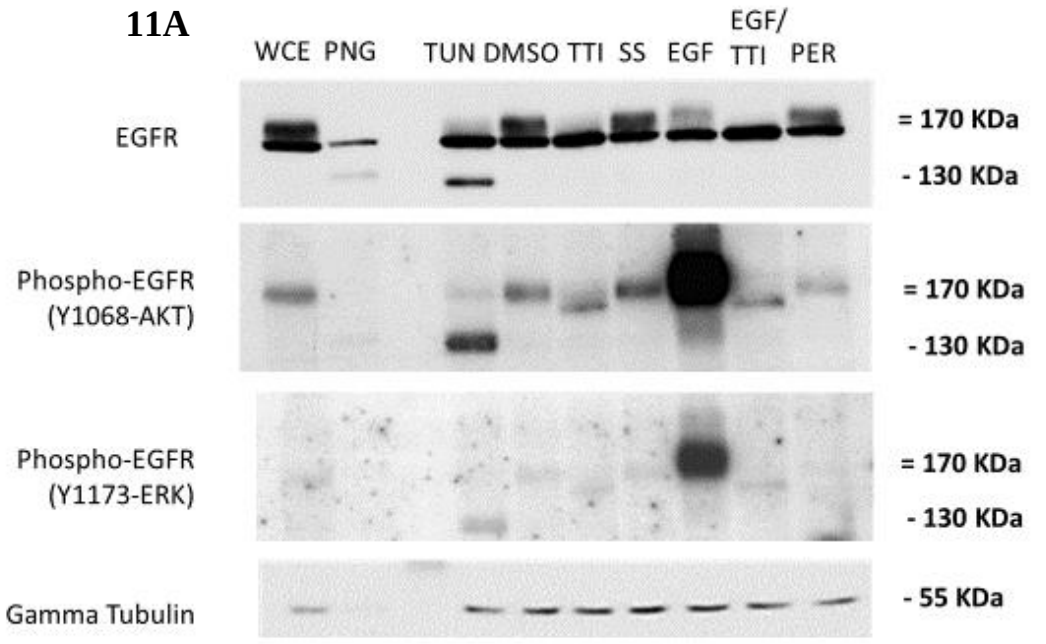
WCE PNG
TUN DMSO TTI SS EGF
EGF/ TTI
PER
EGFR
= 170 KDa
- 130 KDa
Phospho-EGFR (Y1068-AKT)
= 170 KDa
- 130 KDa
Phospho-EGFR (Y1173-ERK)
= 170 KDa
- 130 KDa
Gamma Tubulin
- 55 KDa

11B

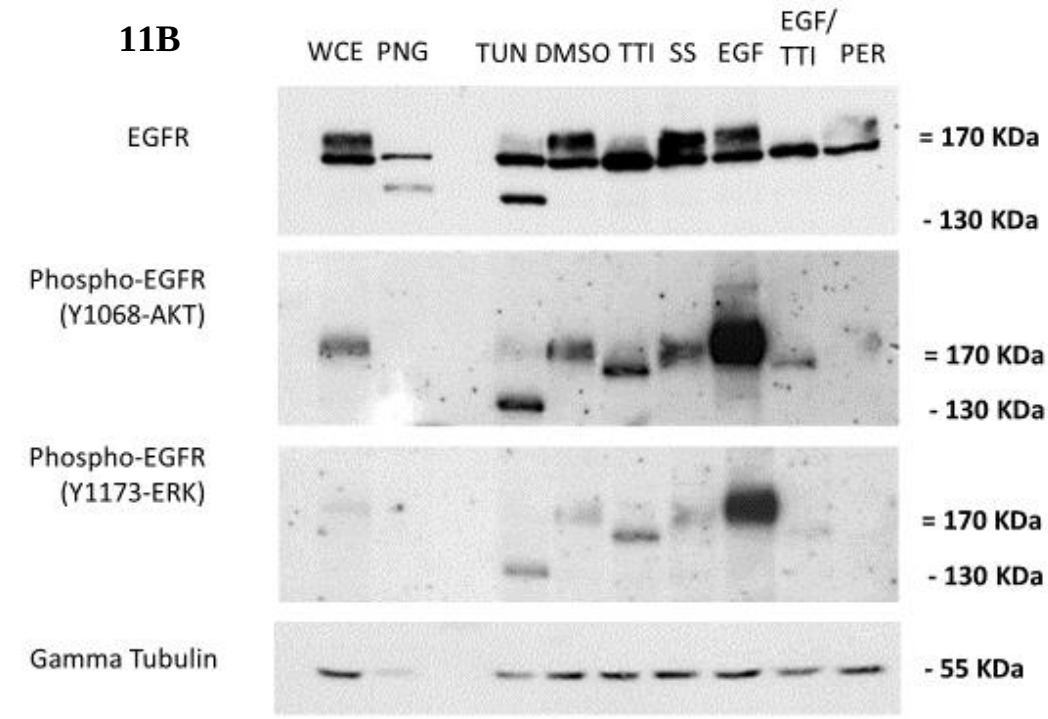
WCE PNG
TUN DMSO TTI SS EGF
EGF/ TTI
PER
EGFR
= 170 KDa
- 130 KDa
Phospho-EGFR (Y1068-AKT)
= 170 KDa
- 130 KDa
Phospho-EGFR (Y1173-ERK)
= 170 KDa
- 130 KDa
Gamma Tubulin
- 55 KDa

11C

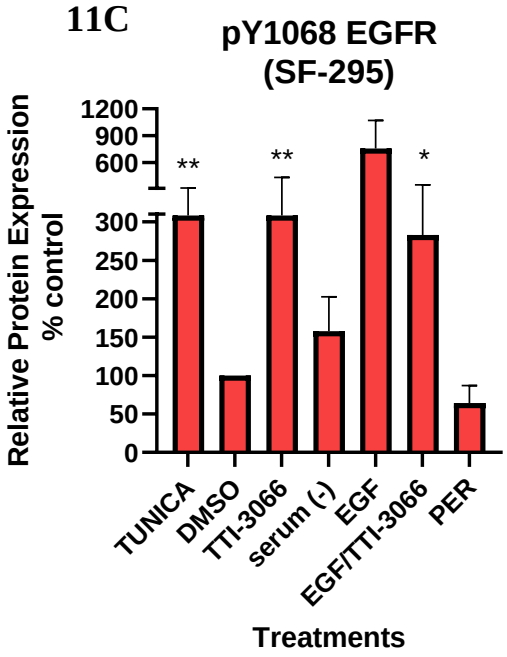
pY1068 EGFR
(SF-295)
Relative Protein Expression
% control
1200
900
600
300
250
200
150
100
50
0
**
**
*
TUNICA
DMSO
TTI-3066
serum (-)
EGF
EGF/TTI-3066
PER
Treatments

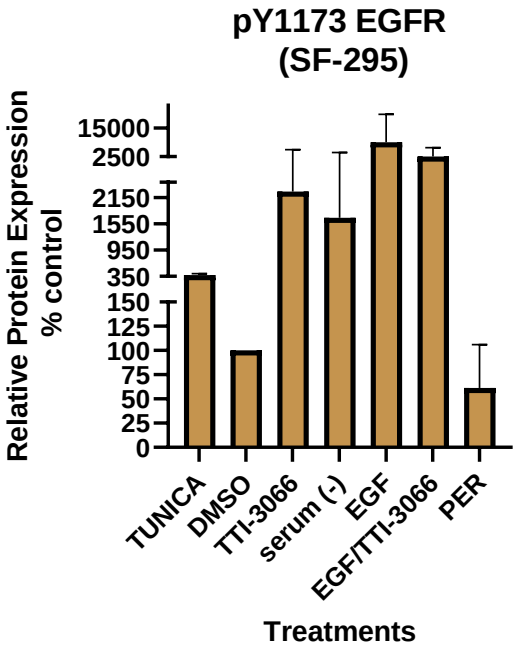
pY1173 EGFR
(SF-295)
Relative Protein Expression
% control
15000
2500
2150
1550
950
350
150
125
100
75
50
25
0
TUNICA
DMSO
TTI-3066
serum (-)
EGF
EGF/TTI-3066
PER
Treatments

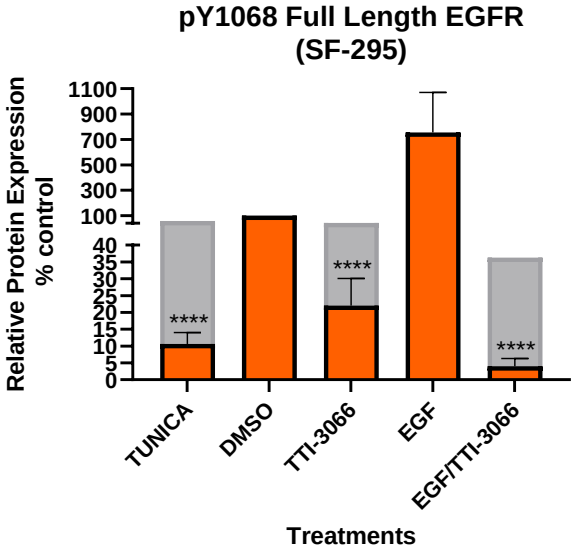
pY1068 Full Length EGFR
(SF-295)
Relative Protein Expression
% control
1100
900
700
500
300
100
40
35
30
25
20
15
10
5
0
****
****
****
TUNICA
DMSO
TTI-3066
EGF
EGF/TTI-3066
Treatments

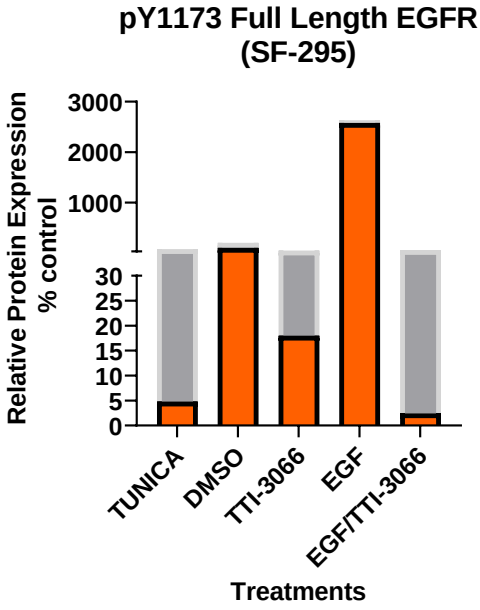
pY1173 Full Length EGFR
(SF-295)
Relative Protein Expression
% control
3000
2000
1000
30
25
20
15
10
5
0
TUNICA
DMSO
TTI-3066
EGF
EGF/TTI-3066
Treatments

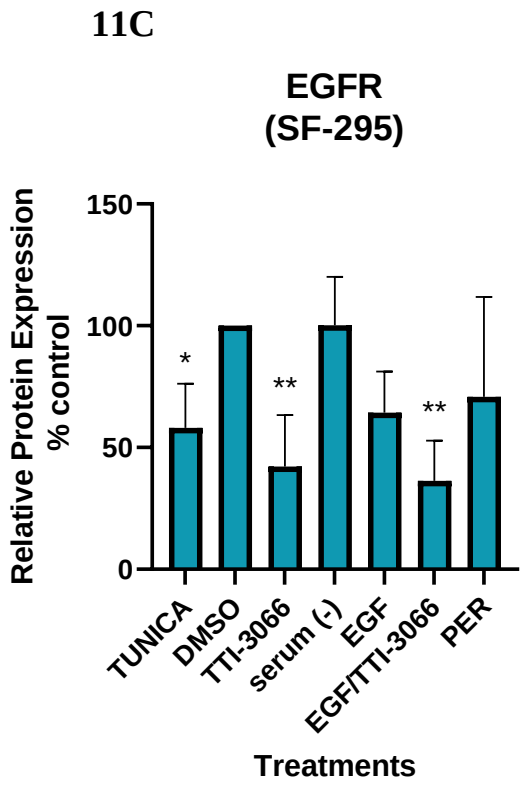

Figure 11: TTI-3066 treatment in SF-295 cells mediates de-glycosylation of EGFR & can potentially reduce levels of EGF-induced phospho-EGFR to a greater extent
A) Various treatments for SF-295 cells. Right portion of the blot demonstrates loss of glycosylation in EGFR seen with PNGase F treatment (PNG) and 10 μM Tunicamycin (TUN). Left protein of the blot was performed in an attempt to address whether schweinfurthin dysregulates downstream signaling of EGFR at the level of increasing the phosphorylated of partially mature EGFR species. Cells were serum starved for 4 hours instead of 3 hours, resulting in a higher intracellular concentration of EGF than 10 ng/mL that likely act through mass action to internalize and re-route EGFR species towards a degradative route. EGF stimulation lasted for 10 minutes. Perifosine served as a positive control for later analyses as an AKT inhibitor. All controls were compared to the combination of EGF stimulation followed by 100 nM TTI-3066 treatment for 24 hours (EGF/TTI) and 100 nM TTI-3066 treatment alone (TTI). WCE represents whole cell extract that used in PNGase treatments. **B)** Representative images for antibody detection of EGFR, phospho-EGFR(Y1068), phospho-EGFR(Y1173), and γ-tubulin. See A for description. **C)** Quantification of blots were performed with Image Studio and GraphPad Prism software. Phospho-EGFR (Y1068) and phospho-EGFR (Y1173) were normalized to EGFR. Full length phospho-EGFR(Y1068) and full length phospho-EGFR(Y1173) normalized to EGFR. Values represent mean (N=3) ± SD. *, **, and **** indicates mean values with a p-value < 0.03, p-value <0.002, or p-value <0.0001 respectively, as performed with one-way ANOVA (post hoc Dunnett's test).

Phosphorylation levels of AKT and MAPK were also analyzed in conjunction to analyses on EGFR expression. Total levels of AKT were probed to see if tunicamycin, EGF, TTI-3066, EGF/TTI-3066, or perifosine would alter its expression (Fig. 12). For the most part, vehicle (DMSO) treated SF-295 cells displayed two bands for AKT. Compared to this control, EGF and tunicamycin treatments seemed to display a subtle increase or decrease in AKT expression for one biological replicate. Normalization and quantification of AKT expression, however, indicates that tunicamycin, EGF, TTI-3066, EGF/TTI-3066, and perifosine had no effect on total levels of AKT. Detection of phospho-AKT with an antibody directed against serine 473 reveals that EGF did not increase phospho-AKT(S473) levels as expected within SF-295 cells, with similar phosphorylation levels to that of vehicle (DMSO) treated control cells. Similarly, tunicamycin treatments also impaired phospho-AKT levels while both TTI-3066 and EGF/TTI-3066 treatments mirrored this magnitude of decreased phosphorylation in AKT (Fig. 12).

In the case of perifosine, impairment of AKT phosphorylation was greater than that seen with schweinfurthin treatment, but EGF/TTI-3066 treatment surpassed perifosine in its inhibitory effects on phospho-AKT expression. Investigations of MAPK levels in SF-295 cells undergoing treatments indicate a substantial increase in MAPK expression under EGF treatment also five-fold of that seen in vehicle (DMSO) treated SF-295 cells (Fig. 13). Treatments with tunicamycin, TTI-3066, and EGF/TTI-3066, however, did not affect MAPK levels in SF-295 cells. Treatments with these four compounds did not alter phospho-ERK(1/2) levels significantly from that seen in vehicle (DMSO) treated SF-295 cells (Fig. 13).

12A

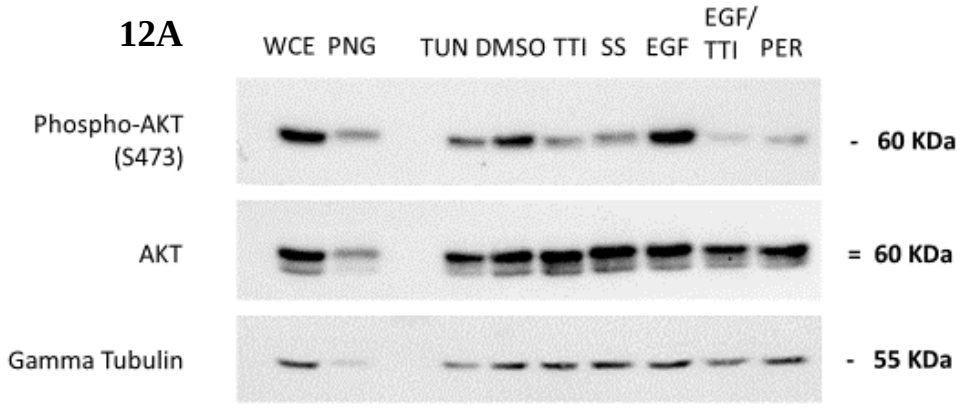
WCE PNG
TUN DMSO TTI SS EGF
EGF/ TTI
PER
Phospho-AKT (S473)
- 60 KDa
AKT
= 60 KDa
Gamma Tubulin
- 55 KDa

12B

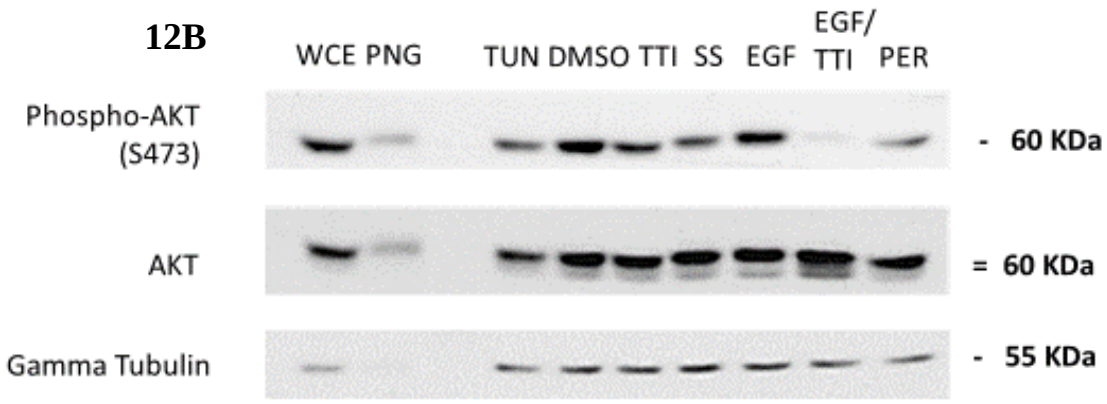
WCE PNG
TUN DMSO TTI SS EGF
EGF/ TTI
PER
Phospho-AKT (S473)
- 60 KDa
AKT
= 60 KDa
Gamma Tubulin
- 55 KDa

12C

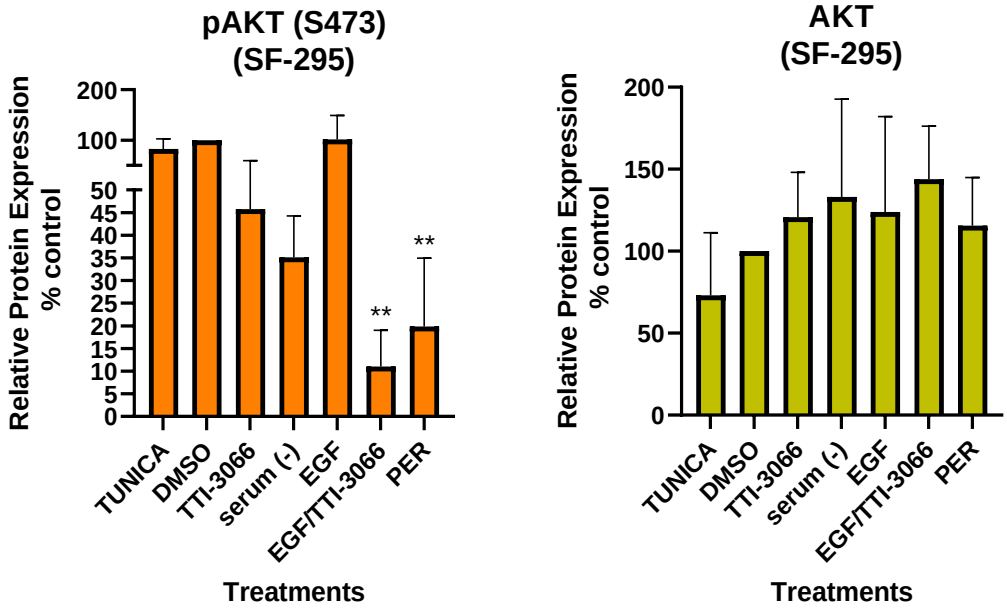
pAKT (S473) (SF-295)
Relative Protein Expression % control
200
100
50
45
40
35
30
25
20
15
10
5
0
**
**
TUNICA
DMSO
TTI-3066
serum (-)
EGF
EGF/TTI-3066
PER
Treatments
AKT (SF-295)
Relative Protein Expression % control
200
150
100
50
0
TUNICA
DMSO
TTI-3066
serum (-)
EGF
EGF/TTI-3066
PER
Treatments

Figure 12: TTI-3066, in combination with a bolus of EGF, may sensitize SF-295 cells to greater reductions in AKT activity, according to lower levels of phospho-AKT (S473). **A)** Various treatments for SF-295 cells, see Fig. 11 for abbreviations. Left protein of the blot was performed in an attempt to address whether schweinfurthin decouples phospho-EGFR(Y1068) expression from activation of AKT. Cells were serum starved for 4 hours instead of 3 hours, resulting in a higher intracellular concentration of EGF than 10 ng/mL. Perifosine served as a positive control as an AKT inhibitor. All controls were compared to the combination of EGF stimulation followed by 100 nM TTI-3066 treatment for 24 hours (EGF/TTI) and 100 nM TTI-3066 treatment alone (TTI). **B)** Representative images for antibody detection of phospho-AKT(S473) and AKT. See A for description. **C)** Quantification of blots were performed with Image Studio and GraphPad Prism software. Phospho-AKT (S473) was normalized to AKT. Values represent mean (N=3) ± SD. ** indicates mean values with a p-value <0.002 as performed with one-way ANOVA (post hoc Dunnett's test).

13A

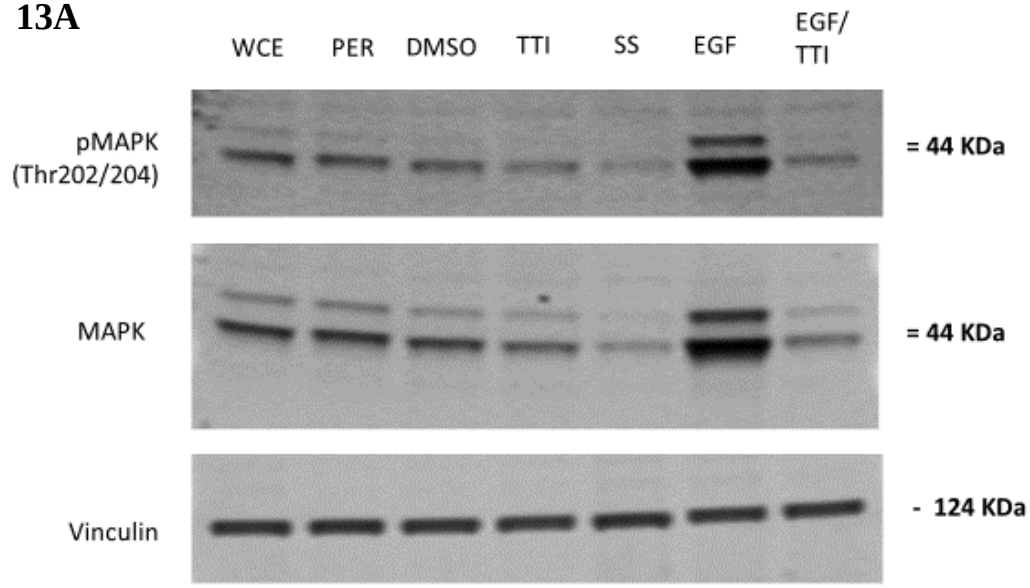
WCE
PER
DMSO
TTI
SS
EGF
EGF/
TTI
pMAPK
(Thr202/204)
= 44 KDa
MAPK
= 44 KDa
Vinculin
- 124 KDa

13B

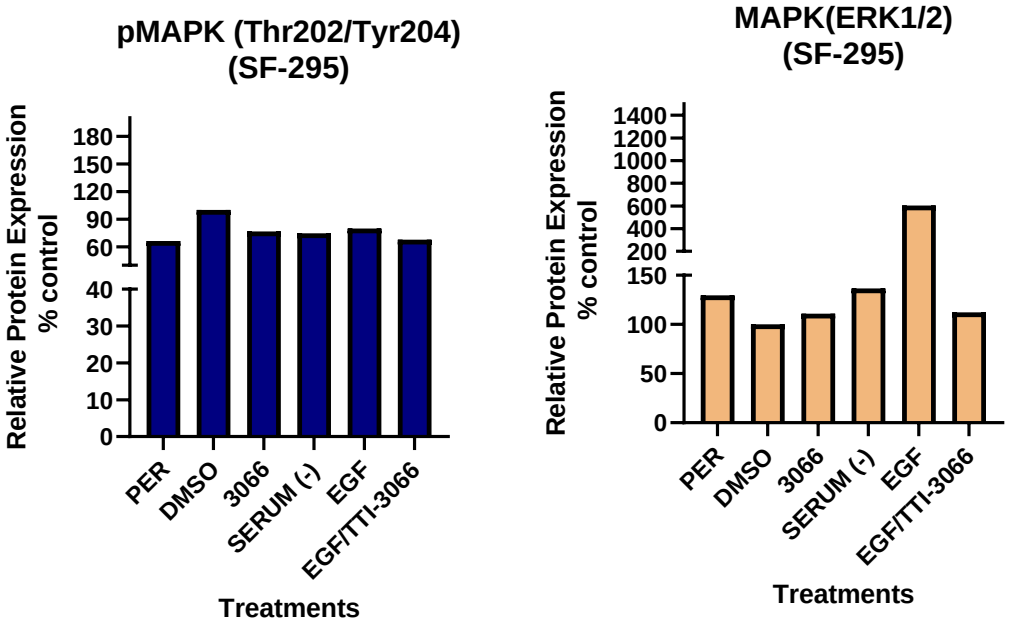
pMAPK (Thr202/Tyr204)
(SF-295)
Relative Protein Expression
% control
180
150
120
90
60
40
30
20
10
0
PER
DMSO
3066
SERUM (-)
EGF
EGF/TTI-3066
Treatments
MAPK(ERK1/2)
(SF-295)
Relative Protein Expression
% control
1400
1200
1000
800
600
400
200
150
100
50
0
PER
DMSO
3066
SERUM (-)
EGF
EGF/TTI-3066
Treatments

Figure 13: TTI-3066 does not affect phospho-MAPK(Thr202/Tyr204) levels in SF-295 cells, in spite of prior results of a trend and irrespective of EGF addition.
A) SF-295 cells were treated with 100 nM of TTI-3066 (TTI) and contrasted to treatments such as perifosine (PER), a control for phospho-MAPK levels, EGF (at 10 ng/mL for 10 min. after 4 hours serum starvation), and a combination treatment of 10 ng/mL of EGF for 10 minutes followed by 100 nM of TTI-3066 for 24 hours. **B)** Quantification of blots were performed with Image Studio. Phospho-MAPK (Thr202/Tyr204) was normalized to MAPK.
Values represent mean N=2. Note: blots do not necessarily reflect trends from graphs.

Prior work has suggested that schweinfurthins disrupt one of the last steps of N-linked glycosylation for glycoproteins undergoing complex glycan modifications, terminal sialylation. To explore this possibility, another protein that undergoes terminal sialylation, similar to EGFR, with a complex array of glycans, was investigated. Detection of LDLR was pursued since the protein has three N-linked glycans and ~12 O-linked glycan sites, most of which are capped by sialyl sugars at the trans-golgi. Detection of LDLR achieved using an antibody revealed opposing patterns of responses between TTI-3066 treated SF-295 cells and tunicamycin treated SF-295 cells (Fig. 14). Levels of fully modified LDLR decreased with tunicamycin treatment compared to vehicle (DMSO) treated SF-295 cells. This is due to the visible increase in a single unmodified species of LDLR at ~130 KDa that greatly exceeded levels seen in vehicle (DMSO) treated SF-295 cells. Quantification of this species was not achieved during analyses. In contrast, treatments with TTI-3066, EGF, EGF/TTI-3066, or perifosine did not seem to appear to change levels of LDLR, compared to that seen in vehicle (DMSO) treated SF-295 cells. Quantification of bands, however, indicates some level of increase in LDLR expression in SF-295 cells after TTI-3066 and EGF/TTI-3066 treatments. SF-295 cells treated with TTI-3066, EGF, EGF/TTI-3066, or perifosine did not display a second, unmodified species of LDLR similar to that seen with tunicamycin treatments (Fig. 14).

14A

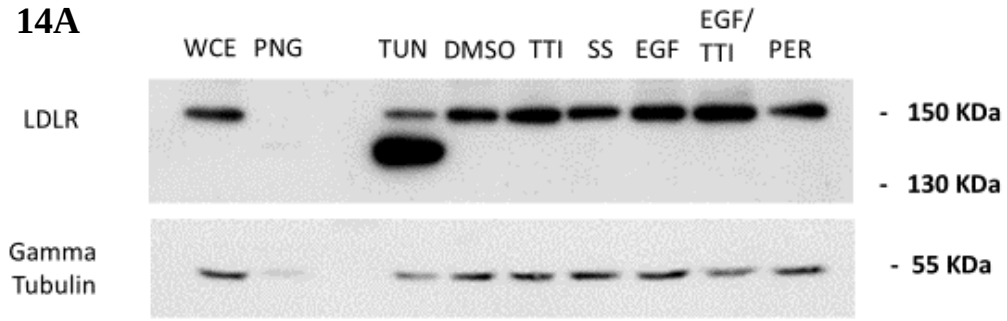
WCE
PNG
TUN
DMSO
TTI
SS
EGF
EGF/ TTI
PER
LDLR
- 150 KDa
- 130 KDa
Gamma Tubulin
- 55 KDa

14B

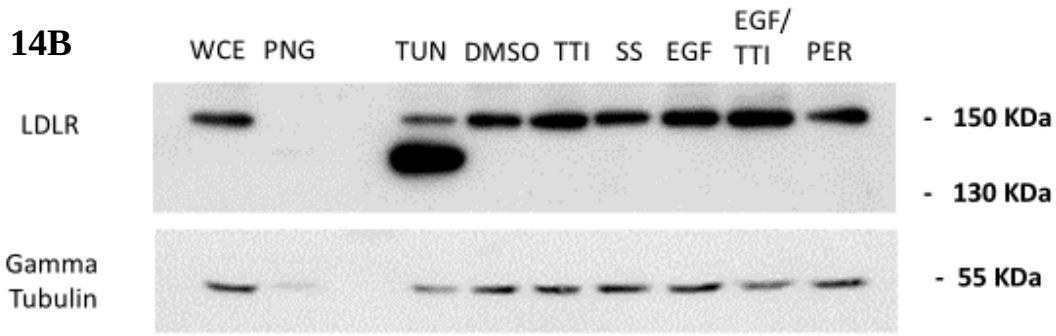
WCE
PNG
TUN
DMSO
TTI
SS
EGF
EGF/ TTI
PER
LDLR
- 150 KDa
- 130 KDa
Gamma Tubulin
- 55 KDa

14C

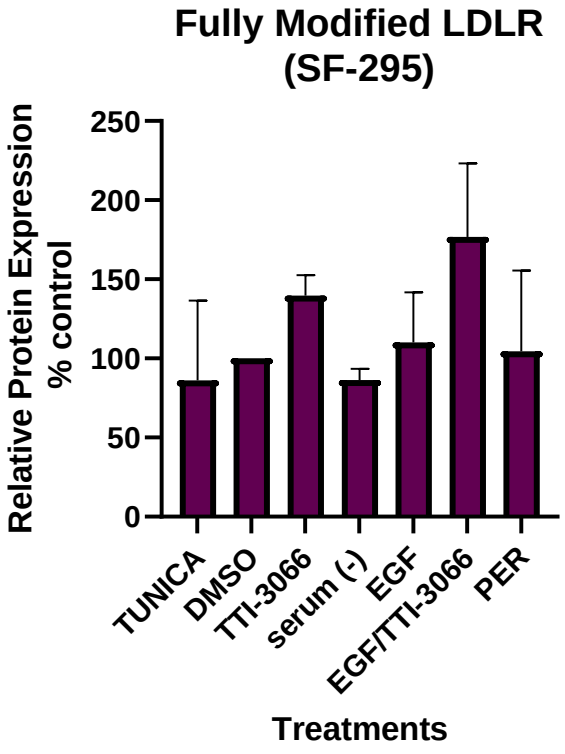
Fully Modified LDLR
(SF-295)
Relative Protein Expression
% control
250
200
150
100
50
0
TUNICA
DMSO
TTI-3066
serum (-)
EGF
EGF/TTI-3066
PER
Treatments

Figure 14: LDLR, a N-linked glycosylated protein, is susceptible to tunicamycin treatment but is not affected by TTI-3066 treatment in SF-295 cells.
A) Various treatments on SF-295 cells from prior experiments, see Fig. 11& 12 for details. LDLR has 3 N-linked glycans and 11 to 12 O-linked glycans which are capped in the golgi apparatus with terminal sialyl groups, similar to EGFR. Yet, TTI-3066 does not reduce the apparent molecular weight of LDLR. **B)** Representative blot from antibody detection of LDLR
C) Quantification of blots were performed with Image Studio and GraphPad Prism software with no statistical significance found. Values represent mean (N=3) ± SD.

Coupling of EGFR-AKT signaling in the context of schweinfurthin treatment was re-evaluated within SF-295 cells since initial findings showed that initial setups of EGF addition overstimulated these cells. Both acute and prolonged stimulation of EGFR with EGF was investigated within SF-295 cells. SF-295 cells were serum starved for 3 hours before a 10-minute treatment with 10 ng/mL EGF followed by TTI-3066 treatment (Fig. 15).

SF-295 cells were also co-incubated with 1 ng/mL EGF and TTI-3066 treatments as an alternative method to stimulate downstream EGFR signaling within these cells. Detection of EGFR with an antibody reveals that vehicle (DMSO) treated SF-295 cells displayed at least two bands which are believed to be the fully modified and partially/unmodified forms of EGFR. Treatments of SF-295 cells with EGF at both concentrations without TTI-3066 reveals a visible and sometime slight reduction in mature EGFR levels. Further quantification reveals that total levels of EGFR in SF-295 cells treated with 10 ng/mL EGF for 10 minutes are higher than that seen in vehicle (DMSO) treated SF-295 cells. In contrast, a modest decrease in total levels of EGFR is seen in SF-295 cells treated for 24 hours with 1 ng/mL EGF (Fig. 15). Detection of EGFR with an antibody reveals that SF-295 cells treated with 10 ng/mL EGF, followed by TTI-3066 for either 18 hours or 24 hours, experience either a transient increase in the levels of EGFR at 18 hours (not shown) or no apparent changes in EGFR expression even after 24 hours of TTI-3066 treatment. SF-295 cells treated with 1 ng/mL of EGF showed a similar trend in EGFR levels to that seen within cells treated with 10 ng/mL of EGF.

Phosphorylation of EGFR at Y1068 and Y1173 was also investigated to determine the impact of EGF/TTI-3066 treatment on downstream activation of AKT and MAPK, respectively, within SF-295 cells. Detection of phospho-EGFR(Y1068) using an antibody shows that a single band of EGFR is phosphorylated in vehicle (DMSO) treated SF-295 cells (Fig. 15). This signal overlays the phospho-EGFR(Y1068) signal captured on film that is believed to be the mature form of EGFR. This band slightly smears upward when SF-

295 cells are treated with 10 ng/mL of EGF for 10 minutes, believed to represent ligand-bound, mature forms of EGFR. Phospho-EGFR(Y1068) levels in this EGF treatment are quantitatively two-folds higher than that seen in vehicle (DMSO) treated SF-295 cells. This upper smear disappears in SF-295 cells treated with 10 ng/mL of EGF and schweinfurthin (Fig. 15). Total phospho-EGFR(Y1068) levels in these treated cells returns to that of vehicle (DMSO) treated cells. Intriguingly, SF-295 cells treated with 10 ng/mL of EGF displayed a lower band detected by an antibody against phospho-EGFR(Y1068) that does not migrate with that seen in SF-295 cells treated with vehicle (DMSO). Our interpretation is that this band, not seen in vehicle (DMSO) treated SF-295 cells, represents a partially modified/immature form of EGFR. Upon re-evaluation of pan EGFR signals, it is possible that much of the EGFR species seen in SF-295 cells treated with 10 ng/mL EGF + TTI-3066 are fast migrating, immature species of EGFR relative to the lowest band seen in vehicle (DMSO) treated SF-295 cells. This is best seen in the context of the signals detected by the phospho-EGFR(Y1068) antibody as discussed.

In one replicate, a faint second band is present in SF-295 cells treated with 10 ng/mL of EGF as well as SF-295 cells treated with EGF/TTI-3066 for 18 or 24 hours (Fig. 15). This overlays the EGFR signal detected by an antibody specific to EGFR that definitively corresponds to the position of what is believe to be the immature form of the receptor.

In SF-295 cells treated with 1 ng/mL of EGF for 24 hours, phospho-EGFR(Y1068) levels, as detected with an antibody against this site, were relatively similar to that seen in vehicle (DMSO) treated SF-295 cells (Fig. 15). For the most part, much of the phosphorylated signal at Y1068 was predominantly found for the topmost band in SF-295 cells treated with either vehicle (DMSO) or 1 ng/mL EGF as detected with this site-specific, phospho-EGFR(Y1068) antibody. This band however may not represent the identical EGFR species between both treatments. Similar to prior treatments with 10 ng/mL EGF + TTI-3066, SF-295 cells treated with 1 ng/mL EGF, irrespective of co-treatment with TTI-3066, display this

topmost band of Y1068 phosphorylation at a slightly lower apparent molecular weight than that seen in SF-295 cells treated with vehicle (DMSO). Hence, it is believed that this band represents partially modified/immature forms of EGFR absent in vehicle (DMSO) treated SF-295 cells (Fig. 15). In addition, this band in SF-295 cells treated with 1 ng/mL EGF, irrespective of schweinfurthin addition, shows a split in phosphorylation signal that we believe are multiple immature species of EGFR, represented as two distinct bands in two out of three experiments. This was detected with an antibody against phospho-EGFR(Y1068). Quantitative analyses of the bands indicates that total levels of Y1068 phosphorylation went up in SF-295 cells treated with 10 ng/mL EGF and TTI-3066 (Fig. 15). This was not the case when analyzing just the top band of phospho-EGFR(Y1068), which is believed to be the mature form of EGFR.

Phosphorylation of EGFR at Y1173 appeared as three distinct bands in vehicle (DMSO) treated SF-295 cells, based on antibody detection against this site. Overlay of this signal from the topmost band was compared to that detected with an antibody against EGFR at the same position within vehicle (DMSO) treated SF-295 cells (Fig. 15). This topmost band of phosphorylated EGFR seen in vehicle (DMSO) treated SF-295 cells corresponds to what is believed to be the mature form of EGFR. Detection of phospho-EGFR(Y1173) levels with an antibody reveals an increase in phosphorylation for all three species of EGFR when SF-295 cells are treated with 10 ng/mL of EGF for 10 minutes. This signal is the most increased for the topmost band seen in SF-295 cells treated with 10 ng/mL EGF, compared to that seen in vehicle (DMSO) treated SF-295 cells. The upward smear of the band is believed to indicate that this form of EGFR is bound to EGF (Fig. 15). SF-295 cells pre-conditioned with 10 ng/mL of EGF before TTI-3066 treatment displayed, as detected with an antibody against phospho-EGFR(Y1173), less EGF-induced phospho-EGFR(Y1173) expression. Much of this phosphorylation was limited to partially modified forms of EGFR, since previous detection of EGFR with an antibody showed that fully modified EGFR is lost within SF-295 cells treated

with 10 ng/mL EGF + TTI-3066. Hence, detection of phospho-EGFR(Y1173) levels with an antibody revealed that SF-295 cells treated with 10 ng/mL EGF + TTI-3066 had a lack of phosphorylation that corresponded to the topmost band seen within SF-295 cells treated with vehicle (DMSO) (Fig. 15).

Detection of phospho-EGFR(Y1173) levels within SF-295 cells treated with 1 ng/mL of EGF for 24 hours also displayed an increase in total phospho-EGFR(Y1173) expression, compared that seen in vehicle (DMSO) treated SF-295 cells (Fig. 15). However, this increase in phospho-EGFR(Y1173) expression that was detected with an antibody against phospho-EGFR(Y1173) was limited to intermediate band(s) of EGFR shared in common with thosepresent in vehicle (DMSO) treated SF-295 cells. These intermediates are believed to be immature forms of EGFR. SF-295 cells treated with both 1 ng/mL of EGF and TTI-3066 show, according to detection with an antibody against phospho-EGFR(Y1173), a modest, time-dependent increase in phospho-EGFR(Y1173) levels compared to vehicle (DMSO) treated SF-295 cells (Fig. 15). Levels of phospho-EGFR(Y1173) levels in SF-295 cells treated with both 1 ng/mL EGF and TTI-3066, measured by a site-specific antibody, are found at similar intermediate forms of EGFR as that seen in SF-295 cells treated with 1 ng/mL of EGF.

A549 cells were also investigated under the same treatments as that done within SF-295 cells to see whether or not EGF stimulation changes the effects of TTI-3066 on these cells. Detection of EGFR with an EGFR-specific antibody revealed the presence of at least 2 to 3 forms of EGFR in vehicle (DMSO) treated A549 cells (Fig. 15). Out of these species, one is believed to be a fully modified/mature form of EGFR and two are believed to be partially modified/immature forms of EGFR. A549 cells treated with 10 ng/mL of EGF for 10 minutes displayed a slight reduction in EGFR expression relative to that seen in vehicle (DMSO) treated A549 cells. This reduction, as detected by anti-EGFR, was reversed in A549 cells treated with 10 ng/mL EGF + TTI-3066, back to the levels seen in vehicle (DMSO) treated A549 cells. When A549 cells were treated for 24 hours with 1 ng/mL of EGF, detection of EGFR with an antibody indicated similar EGFR levels to that seen in A549 cells treated with vehicle (DMSO). Detection of EGFR levels with an antibody against EGFR also showed that A549 cells treated with 1 ng/mL of EGF + TTI-3066 had similar levels of EGFR to that seen in vehicle (DMSO) treated A549 cells. In all these treatments, there was no shift in the apparent molecular weight of EGFR, based on antibody detection (Fig. 15).

Detection of phospho-EGFR(Y1068) with an antibody indicates two distinct phospho-EGFR(Y1068) bands expressed in vehicle (DMSO) treated A549 cells. The top band, which is believed to represent the mature form of EGFR, is highly phosphorylated according to detection. A subtle to modest level of phosphorylation is evident in the lower, second band which is believed to be the immature form(s) of EGFR in vehicle (DMSO) treated A549 cells based on this antibody detection (Fig. 15). A549 cells treated with 10 ng/mL EGF display a shift in phosphorylated EGFR species towards a higher apparent molecular weight form, believed to be ligand-bound. This increase in apparent molecular weight is higher than that seen in vehicle (DMSO) treated A549 cells, as detected with an antibody against phospho-EGFR(Y1068). In contrast, A549 cells treated with 1 ng/mL of EGF for 24 hours displays

similar levels of phospho-EGFR(Y1068) expression as that seen in vehicle (DMSO) treated A549 cells. Treatment with TTI-3066 after stimulation with either 10 ng/mL EGF or 1 ng/mL EGF in A549 cells showed, according to antibody detection, similar levels of phospho-EGFR(Y1068) as that seen in vehicle (DMSO) treated A549 cells (Fig. 15).

Similar to SF-295 cells, A549 cells treated with vehicle (DMSO) also displayed three distinct bands of phospho-EGFR(Y1173) expression, as detected with a site-specific antibody for phospho-EGFR(Y1173). The topmost band from this phospho-EGFR(Y1173) signal, according to this antibody detection as well as anti-EGFR, is believed to be the mature form of EGFR. This form is likely to be ligand bound since this signal appears as an upward smear (Fig. 15). Detection of phospho-EGFR(Y1173) expression also indicates that A549 cells treated with 10 ng/mL EGF display an increase in phospho-EGFR(Y1173) levels relative to that seen in vehicle (DMSO) treated A549 cells. This increase in phosphorylation, however, is mostly seen with the topmost band of EGFR found in A549 cells treated with 10 ng/mL EGF (Fig. 15). A549 cells treated with both 10 ng/mL of EGF and TTI-3066 more or less showed, according to antibody detection of phospho-EGFR(Y1173), similar (or slightly lower) levels of phospho-EGFR(Y1173) expression to that seen in vehicle (DMSO) treated A549 cells. On the other hand, A549 cells treated for 24 hours with 1 ng/mL of EGF showed two patterns of phospho-EGFR(Y1173) expression. The same was the case for A549 cells co-treated with 1 ng/mL of EGF + TTI-3066. As detected by an antibody against phospho-EGFR(Y1173) expression, the two topmost bands of EGFR in one replicate of A549 cells treated with 1 ng/mL EGF showed increases in phospho-EGFR(Y1173) expression (Fig. 15). In contrast, two out of three replicates showed a decrease in phospho-EGFR(Y1173) levels for all three bands of EGFR, relative to vehicle (DMSO) treated A549 cells. For one replicate, as detected by an antibody against phospho-EGFR(Y1173) expression, A549 cells treated with 1 ng/mL of EGF and TTI-3066 showed similar levels of phospho-EGFR(Y1173) expression to that seen in

A549 cells treated with 1 ng/mL EGF. In two out of three replicates, A549 cells co-treated with 1 ng/mL of EGF and TTI-3066 also had similar phospho-EGFR(Y1173) levels comparable to that seen in vehicle (DMSO) treated A549 cells, as detected by antibody against phospho-EGFR(Y1173) (Fig. 15).

15A

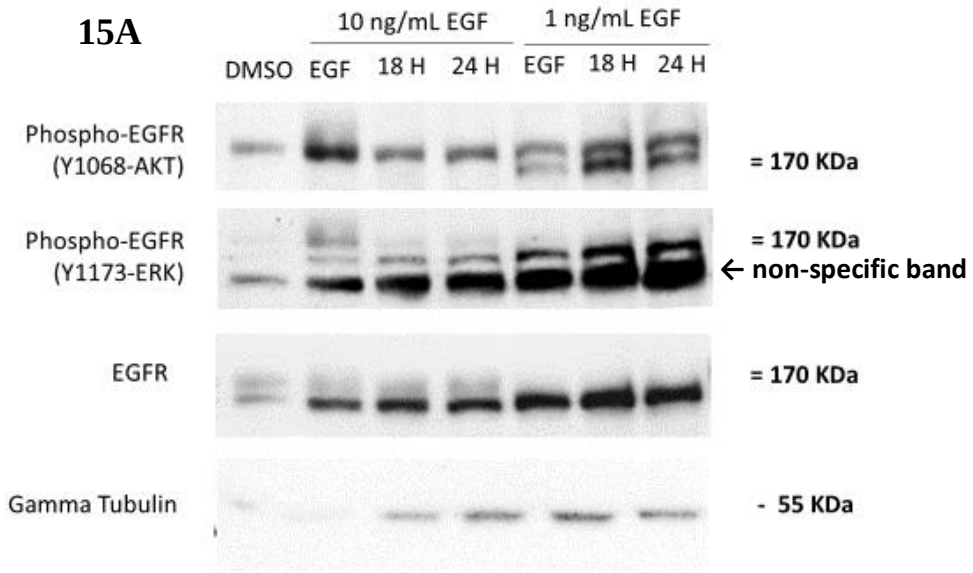
10 ng/mL EGF
1 ng/mL EGF
DMSO
EGF
18 H
24 H
EGF
18 H
24 H
Phospho-EGFR (Y1068-AKT)
= 170 KDa
Phospho-EGFR (Y1173-ERK)
= 170 KDa
← non-specific band
EGFR
= 170 KDa
Gamma Tubulin
- 55 KDa

15B

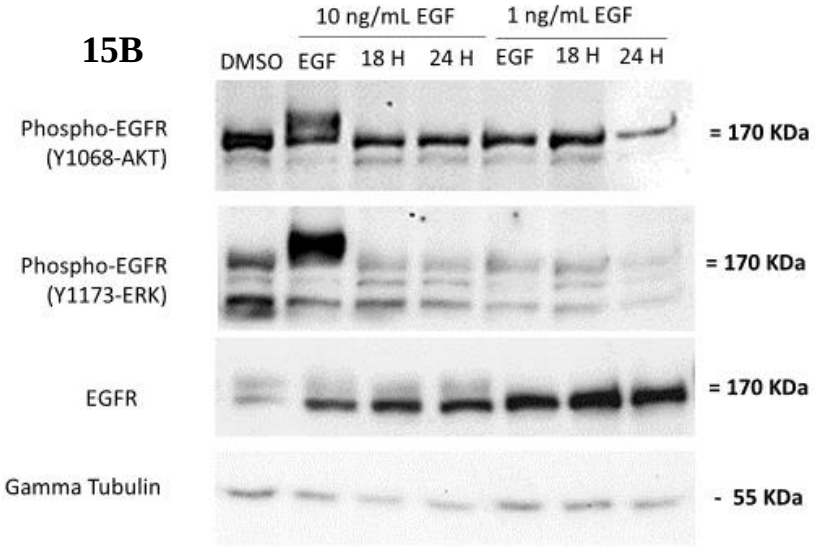
10 ng/mL EGF
1 ng/mL EGF
DMSO
EGF
18 H
24 H
EGF
18 H
24 H
Phospho-EGFR (Y1068-AKT)
= 170 KDa
Phospho-EGFR (Y1173-ERK)
= 170 KDa
EGFR
= 170 KDa
Gamma Tubulin
- 55 KDa

15C

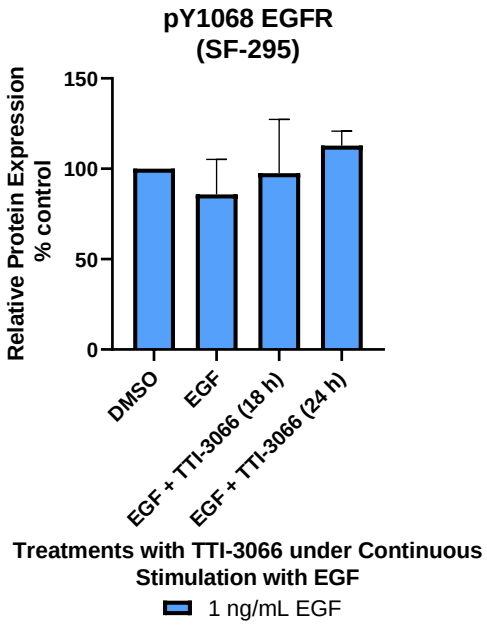

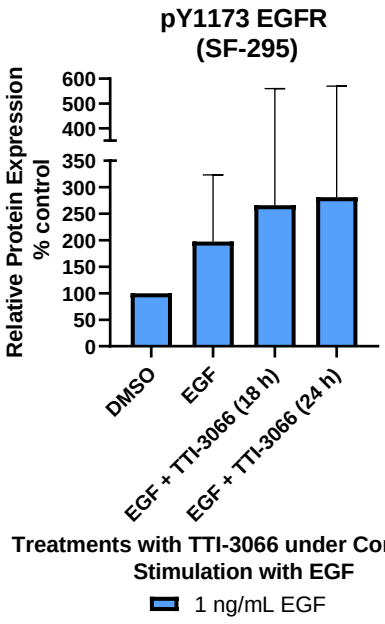

Treatments with TTI-3066 under Continuous Stimulation with EGF

1 ng/mL EGF

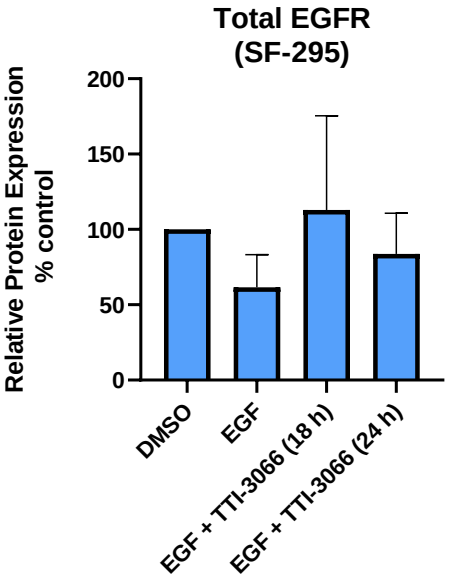

Treatments with TTI-3066 under Continous Stimulation with EGF

1 ng/mL EGF

15C

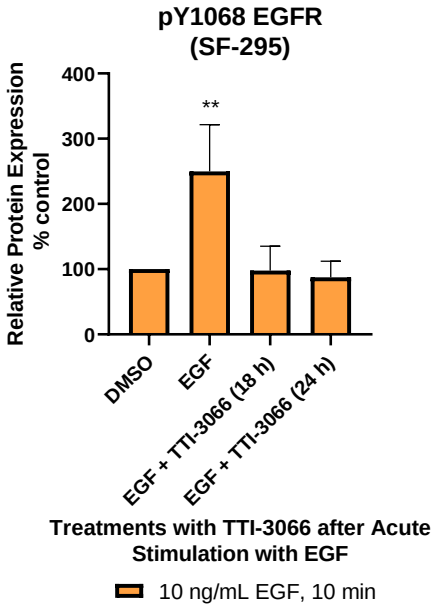
pY1068 EGFR
(SF-295)
Relative Protein Expression
% control
400
300
200
100
0
**
DMSO
EGF
EGF + TTI-3066 (18 h)
EGF + TTI-3066 (24 h)
Treatments with TTI-3066 after Acute
Stimulation with EGF
10 ng/mL EGF, 10 min

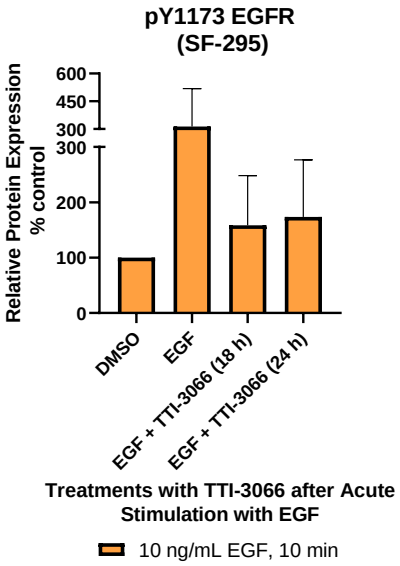
pY1173 EGFR
(SF-295)
Relative Protein Expression
% control
600
450
300
300
200
100
0
DMSO
EGF
EGF + TTI-3066 (18 h)
EGF + TTI-3066 (24 h)
Treatments with TTI-3066 after Acute
Stimulation with EGF
10 ng/mL EGF, 10 min

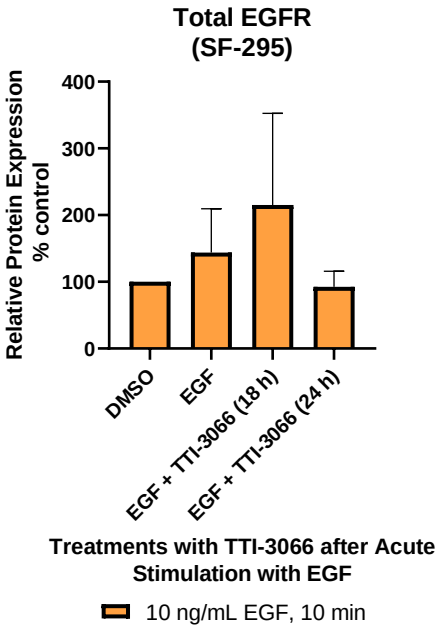
Total EGFR
(SF-295)
Relative Protein Expression
% control
400
300
200
100
0
DMSO
EGF
EGF + TTI-3066 (18 h)
EGF + TTI-3066 (24 h)
Treatments with TTI-3066 after Acute
Stimulation with EGF
10 ng/mL EGF, 10 min

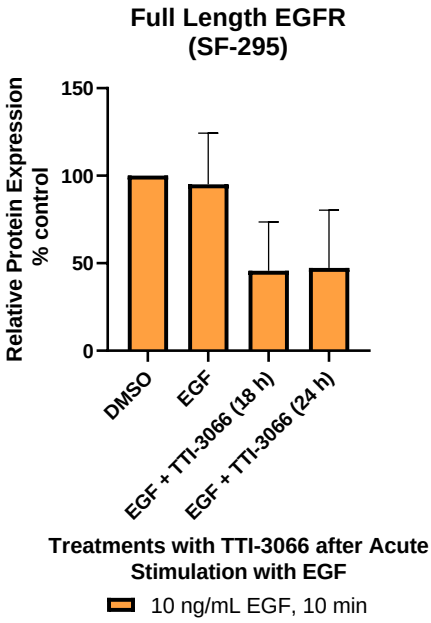
Full Length EGFR
(SF-295)
Relative Protein Expression
% control
150
100
50
0
DMSO
EGF
EGF + TTI-3066 (18 h)
EGF + TTI-3066 (24 h)
Treatments with TTI-3066 after Acute
Stimulation with EGF
10 ng/mL EGF, 10 min

15C

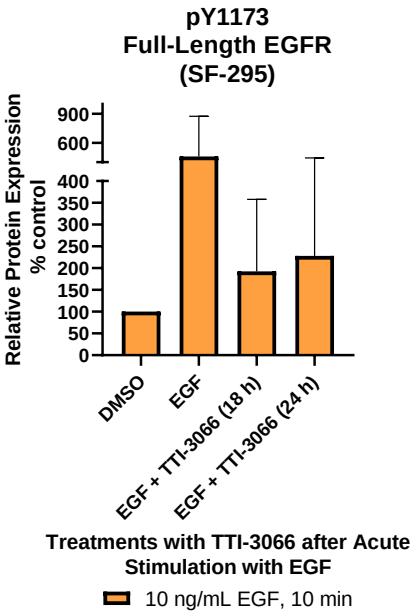
pY1173
Full-Length EGFR
(SF-295)
Relative Protein Expression
% control
900
600
400
350
300
250
200
150
100
50
0
DMSO
EGF
EGF + TTI-3066 (18 h)
EGF + TTI-3066 (24 h)
Treatments with TTI-3066 after Acute
Stimulation with EGF
10 ng/mL EGF, 10 min

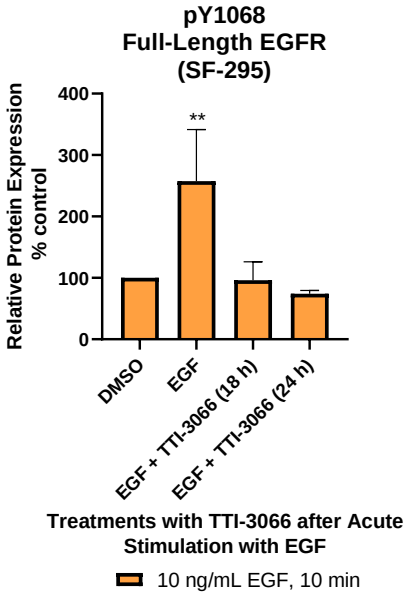
pY1068
Full-Length EGFR
(SF-295)
Relative Protein Expression
% control
400
300
200
100
0
**
DMSO
EGF
EGF + TTI-3066 (18 h)
EGF + TTI-3066 (24 h)
Treatments with TTI-3066 after Acute
Stimulation with EGF
10 ng/mL EGF, 10 min

15D

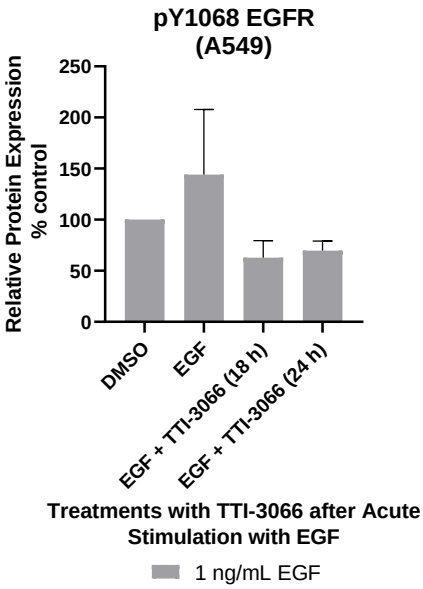
pY1068 EGFR
(A549)
Relative Protein Expression
% control
250
200
150
100
50
0
DMSO
EGF
EGF + TTI-3066 (18 h)
EGF + TTI-3066 (24 h)
Treatments with TTI-3066 after Acute
Stimulation with EGF
1 ng/mL EGF

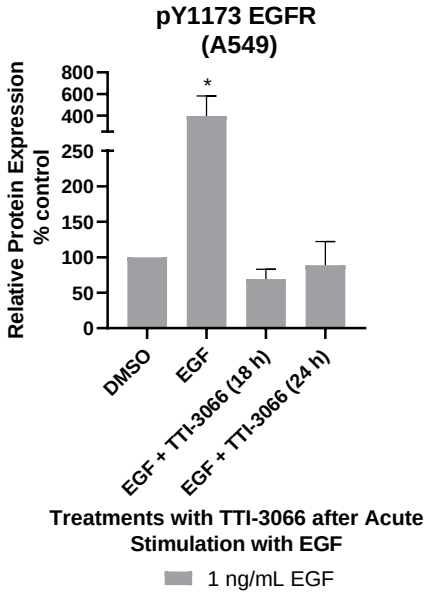
pY1173 EGFR
(A549)
Relative Protein Expression
% control
800
600
400
250
200
150
100
50
0
*
DMSO
EGF
EGF + TTI-3066 (18 h)
EGF + TTI-3066 (24 h)
Treatments with TTI-3066 after Acute
Stimulation with EGF
1 ng/mL EGF

15D

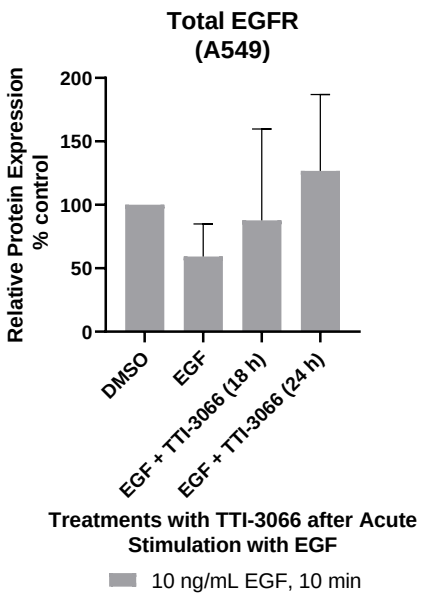
Total EGFR
(A549)
Relative Protein Expression
% control
200
150
100
50
0
DMSO
EGF
EGF + TTI-3066 (18 h)
EGF + TTI-3066 (24 h)
Treatments with TTI-3066 after Acute
Stimulation with EGF
10 ng/mL EGF, 10 min

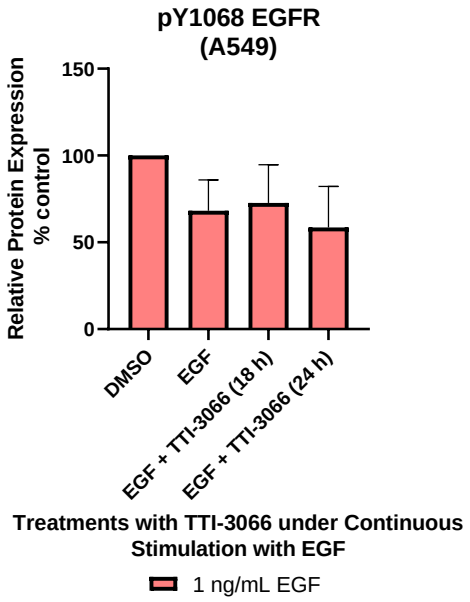
pY1068 EGFR
(A549)
Relative Protein Expression
% control
150
100
50
0
DMSO
EGF
EGF + TTI-3066 (18 h)
EGF + TTI-3066 (24 h)
Treatments with TTI-3066 under Continuous
Stimulation with EGF
1 ng/mL EGF

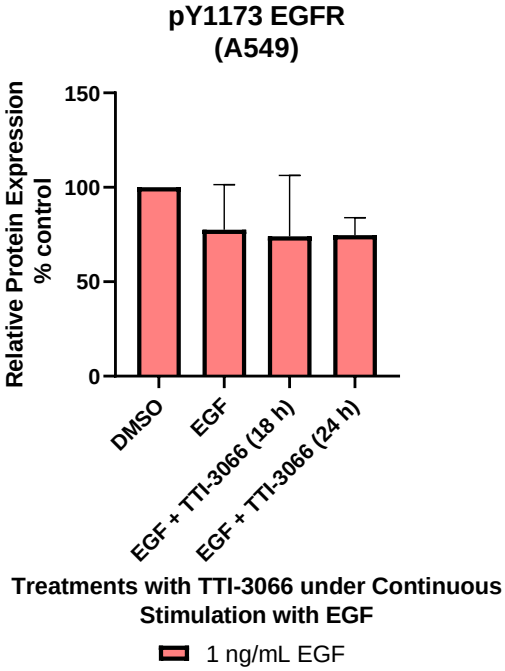
pY1173 EGFR
(A549)
Relative Protein Expression
% control
150
100
50
0
DMSO
EGF
EGF + TTI-3066 (18 h)
EGF + TTI-3066 (24 h)
Treatments with TTI-3066 under Continuous
Stimulation with EGF
1 ng/mL EGF

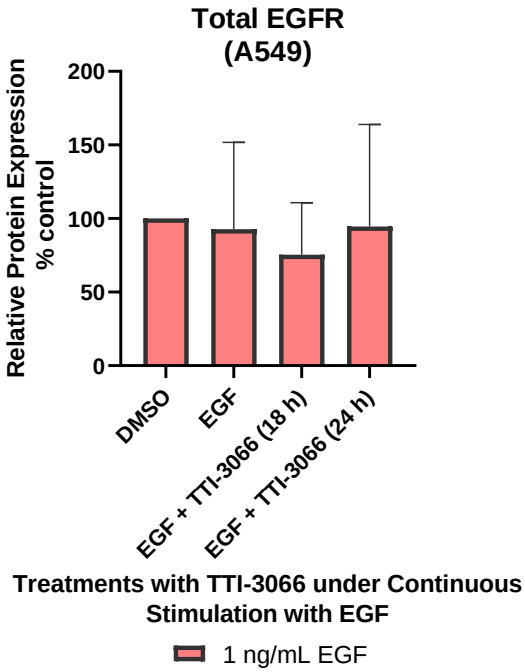
Total EGFR
(A549)
Relative Protein Expression
% control
200
150
100
50
0
DMSO
EGF
EGF + TTI-3066 (18 h)
EGF + TTI-3066 (24 h)
Treatments with TTI-3066 under Continuous
Stimulation with EGF
1 ng/mL EGF

Figure 15: 10 ng/mL of EGF is needed for activation of EGFR signaling & addition of TTI-3066 reduces phospho-EGFR signals in SF-295 cells, not A549 cells in this condition. **A)** SF-295 cells were treated under an acute stimulation of EGF (10 ng/mL for 10 minutes after 3 hours of serum starvation) and at physiological concentrations of EGF (1 ng/mL for the duration of the experiment with EGF only treatment lasting 24 hours). Note that beyond 12 hours, it was assumed that EGF concentrations will be a bit higher than physiological concentrations found in a tumor microenvironment. While 10 ng/mL of EGF increased phosphorylation of EGFR which was reduced in TTI-3066 treated cells, 1 ng/mL of EGF did not induce phosphorylation of mature EGFR and may have even buffered the effects of TTI-3066. Note that phospho-EGFR(Y1173) signals in SF-295 cells displays a non-specific band, see discussion. **B)** A549 cells were also investigated under the same conditions as described in A. 10 ng/mL of EGF induced EGFR phosphorylation but, similar to known resistance of A549 cells to schweinfurthins, the addition of EGF does not reverse the lack of response A549 cells have with regards to EGFR activation nor does it increase activation of the receptor. **C & D)** Quantification of blots were performed with Image Studio and GraphPad Prism software. Phospho-EGFR (Y1068) and phospho-EGFR (Y1173) were normalized to EGFR. Values represent mean (N=3) ± SD. * and ** indicates mean values with a p-value < 0.03 or p-value <0.002, respectively,as performed with one-way ANOVA (post hoc Dunnett's test). Note: blots do not necessarily reflect trends from graphs.

The presence of EGF was unable to buffer schweinfurthin-mediated reductions in both mature levels of EGFR expression as well as its phosphorylations. To investigate whether phospho-EGFR(Y1068) levels are de-coupled from AKT due to these effects, the downstream effector, AKT, was studied within both SF-295 cells and A549 cells (Fig. 16). Detection of AKT with an antibody indicates that SF-295 cells treated with vehicle (DMSO) display two bands. These two bands are believed to represent different phosphorylated forms of AKT in which the topmost band represents phosphorylated AKT, and the bottom band represents non-phosphorylated AKT. Signal intensity of the top band was greater than that of the second band, which is believed to reflect a higher phospho-AKT to AKT ratio in SF-295 cells treated with vehicle (DMSO) (Fig. 16). Detection of AKT with an antibody reveals that SF-295 cells treated with either 1 ng/mL EGF or 10 ng/mL EGF undergo a modest to significant increase in AKT levels compared to that seen in vehicle (DMSO) treated SF-295 cells. This increase is only seen for the topmost band of AKT, believed to be the phosphorylated form of the protein. Follow up of schweinfurthins after EGF stimulation with 10 ng/mL EGF in SF-295 cells leads to variable patterns in AKT expression (Fig. 16). Detection with an antibody against AKT reveals that in two out of three replicates, SF-295 cells treated with EGF and TTI-3066 show a slight increase in AKT levels relative to that in SF-295 cells treated with 10 ng/mL EGF. This pattern was reversed in the other replicate, showing a slight decrease in AKT levels compared to SF-295 cells treated with 10 ng/mL EGF. SF-295 cells treated with 1 ng/mL EGF and TTI-3066 show no detectable difference in AKT expression, as detected by an antibody, compared to that of SF-295 cells treated with 1 ng/mL EGF (Fig. 16).

Activation of AKT, as measured through detection of phospho-AKT (S473) expression with an antibody, revealed a single band of phospho-AKT(S473) expression within SF-295 cells treated with vehicle (DMSO) (Fig. 16). This phosphorylated signal overlays the topmost band of AKT expression, as detected with an antibody against AKT. SF-295 cells treated with 10 ng/mL EGF show an increased intensity of phospho-AKT(S473) signal compared to that seen in vehicle (DMSO) treated SF-295 cells, as detected with an antibody against this site.

SF-295 cells treated with both 10 ng/mL EGF and TTI-3066, as detected by anti-phospho-AKT(S473), reveal a time-dependent decrease in phospho-AKT(S473) expression for two out of three replicates (Fig. 16). For the other replicate, phospho-AKT(S473) levels go down after 18 hours of TTI-3066 treatment, only to slightly increase when SF-295 cells are treated up to 24 hours with TTI-3066. These patterns of phosphorylation were identified relative to that seen and detected with a phospho-AKT(S473) antibody in vehicle (DMSO) treated SF-295 cells.

SF-295 cells treated with 1 ng/mL EGF, from antibody detection of phospho-AKT(S473), displayed similar levels of phospho-AKT(S473) signal compared to that in vehicle (DMSO) treated SF-295 cells. SF-295 cells co-treated with 1 ng/mL EGF and TTI-3066 show little effect on phospho-AKT(S473) levels, which remained similar to that seen in both vehicle (DMSO) treated SF-295 cells as well as that seen in SF-295 cells treated with 1 ng/mL EGF. This observation was made according to antibody detection against phospho-AKT(S473).

Vehicle (DMSO) treated A549 cells also displayed at least two bands detected by an antibody against AKT (Fig. 16). AKT expression within these A549 cells are believed to be of equal ratio of phospho-AKT to AKT expression due to the similar intensities of each of the bands. A549 cells treated with either 1 ng/mL EGF or 10 ng/mL EGF reveal similar AKT expression to that seen in A549 cells treated with vehicle (DMSO). Antibody detection of AKT in A549 cells treated with either 1 ng/mL EGF + TTI-3066, or 10 ng/mL EGF + TTI-3066, also revealed similar levels of AKT to that seen in vehicle (DMSO) treated A549 cells.

A549 cells treated with 10 ng/mL EGF and TTI-3066 showed a transient decrease in phospho-AKT(S473) expression according to antibody detection against this site. This is not seen in vehicle (DMSO) treated A549 cells under the same conditions and is reversed in these EGF/TTI-3066 treated A549 cells after 24 hours of TTI-3066 treatment (Fig. 16). At this timepoint, the levels of phospho-AKT(S473) expression detected by an antibody against phospho-AKT(S473) are higher than that seen in vehicle (DMSO) treated A549 cells. A549 cells treated with 1 ng/mL EGF had similar pattern of phospho-AKT(S473) expression as that seen in A549 cells treated with 10 ng/mL EGF, according to antibody detection. However, A549 cells treated with 1 ng/mL EGF and TTI-3066 displayed higher phospho-AKT(S473) levels that exceed that seen in A549 cells treated with 1 ng/mL EGF, but not that of A549 cells treated with vehicle (DMSO). This was also detected with an antibody against phospho-AKT(S473) (Fig. 16).

16A

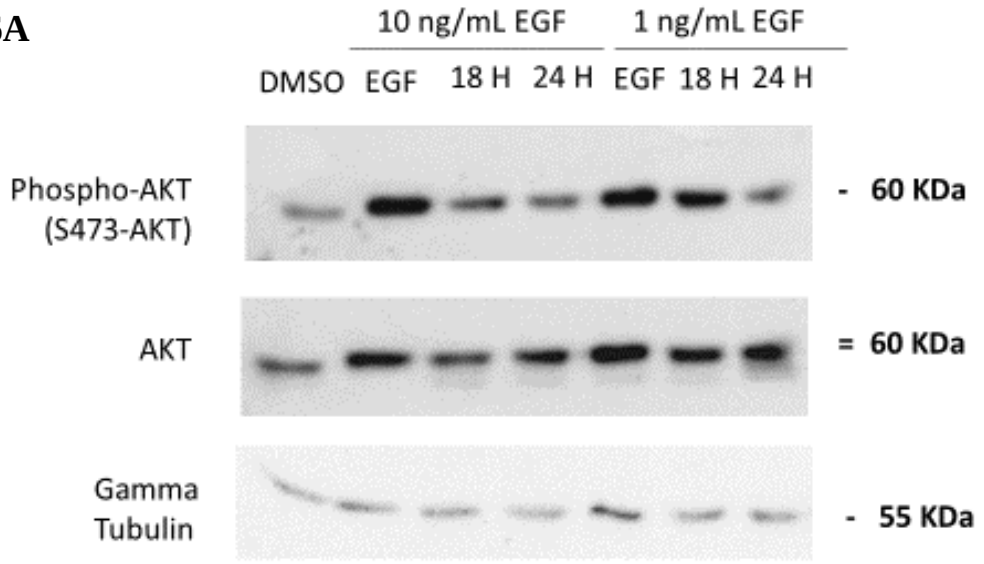
10 ng/mL EGF
1 ng/mL EGF
DMSO EGF 18 H 24 H EGF 18 H 24 H
Phospho-AKT
(S473-AKT)
- 60 KDa
AKT
= 60 KDa
Gamma
Tubulin
- 55 KDa

16B

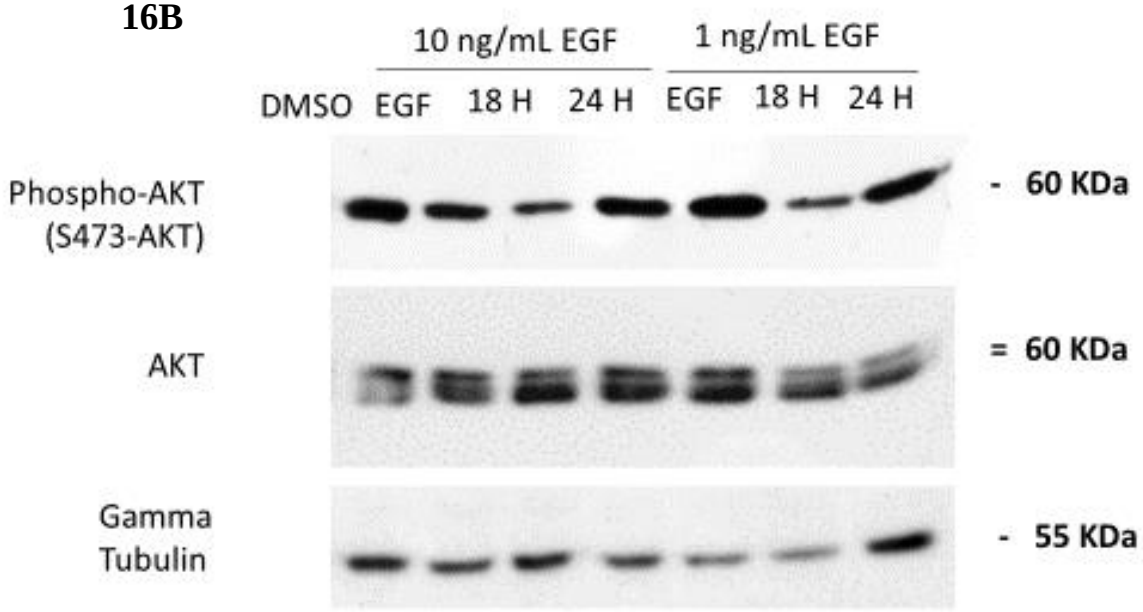
10 ng/mL EGF
1 ng/mL EGF
DMSO EGF 18 H 24 H EGF 18 H 24 H
Phospho-AKT
(S473-AKT)
- 60 KDa
AKT
= 60 KDa
Gamma
Tubulin
- 55 KDa

16C

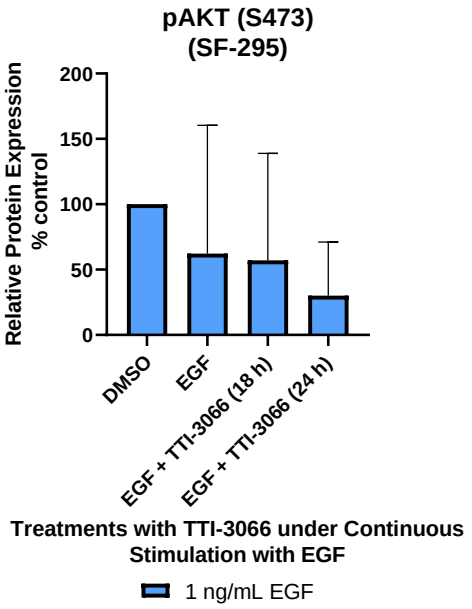
pAKT (S473)
(SF-295)
Relative Protein Expression
% control
200
150
100
50
0
DMSO
EGF
EGF + TTI-3066 (18 h)
EGF + TTI-3066 (24 h)
Treatments with TTI-3066 under Continuous Stimulation with EGF
1 ng/mL EGF

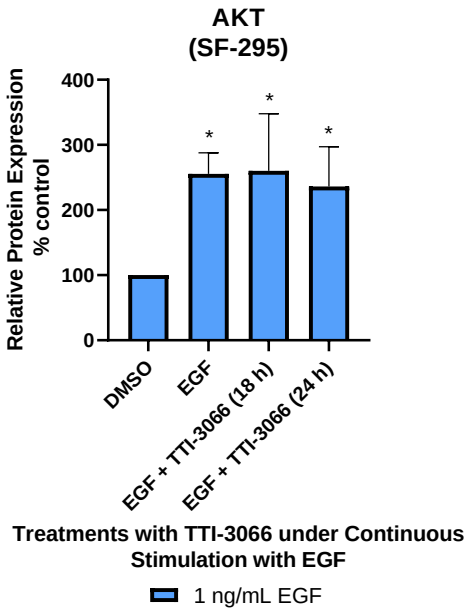
AKT
(SF-295)
Relative Protein Expression
% control
400
300
200
100
0
*
*
*
DMSO
EGF
EGF + TTI-3066 (18 h)
EGF + TTI-3066 (24 h)
Treatments with TTI-3066 under Continuous Stimulation with EGF
1 ng/mL EGF

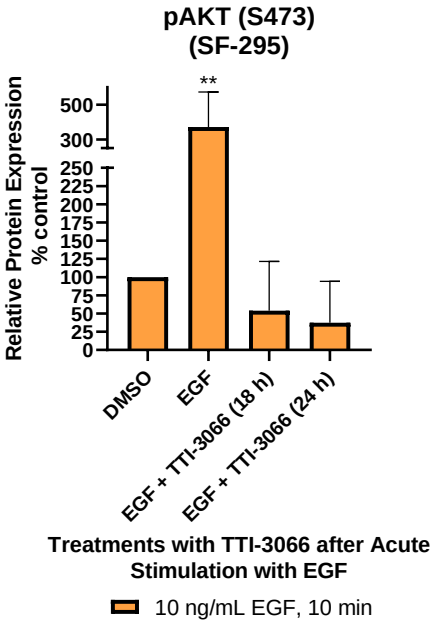
pAKT (S473)
(SF-295)
Relative Protein Expression
% control
**
500
300
250
225
200
175
150
125
100
75
50
25
0
DMSO
EGF
EGF + TTI-3066 (18 h)
EGF + TTI-3066 (24 h)
Treatments with TTI-3066 after Acute Stimulation with EGF
10 ng/mL EGF, 10 min

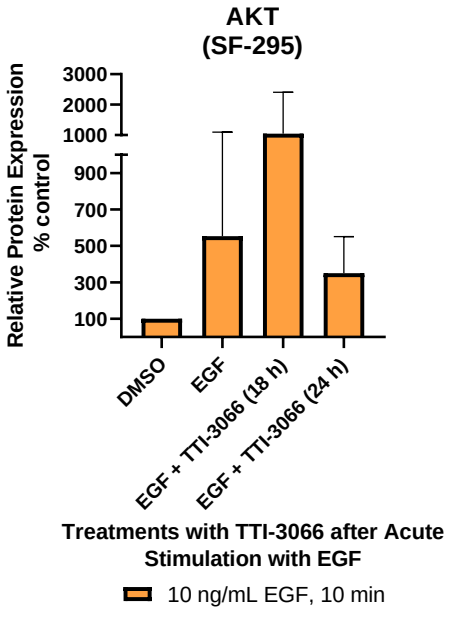
AKT
(SF-295)
Relative Protein Expression
% control
3000
2000
1000
900
700
500
300
100
DMSO
EGF
EGF + TTI-3066 (18 h)
EGF + TTI-3066 (24 h)
Treatments with TTI-3066 after Acute Stimulation with EGF
10 ng/mL EGF, 10 min

Figure 16: 10 ng/mL EGF + TTI-3066 does not buffer SF-295 cells from de-coupling effects seen on EGFR and AKT nor does it reveal AKT activation in A549 cells. A) SF-295 cells were treated as described in Fig. 15. 10 ng/mL of EGF was sufficient in inducing phospho-AKT(S473) levels. 1 ng/mL of EGF turns out to possibly increase phospho-AKT(S473) levels in some cases, but fluctuated in its ability to do so consistently. TTI-3066 addition after EGF stimulation led to a time-dependent decrease in phospho-AKT(S473) levels. **B)** A549 cells were treated as described in Fig. 13. 10 ng/mL of EGF was the appropriate concentration to stimulate phospho-AKT(S473) levels to go up. However, TTI-3066 treatment did not affect phospho-AKT(473) relative to vehicle (DMSO) treated A549 cells, consistent with findings of when A549 cells were treated with TTI-3066 without EGF stimulation. **C)** Quantification of blots were performed with Image Studio and GraphPad Prism software. Phospho-AKT (S473) was normalized to AKT. Values represent mean (N=3) ± SD. * and ** indicates mean values with a p-value < 0.03 or p-value <0.002, respectively, as performed with one-way ANOVA (post hoc Dunnett's test).

It is uncertain whether SF-295 cells treated with both EGF and TTI-3066 display less MAPK activation. Results with A549 cells, however, suggests that treatments with TTI-3066 have little effect on both phosphorylation of EGFR(Y1173) and phosphorylation of MAPK(Thr202/Tyr204). Therefore, the following experiments were limited to SF-295 cells to study the effects of EGF+ TTI-3066 treatments on MAPK activity (Fig. 17). SF-295 cells treated with vehicle (DMSO) displayed two bands for MAPK based on detection with an antibody against MAPK. Both bands are believed to represent different forms of MAPK (ERK1 and ERK2). SF-295 cells treated with 10 ng/mL of EGF showed increases in total MAPK levels relative to that seen in vehicle (DMSO) treated SF-295 cells. SF-295 cells treated with 10 ng/mL EGF and TTI-3066 showed a time dependent decrease in MAPK levels which were lower than that seen in vehicle (DMSO) treated SF-295 cells. Detection with an antibody against MAPK reveal that this decrease seen within SF-295 cells treated with 10 ng/mL EGF and TTI-3066 was evident for both bands (ERK1 and ERK2). SF-295 cells treated for 24 hours with 1 ng/mL EGF showed no difference in MAPK levels from that seen in vehicle (DMSO) treated SF-295 cells, as detected by an antibody against MAPK. Detection of MAPK with this antibody revealed that SF-295 cells treated with 1 ng/mL EGF and TTI-3066 also showed no difference in MAPK levels from that seen in vehicle (DMSO) treated SF-295 cells (Fig. 17).

Ras-mediated activation of MAPK at Thr202/Tyr204 was next investigated (Fig. 17). Detection of phospho-MAPK(Thr202/Tyr204) with an antibody revealed that vehicle (DMSO) treated SF-295 cells displayed two bands of phospho-MAPK. SF-295 cells treated with 10 ng/mL EGF displayed no significant activation of MAPK, according to detection with a phospho-MAPK(Thr202/204) antibody, compared to that seen in vehicle (DMSO) treated SF-295 cells. SF-295 cells treated with 10 ng/mL EGF and TTI-3066 also display no significant change to phospho-MAPK levels, as detected with a site-specific antibody for phospho-MAPK(Thr202/Tyr204). This was observed relative to that seen in SF-295 cells treated with vehicle (DMSO), although a slight non-significant increase was seen at the 24-hour timepoint for SF-295 cells treated with 10 ng/mL EGF + TTI-3066. SF-295 cells treated with 1 ng/mL of EGF showed similar phospho-MAPK levels detected by a phospho-MAPK(Thr202/Tyr204) antibody as that seen in vehicle (DMSO) treated SF-295 cells. Detection of phospho-MAPK(Thr202/204) levels with an antibody in SF-295 cells treated with 1 ng/mL EGF + TTI-3066 showed no significant difference in phospho-MAPK levels to that seen in vehicle (DMSO) treated SF-295 cells. Relative to vehicle (DMSO) treated SF-295 cells, SF-295 cells treated with 1 ng/mL EGF + TTI-3066 for 24 hours seemed to show a non-significant decrease in phospho-MAPK(Thr202/204) levels. All effects on phospho-MAPK(Thr202/204) levels were more or less seen equally for two bands, believed to be different forms of phospho-MAPK (Fig. 17).

17A

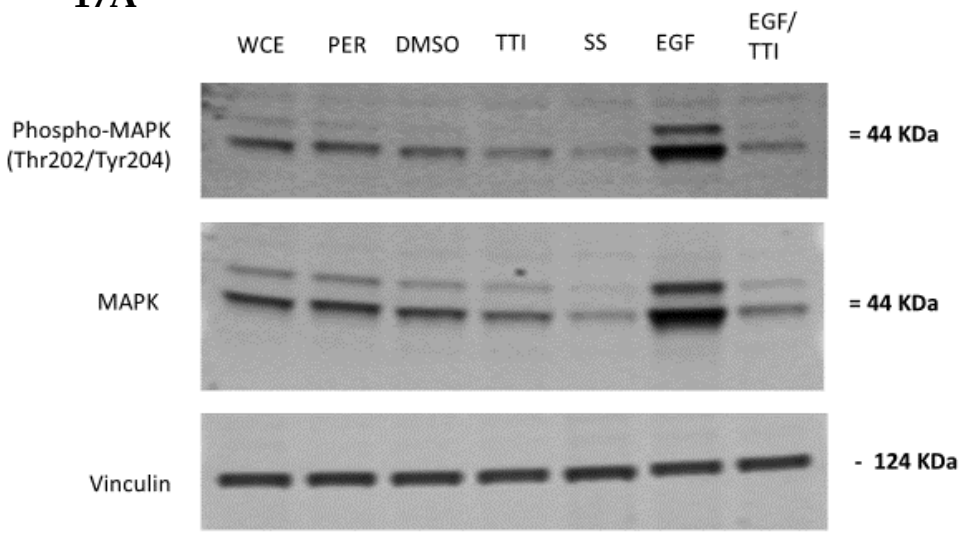
WCE
PER
DMSO
TTI
SS
EGF
EGF/
TTI
Phospho-MAPK
(Thr202/Tyr204)
= 44 KDa
MAPK
= 44 KDa
Vinculin
- 124 KDa

17B

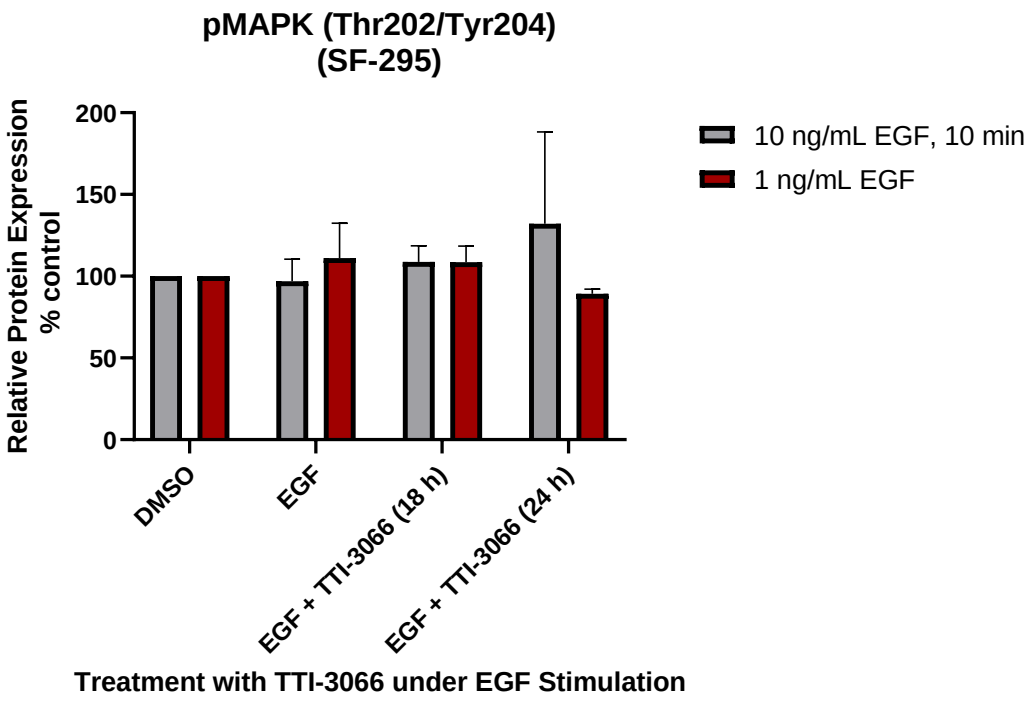
pMAPK (Thr202/Tyr204)
(SF-295)
Relative Protein Expression
% control
200
150
100
50
0
DMSO
EGF
EGF + TTI-3066 (18 h)
EGF + TTI-3066 (24 h)
10 ng/mL EGF, 10 min
1 ng/mL EGF
Treatment with TTI-3066 under EGF Stimulation

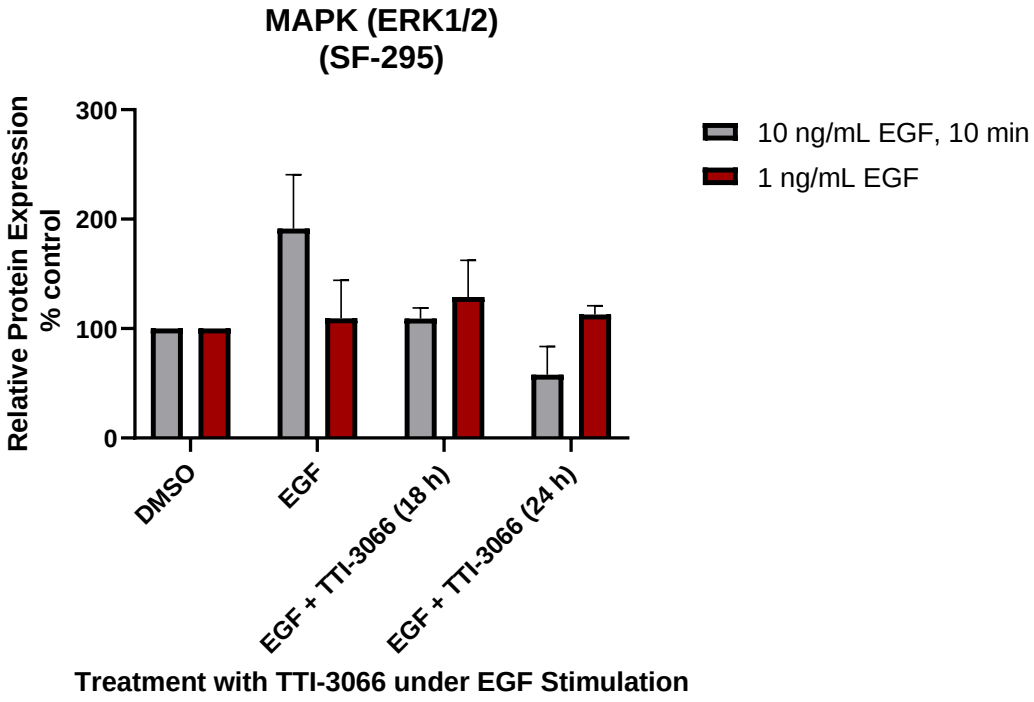
MAPK (ERK1/2)
(SF-295)
Relative Protein Expression
% control
300
200
100
0
DMSO
EGF
EGF + TTI-3066 (18 h)
EGF + TTI-3066 (24 h)
10 ng/mL EGF, 10 min
1 ng/mL EGF
Treatment with TTI-3066 under EGF Stimulation

Figure 17: Modification of EGF stimulation in SF-295 cells did not alter phospho-MAPK (Thr202/Tyr204) levels in response to combined EGF/TTI-3066 treatment. A) SF-295 cells were treated under an acute stimulation of EGF (10 ng/mL for 10 minutes after 3 hours of serum starvation) and at physiological concentrations of EGF (1 ng/mL for the duration of the experiment with EGF only treatment lasting 24 hours) with and without TTI-3066. The addition of EGF followed by TTI-3066 bolsters support that schweinfurthins dysregulate the PI3K/AKT pathway not the Ras/MAPK pathway in SF-295 cells. **B)** Quantification of blots were performed with Image Studio and GraphPad Prism software. Phospho-MAPK (Thr202/Tyr204) was normalized to MAPK. Values represent mean N=2. Note: blots do not necessarily reflect trends from graphs.

Chapter 5

Discussion

Schweinfurthins are natural compounds whose toxic effects are multi-faceted and effective against the cytoskeleton, the mevalonate pathway, small GTPase function, and cell fate [4,8]. Many of these properties are limited to cancer cells [4,8]. Additionally, based on high throughput testing by NCI, difficult-to-treat cancers like glioblastomas fall under the category of being sensitive to schweinfurthins [4,8]. Schweinfurthins, however, are not universally cytotoxic to all cancer cell lines. For instance, schweinfurthins are not selective against certain cancer cells, like those of non-small cell lung cancers [4,8]. Several studies that originate from our group cover the unique mechanism of action for schweinfurthins as well as other mevalonate pathway inhibitors. Notably, schweinfurthins have been demonstrated to synergize with lovastatin, sharing some characteristics with it in terms of mechanism, such as decreasing cholesterol and isoprenoid FPP and GGPP pools within cancer cells [8,12].

Isoprenoid substrates like FPP and GGPP are classically known to modify small GTPases, modulating not just their diverse activities, but also their localization at the membranes of different cell compartments [17,18,19,20,58,59,60,61,62]. One of the far-reaching effects, should prenylation be disrupted on small GTPases, has been well-documented in the case of EGFR signaling and lovastatin treatments [17]. Dimitroulakos et. al. 2010 reports that lovastatin treatments affect prenylation of RhoA, to the extent that EGFR activity is compromised [17]. Such activities range from lack of dimerization and phosphorylation of EGFR, to a reduction in downstream, coupled signaling between EGFR(Y1068) and AKT [15,17]. There is one study that links schweinfurthin-mediated cytotoxicities to an impairment in RhoA activity [10]. Turbyville et. al. 2010 suggests that EGF-induced RhoA-GTP levels decrease upon schweinfurthin

treatment, at least for malignant peripheral nerve sheath tumor cells [10]. This study implies that there may be similar effects in SF-295 glioblastoma cells as well [10]. Yet, schweinfurthin-mediated cytotoxicities are likely to be affected by more than just a lack of prenylation in RhoA small GTPases. These cytotoxicities, for instance, may be linked to effects related to EGFR processing, distribution, and signaling [7,18].

Deconstruction of this possibility begins with studies from our group with the use of an inhibitor to the RhoA family of proteins within SF-295 glioblastoma cells and A549 non-small cell lung cancer cells, two cancer cell lines that are sensitive and insensitive to the effects of schweinfurthins, respectively [11]. Noticeably, cytoskeletal changes from a RhoA inhibitor were not similar to that caused by schweinfurthins on these two cancer cell lines [11]. Further work from Irwin et. al. 2011 also suggests that changes in protein prenylation status from lovastatin may partially explain the loss of EGFR-mediated AKT activation [18]. These findings investigate breast cancer cell lines resistant to the effects of an EGFR tyrosine kinase inhibitor, gefitinib [18]. Activation of AKT did not decrease upon treatment with gefitinib for these cancer cell lines, despite the property of gefitinib to impair tyrosine kinase activity of EGFR [18]. AKT activation, however, decreased when gefitinib was combined with mevalonate pathway inhibitors, like a squalene synthase inhibitor or lovastatin, which deplete cholesterol [18].

Irvin et. al. 2011 rationalizes that the lack of an effect on AKT from gefitinib treatment within certain breast cancer cell lines may be due to EGFR proteins being sequestered to specific membrane compartments, lipid rafts, within gefitinib-resistant cells, not gefitinib-sensitive cells [18]. It is important to note that this explanation may overlook other aspects to lovastatin-mediated disruptions of EGFR-AKT signaling. Later studies using methyl-β-cyclodextrin to deplete membrane cholesterol indicate that EGFR still dimerizes, undergoes autophosphorylation, and signals to effectors like MAPK [63]. In other words, the effects of schweinfurthins are unlikely to be isolated to a decrease in cholesterol levels within lipid rafts or less prenylated RhoA levels.

Given the gaps in knowledge in mechanisms behind schweinfurthin-mediated toxicities in cancer cells, we proposed a hypothesis that looks at the effects of schweinfurthin analogs on SF-295 cells and A549 cells. Historical precedence exists with the use of these cancer cell lines to flesh out various pleiotropic aspects of schweinfurthins related, but not limited to, ER stress, p-glycoprotein transporters (ABCA1/ ABCG1), PKM2, OSBPs, and Hedgehog signaling [65]. Incidentally, both GBM and NSCLC cells have been reported to have high levels of EGFR, with reports that EGFR levels are two to three orders of magnitude higher in GBM lines and approximately 100,000 receptors/cell within A549 cells [36,37]. For the purposes of our experiments, EGFR itself was chosen as a valid candidate to generalize the effects of schweinfurthins to pro-survival signaling receptors. We hypothesize that schweinfurthins would selectively impair pro-survival signaling at the level of EGFR/Ras within SF-295 cells, not A549 cells. We rationalize that A549 cells, which are resistant to schweinfurthins, would have a mechanism of compensation against compromised EGFR/Ras activity after looking into various mutations within SF-295 cells and A549 cells that relate to EGFR. We suggest that this mechanism of compensation can be further probed into by zeroing in on the assumption that A549 cells may be able to signal downstream from EGFR due to an oncogenic mutation in

K-Ras. Additionally, several studies have suggested that the Ras family of small GTPases, and K-Ras, in particular, may have more adaptive capabilities to signal under conditions where FPP levels and cholesterol levels are depleted [21,33,55,57,58,59,60,61,62]. For instance, K-Ras, a farnesylated protein, does not necessarily require cholesterol for membrane localization and can alternatively be prenylated with a moiety from GGPP instead of FPP [21].

Another insight that led to this hypothesis relates to an observation that a multiple myeloma cancer cell line, RPMI-8226, displays slower reductions in fully modified Ras levels upon co-treatment with lovastatin and schweinfurthin [8,22]. Such an effect was not evident within another multiple myeloma cancer cell line, U266 [8,22]. This effect on Ras levels is similar to that seen with both of these cancer cell lines when treated with lovastatin alone [22]. This directed our attention towards potential mutations that may be involved, leading to the discovery that RPMI-8226 cancer cells have an oncogenic mutation in K-Ras [54].

We next investigated the sensitivities of these cancer lines to both schweinfurthins and lovastatin. The cytotoxic profiles of both compounds were similar in that RPMI-8226 cells were sensitive to the effects of schweinfurthins and/or lovastatin while U266 cells were resistant to the effects of schweinfurthins and/or lovastatin [8,22]. One potential reason for this is that RPMI-8226 cells are known to have lower total FPP/GGPP pools than U266 cells [22]. This led us to question whether cancer cells with higher basal levels of FPP/GGPP pools could be more susceptible to schweinfurthins if K-Ras was mutated.

An alternative readout for this hypothesis was specifically investigated based on the works of other researchers to simplify our investigations. A study by Bao et. al. 2015 reports the effects of schweinfurthins on the integrity of the trans-Golgi network, which disrupts the localization and signaling of glycoproteins [7]. A seminal finding from this investigation was the observation that the apparent molecular weight of EGFR was reduced as a consequence of less glycosylation/terminal sialylation, of these receptors [7]. This was loosely linked to impairment of the PI3K/AKT/mTOR pathway, though the connection was more a correlation according to western blot experiments from Bao et. al. 2015 [7].

Contrary to findings from Bao et. al. 2015, our group has not seen these schweinfurthin-mediated effects across all cancer cells [7]. SF-295 cells and A549 cells are sensitive and insensitive to the effects of schweinfurthins, respectively. Preliminary findings from our group supports an apparent decrease in molecular weight of EGFR seen within SF-295 cells, but not A549 cells [66]. This may explain schweinfurthin-mediated toxicities in cancer cells that are sensitive to schweinfurthins. As previously mentioned, EGFR, if not fully glycosylated or in its fully mature state, will display compromised dimerization and autophosphorylation for downstream signaling, which in turn, affects cell survival [7]. Although A549 cells display a decrease in total levels of EGFR, this is not likely to contribute to schweinfurthin-mediated cytotoxicities since AKT activity was found to not change like that in SF-295 cells [66].

It was surmised that treatments with schweinfurthins may lower EGF-induced activation of AKT in SF-295 and A549 cells, but that A549 cells may require a higher concentration of schweinfurthins to disrupt EGFR/AKT signaling [66]. Our group seeks to confirm these ideas and trends with additional experiments and to use downstream effectors of EGFR as readouts for differences in Ras signaling between both cancer cell lines.

Our first preliminary investigations began with MTT assays to determine the optimal concentrations of both TTI-3066 and TTI-4242 that ensure both cell viability and a schweinfurthin-mediated effect (Fig. 5). Two cancer cell lines with differential sensitivities to schweinfurthins (SF-295, GBM, sensitive; A549, NSCLC, resistant) were tested with each schweinfurthin analog (Fig. 5). Each compound was serially diluted to achieve logarithmic concentrations for generation of dose response curves and to approximate an EC_{50} for western blot experiments (Fig. 5). One of our two schweinfurthins came from a compromised stock, but was continued for the duration of MTT experiments to demonstrate the selective properties of schweinfurthins between SF-295 cells and A549 cells (Fig. 5). Based on a log dose response curve of TTI-3066 treatment in SF-295 cells, 100 nM was chosen as the concentration for treating SF-295 cells and A549 cells with the different schweinfurthins over a 24-hour time course (Fig. 5).

Detection of EGFR with an antibody indicates a maximum of three different EGFR species in vehicle (DMSO) treated SF-295 cells and A549 cells, though more may be present, but not spatially separated enough on SDS-PAGE (Fig. 6; Fig. 8). This was consistent with prior studies that revealed various glycosylated forms of EGFR ranging from fully modified and glycosylated, to partially modified and glycosylated, to even completely unmodified forms of EGFR. The fully glycosylated form(s) of the receptor displays basal levels of EGFR(Y1068) phosphorylation and EGFR(Y1173) phosphorylation seen in both cancer cell lines (Fig. 6; Fig. 8). Both cancer cell lines also display other EGFR species of lower apparent molecular weight, but these showed minimal to no phosphorylation at these residues (Fig. 6; Fig. 8). In some cases, the top two bands are believed to represent ligand-bound and unbound receptors since specific detection of phospho-EGFR(Y1068) or phospho-EGFR(Y1173) with an antibody reveals more than one band with a positive signal for phosphorylation (Fig. 6; Fig. 8).

Glycosylated mature EGFR within our experiments runs at 170-175 kDa, which is also consistent with prior studies (Fig. 6; Fig. 8). Addition of either schweinfurthin to SF-295 cells results in an apparent reduction in molecular weight of EGFR ~6 to 12 hours into treatment (Fig. 6; Fig. 8). Detection of phospho-EGFR(Y1068) or phospho-EGFR(Y1173) with an antibody within these cells reveals a non-significant trend towards an increase in phosphorylation for these partially modified, immature species of EGFR (Fig. 6; Fig. 8). This appearance of EGFR plus the shift in phosphorylation towards lower apparent molecular weight species was only seen in SF-295 cells, not A549 cells (Fig. 6; Fig. 8).

Together, these results may signify an uncoupling of EGFR from AKT, as suggested by Bao et. al. 2015, and may extend to an uncoupling between EGFR and MAPK.

This latter relationship was looked into within a custom panel of cancer cell lines. Results from this analysis do not show this to be the case in Bao et. al. 2015, but was re-evaluated in SF-295 cells and A549 cells. This was done in the context of asking whether or not schweinfurthins could selectively impair MAPK activation in these two cancer cell lines. Several of the trends with regards to detection of phospho-EGFR(Y1068) and phospho-EGFR(Y1173) levels within schweinfurthin-treated SF-295 cells have, despite non-significance, substantial effect sizes at multiple time points of treatments (Fig. 6; Fig. 8). Variability within results was a setback in the execution of these experiments since signal intensity of the bands, as detected by phospho-EGFR antibodies, was low. Though not pursued in these experiments, primary antibodies were replaced such that each phospho-specific antibody was from a different species. This allowed for detection to be pursued sequentially after washing blot(s) thoroughly, without need to strip after each probe. This and subsequent optimization of cell numbers (per treatment plate) in the following experiments overcame the issues faced within this experiment.

Our next approach was to investigate how TTI-3066 and TTI-4242 affected the activation of AKT, one of several downstream effectors of EGFR. Detection of AKT with a specific antibody displays most often two bands, but sometimes one band, for AKT seen in vehicle (DMSO) treated SF-295 cells and vehicle (DMSO) treated A549 cells (Fig. 7; Fig. 9). The top band was believed to represent the phosphorylated form of AKT while the bottom band was believed to represent the non-phosphorylated form of AKT in both cancer cell lines (Fig. 7; Fig. 9). Treatment with either schweinfurthin reveals a time-dependent decrease in phospho-AKT(S473) levels within SF-295 cells that matches the time-frame in which phospho-EGFR(Y1068) levels shifted to lower apparent molecular weight forms of EGFR (Fig. 7; Fig. 9). A reduction in phospho-AKT(S473) signals was not evident in schweinfurthin-treated A549 cells (Fig. 7; Fig. 9). In both cancer cell lines, phospho-AKT(S473) bands overlay the top band of AKT, captured via chemiluminescence and film (Fig. 7; Fig. 9).

Subsequent experiments investigated the effect of TTI-3066 on the activation of MAPK in both SF-295 cells and A549 cells (Fig. 10). Detection of MAPK with an antibody displays two bands for MAPK, which are believed to represent ERK1 and ERK2 within both cancer cell lines (Fig. 10). Levels of MAPK fluctuated upon treatment with schweinfurthins in both SF-295 cells and A549 cells, with the levels of both bands going up or down in unison (Fig. 10). This may either be due to a biologically relevant response to schweinfurthins or, more likely, reflects little effect of schweinfurthins on total MAPK levels.

A Ras-mediated phosphorylation site on MAPK (Thr202/Tyr204) was investigated with a specific antibody to see whether or not TTI-3066 could have a selective effect on MAPK activation, dependent on the type of cancer cell line. Detection of phospho-MAPK(Thr202/Tyr204) revealed some variation of signal across the blots (Fig. 10). Normalization of the data, however, suggests that treatments with TTI-3066 induce a time-dependent decrease in phospho-ERK(1/2) levels within SF-295 cells when compared to vehicle (DMSO) treated SF-295 cells (Fig. 10). TTI-3066 did not display this effect in A549 cells, with phosphorylation levels at this site comparable to that of vehicle (DMSO) treated A549 cells (Fig. 10). These results suggest that schweinfurthins, concordant with our own preliminary data and in contrast to findings by Bao et. al., may impair EGFR-mediated activation of AKT and MAPK in a differential manner (Fig. 10). These findings support that only SF-295 cells, not A549 cells, are impacted at the level of EGFR phosphorylation, with much of the phosphorylation taking place at lower apparent molecular weight forms of EGFR. Although this effect is a trend without significance, downstream AKT phosphorylation is reduced significantly and selectively in SF-295 cells, not A549 cells, upon schweinfurthin treatment. Another non-significant pattern that may be biologically relevant, given the large effect sizes, is that Ras-mediated MAPK activation may be impaired in schweinfurthin-sensitive SF-295 cells, not schweinfurthin-insensitive A549 cells.

Decreases in glycosylation and impaired signaling between EGFR and AKT/MAPK were investigated with a set of controls to further support the proposed, differential mechanism of schweinfurthins (Fig. 11). SF-295 cells were treated with various inhibitors alongside both SF-295 cells treated with TTI-3066 and SF-295 cells treated with EGF/TTI-3066 (Fig. 11). Detection of EGFR with an antibody indicates that both conditions showed a shift in apparent molecular weight of EGFR towards lower apparent molecular weight/immature forms

of EGFR (Fig. 11). Tunicamycin was one of the two controls used to show what species of EGFR are formed when N-linked glycosylation is impaired (Fig. 11). Tunicamycin is a classical choice for inhibition of N-linked glycosylation since it impairs the very first step in N-linked glycan processing in the endoplasmic reticulum [27]. Tunicamycin at nanomolar concentrations prevents the transfer of N-linked glycans to dolichol, while higher concentrations have been reported to induce ER-stress. Consistent with several studies that use tunicamycin at concentrations between 1 to 10 µg/mL for impairment of N-linked glycosylation, we chose a concentration of 10 µM of tunicamycin for subsequent treatments (Fig. 11) [67,68].

Treatments with tunicamycin decreased the apparent molecular weight of EGFR from ~175kDa to 130 kDa in SF-295 cells, in agreement with what was previously reported in the literature (Fig. 11) [27,46,48,49,51]. However, detection of EGFR with an antibody displayed a higher intermediate species of EGFR (~160 to 170 kDa) in SF-295 cells treated with tunicamycin (Fig. 11). This EGFR species matches the slow-migrating appearance of the immature form(s) of EGFR seen in SF-295 cells treated with schweinfurthins (Fig. 11). Preliminary work contrasted the effects of tunicamycin with another N-linked glycosylation inhibitor that works at the level of the Golgi, swainsonine (not shown) [27]. Detection of EGFR with an antibody shows that both inhibitors share identical band patterns, where mostly partially modified receptors were seen (not shown). One explanation for this result could be that schweinfurthins, tunicamycin, and swainsonine are capable of impairing N-linked glycan addition at the level of terminal sialyl residues. This loss of sialyl residues on EGFR, as opposed to other protein-level changes, was tested with a glycan trimming enzyme/glycosidase, PNGase F (Fig. 11) [51]. PNGase F treatment on SF-295 lysates was indeed found to produce this form of EGFR, as detected by anti-EGFR (Fig. 11). If this explanation turns out to be the case, this could lend complexity to the interpretation of data from Bao et. al. 2015.

Though a loss of terminal sialyl residues from EGFR may be mediated by schweinfurthins, the loss of glycans from EGFR may not be strictly limited to processes within the trans-Golgi/trans-Golgi network.

Tyrosine phosphorylation on EGFR dictates downstream signaling, depending on which site gets phosphorylated. Schweinfurthin treatments may impair the subsequent signal transduction between EGFR and its effectors, though not all the data was significant to support such an effect. To re-evaluate the impact that schweinfurthins have on the phosphorylation state of EGFR at Y1068 or Y1173, we relied on experiments above in which SF-295 cells were treated with various inhibitors (Fig. 11). Additionally, both SF-295 cells treated with TTI-3066 as well as SF-295 cells treated with 10 ng/mL EGF + TTI-3066 were tested alongside these inhibitors (Fig. 11). Along with tunicamycin, SF-295 cells were treated with perifosine, an AKT inhibitor, to compare its effects on AKT to that of schweinfurthins on AKT (Fig. 11). Perifosine is known to exert toxic effects on tumor cells, partly through decreased membrane recruitment, which in turn, reduces subsequent phosphorylationon AKT (Fig. 11) [69]. Additionally, perifosine has also been shown to decrease MAPK phosphorylation (Fig. 11) [69]. This goes well with our understanding that the AKT pathway and MAPK pathway interact with one another [40].

Given our combined EGF/TTI-3066 treatment, SF-295 cells were also treated with 10 ng/mL EGF as a check to see if both the AKT pathway and MAPK pathway were activated (Fig. 11). SF-295 cells treated with TTI-3066 along with SF-295 cells treated with EGF/TTI-3066 show a reduction in the lower apparent molecular weight of EGFR and an induction in phospho-EGFR(Y1068) and phospho-EGFR(Y1173) expression relative to that seen in vehicle (DMSO) treated SF-295 cells (Fig. 11). In contrast, vehicle (DMSO) treated SF-295 cells and EGF-treated SF-295 cells display one band believed to be the mature form of EGFR upon detection with an antibody against EGFR (Fig. 11). Detection of phospho-EGFR at Y1068 and Y1173 reveals detectable phosphorylation of the mature form of EGFR in both vehicle

(DMSO) treated SF-295 cells and EGF-treated SF-295 cells (Fig. 11). However, the level of increased phosphorylation seen in EGF-treated SF-295 cells compared to vehicle (DMSO) treated SF-295 cells is several magnitudes higher (Fig. 11). Quantification of this phosphorylation in EGF-treated SF-295 cells is likely outside linear ranges of detection, but was included in the data analysis for comparisons.

Subsequent experiments to confirm whether schweinfurthin-mediated shifts in phosphorylation towards immature forms of EGFR would have implications on AKT and MAPK signaling were investigated in the context of these controls. Detection of AKT with an antibody reveals that AKT levels are unaffected in SF-295 cells treated with TTI-3066, EGF/TTI-3066, EGF, and perifosine relative to vehicle (DMSO) treated SF-295 cells (Fig. 12). Analysis of MAPK levels by an antibody also reveals similar lack of change in MAPK levels with the exception of EGF-treated SF-295 cells (Fig. 13). This treatment showed an increase in MAPK levels relative to vehicle (DMSO) treated SF-295 cells (Fig. 13). TTI-3066 treated SF-295 cells, with and without EGF stimulation, and perifosine-treated SF-295 cells showed a decrease in phospho-AKT(S473) expression when compared to vehicle (DMSO) treated SF-295 cells according to phospho-AKT(S473) detection with an antibody (Fig. 11). In contrast, none of the treatments showed changes in phospho-ERK(1/2) (Thr202/204) expression when compared with vehicle (DMSO) treated SF-295 cells, a finding that contradicts initial suspicions that schweinfurthins may cause a decrease in phospho-ERK(1/2) (Thr202/204) levels within 24 hours (Fig. 13). To focus on the coupling status of EGFR(Y1068) and phospho-AKT, EGF treated SF-295 cells did not show a stimulation of phospho-ERK(1/2) nor phospho-AKT expression when probed with the mentioned antibodies (Fig. 12; Fig. 13). Therefore, our studies fell short in confirming that changes in phospho-EGFR (Y1068) expression are closely tied to schweinfurthin-mediated decreases in phospho-AKT expression since it is not certain whether and for how long AKT could have been activated by EGF treatment.

The mass action effect of EGF on EGFR(Y1068) levels suggests that the EGFR-AKT arm of the signaling pathway was activated, but was suppressed by potential internalization and routing of ligand-bound EGFR to endosomes/lysosomes [70,71,72,73,74]. This latter routing may or may not be the case in our experiments. On the one hand, total EGFR expression, as detected by an antibody against EGFR, went down in EGF/TTI-3066 treated SF-295 cells when compared to the levels seen in EGF- and vehicle (DMSO)- treated SF-295 cells (Fig. 11). However, SF-295 cells treated with TTI-3066 also displayed similar decreases in EGFR expression relative to EGF/TTI-3066 SF-295 cells, a finding that wasn't evident in our prior studies above and cannot be fully explained (Fig. 11). The only thing that can be said is that cells in this experiment were grown in RPMI-1640 medium lacking 4 mM supplementation of L-Gln and from lower cell passages which are both differences made in this experiment. Both changes were made in order to reduce cell clumps and improve plating densities of cell number for western blot analyses. Phospho-EGFR(Y1068) levels between TTI-3066 treated SF-295 cells and EGF/TTI-3066 treated SF-295 cells were also similar to one another as detected by an antibody (Fig. 11). The observation that EGF/TTI-3066 treated SF-295 cells had vastly lower levels of phospho-AKT(S473) expression compared TTI-3066 treated SF-295 cells seems to suggest that pre-conditioning of SF-295 cells with high EGF concentrations may increase sensitivity of cells to schweinfurthins than just schweinfurthin treatment alone (Fig. 12). Indeed, some reports have suggested that endosomal EGFR signals differently from EGFR found on the plasma membrane [74]. Both EGFR pools, however, can interact with some of the same effector proteins, such as the p85 subunit of PI3K [74]. With regards to EGFR levels in TTI-3066 treated cells, this experiment may warrant further investigations into observing surface levels of EGFR and its trafficking. Future experiments to address this issue include surface biotinylation/immunoprecipitation of EGFR in schweinfurthin-treated cells before western blots or live cell imaging to track EGFR dynamics in schweinfurthin-treated cells.

Research into the re-design of an experiment to address whether schweinfurthins affect the coupling of EGFR to downstream effectors led to a quandary of sorts. EGF addition was modified such that serum starvation was kept to 3 hours before stimulation of cells with EGF for 10 minutes at 10 ng/mL (Fig. 15; Fig. 16; Fig. 17). This was thought to enable recycling of EGFR to the cell surface such that downstream effectors like AKT can undergo activation, as shown by some preliminary data (data not shown). An alternative to this method is described in the literature. Physiological concentrations of EGF have been estimated to range between 0.5-2 ng/mL in a tumor microenvironment [72]. As such, low concentrations of EGF stimulation have been tested for a period of up to 12 hours, with reports indicating that this level of EGF addition activates AKT, as measured by increases in phospho-EGFR(Y1068) levels [72]. On the other hand, it is uncertain if A549 cells could remain insensitive to schweinfurthins after EGF stimulation, especially against schweinfurthin-mediated reductions in mature EGFR and phospho-AKT levels. Therefore, we tested two different conditions of EGF stimulation in SF-295 cells and A549 cells. One condition consists of EGF stimulation for 10 minutes at 10 ng/mL (with the optimizations described above) before schweinfurthin treatment. The other condition consists of a co-incubation of schweinfurthin with EGF at 1 ng/mL. Positive controls for EGF-induced activation of AKT and MAPK were included with addition of EGF under the described conditions without schweinfurthin addition.

Detection of EGFR with an antibody indicates that SF-295 cells under vehicle (DMSO) treatment express at least three different forms of EGFR in which the topmost band represents the mature form and the bottom bands represents partially modified, “immature” forms of the receptor (Fig. 15). Treatments with 1 ng/mL of EGF display a loss of the topmost band seen in vehicle (DMSO) treated SF-295 cells, believed to be the mature form of the receptor (Fig. 15). This loss is not increased nor reversed in SF-295 cells treated with 1 ng/mL of EGF and schweinfurthin (Fig. 15). At first glance, SF-295 cells that are stimulated with 10 ng/mL of EGF

seem to display little changes in the glycosylation of mature EGFR, when compared to SF-295 cells treated with vehicle (DMSO) (Fig. 15). This seemed to be the case even within SF-295 cells treated with 10 ng/mL EGF + TTI-3066 (Fig. 15). However, detection of EGFR in its phosphorylated state with two site-specific antibodies reveals that the topmost band of EGFR may be at a higher apparent molecular weight in SF-295 cells treated with 10 ng/mL of EGF than that seen in SF-295 cells treated with 10 ng/mL of EGF, followed by schweinfurthin (Fig. 15). Not only that, SF-295 cells treated with 10 ng/mL of EGF display a spike in EGFR levels relative to vehicle (DMSO) treated SF-295 cells (Fig. 15). This spike does not go down when this EGF concentration is combined with TTI-3066 in SF-295 cells, as detected by an antibody against EGFR (Fig. 15). This is consistent with ideas that EGF can create a positive feedback loop to increase expression of EGFR [75].

Detection of phospho-EGFR(Y1068) levels with an antibody was pursued within SF-295 cells treated with either 10 ng/mL of EGF alone or with 10 ng/mL of EGF + TTI-3066 (Fig. 15). Detection of EGFR from vehicle (DMSO) treated SF-295 cells revealed various forms of EGFR, as seen with an antibody directed against EGFR (Fig. 15). Relative to this, apart from the topmost band (which may encompass mature and immature species), all other intermediate forms of EGFR are phosphorylated at Y1068 within vehicle (DMSO), 10 ng/mL EGF, and 10 ng/mL EGF + TTI-3066 treated SF-295 cells (Fig. 15). Much of the effects of EGF and schweinfurthin, therefore, are believed to be most directed at the levels of the topmost band seen in vehicle (DMSO) treated SF-295 cells, as detected from an antibody against phospho-EGFR(Y1068) (Fig. 15). Comparisons between this band in SF-295 cells that were treated with vehicle (DMSO) to the topmost band seen SF-295 cells treated with 10 ng/mL of EGF indicatesa migratory difference for mature forms of EGFR (Fig. 15). According to phospho-EGFR(Y1068) detection with an antibody, SF-295 cells treated with 10 ng/mL EGF showed a band that is higher in apparent molecular weight than the topmost band seen in vehicle

(DMSO) treated SF-295 cells (Fig. 15). In addition to this top band in EGF-treated cells, detection with phospho-EGFR(Y1068) antibody also revealed that SF-295 cells treated with 10 ng/mL EGF have an additional band that is phosphorylated at Y1068, in a lower (maybe similar) position to that of vehicle (DMSO) treated SF-295 cells (Fig. 15). It is believed the topmost band within SF-295 cells treated with 10 ng/mL EGF predominantly represents mature species of EGFR that are bound to EGF (Fig. 15). Treatment with TTI-3066 after pre-conditioning of SF-295 cells with 10 ng/mL of EGF shows that schweinfurthin treatment reduced levels of phospho-EGFR (Y1068) from that seen when SF-295 cells were stimulated with 10 ng/mL EGF (Fig. 15). Detection of phospho-EGFR(Y1068) expression with an antibody reveals this shift in phosphorylation, such that vehicle (DMSO) treated SF-295 cells have about the same pattern and level of phosphorylation as that seen in EGF/TTI-3066 treated SF-295 cells (Fig. 15).

It may be possible that the topmost band seen in vehicle (DMSO) treated SF-295 cells, as detected by an antibody against phospho-EGFR(Y1068), is slightly higher in apparent molecular weight than that seen in SF-295 cells treated with EGF/TTI-3066 (Fig. 15). However, band separation, a limitation in this experiment, hindered comprehensive interpretation (Fig. 15). Hence, EGF/TTI-3066-treated SF-295 cells are believed to display phosphorylated, immature forms of EGFR based on this potential difference in migration, as detected with an antibody against phospho-EGFR (Y1068) (Fig. 15). An explanation for these results is that EGF pre-conditioning of cells may buffer, but not completely eliminate, glycosylation defects on EGFR brought about by schweinfurthins (Fig. 15). It is also presumed that schweinfurthins interfere with EGF binding to EGFR, according to signals detected with anti-phospho-EGFR(Y1068) (Fig. 15). As mentioned, EGF-treated SF-295 cells display phosphorylation of the topmost band/mature forms of EGFR (Fig. 15). In contrast, EGF/TTI-3066-treated SF295 cells lack any phosphorylation at this position, as detected by

anti-phospho-EGFR(Y1068), likely due to the case that there might be a loss of mature EGFR within these cells (Fig. 15). An alternative explanation that overlooks band separation issues is the idea that EGF may be masking schweinfurthin-mediated deglycosylation events taking place during EGFR synthesis since EGF recycling of mature EGFR receptors might be able to sequester/shield some receptors from schweinfurthin-mediated effects.

Phospho-EGFR(Y1173) levels were next evaluated with an antibody against this specific site in SF-295 cells treated either with 10 ng/mL of EGF alone or 10 ng/mL EGF + TTI-3066 (Fig. 15). Detection with this antibody revealed two to three bands for phospho-EGFR(Y1173) expression for all treatments (Fig. 15). It is important to note that, based on the overlay of bands detected using antibodies against EGFR and phospho-EGFR(Y1173), respectively, that the bottommost band detected by phospho-EGFR(Y1173) represents a non-specific protein unrelated to EGFR (Fig. 15). This was not considered in the details of the results except in the figures for brevity and will not be counted hereafter in this discussion of various phospho-EGFR(Y1173) bands detected with this antibody.

SF-295 cells treated with vehicle (DMSO) displayed, for the most part,two different phospho-EGFR(Y1173) forms, as detected by an antibody against this phospho-EGFR site (Fig. 15). The topmost band is believed to represent phosphorylation of the mature form of EGFR while the bottom band is believed to represent phosphorylation of a partially modified form of EGFR (Fig. 15). Overall levels of these phospho-species seen in vehicle (DMSO) treated SF-295 cells, as detected by an antibody against phospho-EGFR(Y1173), increased within SF-295 cells treated with 10 ng/mL of EGF (Fig. 15). The topmost band detected within these EGF-treated SF-295 cells smears upward, as detected by an antibody against phospho-EGFR(Y1173) (Fig. 15). This believe to be EGF bound, mature EGFR species within SF-295 cells treated with 10 ng/mL EGF (Fig. 15). Detection of phospho-EGFR at Y1173 with an antibody reveals that the phosphorylation pattern of EGFR(Y1173) seen in EGF/TTI-3066 treated SF-295 cells is more or

less similar to that of vehicle (DMSO) treated SF-295 cells (Fig. 15). The main exception to this observation is that the topmost band of this phosphorylation pattern in SF-295 cells treated with EGF/TTI-3066 is of lower apparent molecular weight than that seen in vehicle (DMSO) treated SF-295 cells (Fig. 15).This is believed to signify not only the loss of EGF-bound receptors that were seen in EGF treated SF-295 cells, but also a loss of glycosylation from these receptors (Fig. 15).

Results from detection of EGFR and phospho-EGFR(Y1173), with two different antibodies, indicates that a partially modified/immature form of EGFR may be co-migrating at the same position on SDS-PAGE as the fully modified/mature form of EGFR (Fig. 15). However, because of limited band separation from SDS-PAGE, the most assured conclusion from data derived from anti-phospho-EGFR(Y1173) is that SF-295 cells treated with 10 ng/mL of EGF + TTI-3066 display an increase in phospho-EGFR(Y1173) expression for the bottommost band (Fig. 15). This phosphorylation, detected with an antibody against phospho-EGFR(Y1173), was not seen in vehicle (DMSO) treated SF-295 cells (Fig. 15). This suggests that SF-295 cells pre-condition with 10 ng/mL EGF and treated with schweinfurthins display more apparent loss of phosphorylation for mature EGFR species than that seen in SF-295 cells treated with 10 ng/mL EGF alone (Fig. 15).

SF-295 cells treated with 1 ng/mL EGF for 24 hours, or with 1 ng/mL EGF + TTI-3066 for 18 to 24 hours, display results that hint at SF-295 cells being treated with higher concentrations of EGF than anticipated (Fig. 15). One explanation for this is that prior research conducted on low levels of continuous EGF treatment had only reported phospho-EGFR signals present after 12 hours, not 24 hours of EGF treatment [72]. Detection with an antibody against phospho-EGFR(Y1173) expression reveals mostly one (maybe two) species of EGFR within these sets of treatments and a lack of the topmost band seen in vehicle (DMSO) treated SF-295 cells (Fig. 15). These species, also present in vehicle (DMSO) treated SF-295 cells, are

believed to represent partially modified form(s) of EGFR (Fig. 15). With regards to EGFR expression, as detected with an antibody against EGFR and based on quantifications, SF-295 cells treated with 1 ng/mL of EGF for 24 hours show a decrease in EGFR levels when compared to that seen in vehicle (DMSO) treated SF-295 cells (Fig. 15). This decrease was mitigated, however, with the combined treatment of 1 ng/mL EGF and TTI-3066 in SF-295 cells, as detected by an antibody against EGFR (Fig. 15). In sum, phosphorylation of EGFR at Y1068 within SF-295 cells treated with either 1 ng/mL EGF or1 ng/mL EGF + TTI-3066 displayed signals that overlay those of partially modified forms of EGFR upon detection with an antibody against phospho-EGFR(Y1068) (Fig. 15). Detection with an antibody against phospho-EGFR(Y1173) within SF-295 cells treated with either 1 ng/mL EGF or 1 ng/mL EGF + TTI-3066 also displayed signals that overlay that of partially modified forms of EGFR seen in vehicle (DMSO) treated SF-295 cells (Fig. 15). We continued these experiments to see whether downstream effector pathways were activated or not, despite the negative effects of continuous EGF treatment within SF-295 cells on both the levels and phosphorylation of
mature EGFR species.

AKT activation became a prime focus in our investigations to address whether or not TTI-3066 had a de-coupling effect on EGFR and AKT interactions. Detection of AKT with an antibody revealed two species of AKT within most treatments of SF-295 cells (Fig. 16).
As mentioned, these species are believed to represent a phosphorylated form of AKT, if at a higher apparent molecular weight, or non-phosphorylated form of AKT (Fig. 16). Detection with anti-AKT indicates that SF-295 cells treated with 10 ng/mL of EGF display an increase in signal for the top band of AKT and a decrease in signal for the bottom band of AKT, relative to vehicle (DMSO) treated SF-295 cells (Fig. 16). This is consistent with expectations that EGF treatment would increase phospho-AKT levels (Fig. 16). SF-295 cells treated with both 10 ng/mL of EGF and TTI-3066 showed an altered distribution of signal for the two bands of AKT, as detected with

an antibody against AKT (Fig. 16). The top band of AKT showed less signal intensity compared to the bottom band in two out of three replicates of SF-295 cells treated with 10 ng/mL EGF and TTI-3066 when compared to SF-295 cells treated with vehicle (DMSO) (Fig. 16). This change in AKT levels in SF-295 cells upon addition of schweinfurthin after EGF stimulation is believed to reflect schweinfurthin-mediated reductions in EGF-induced AKT activation (Fig. 16).

Overall AKT levels in SF-295 cells treated with 10 ng/mL EGF and TTI-3066 were similar to that of vehicle (DMSO) treated SF-295 cells (Fig. 16). SF-295 cells treated for 24 hours with 1 ng/mL of EGF also displayed a pattern of AKT levels, as detected by an antibody specific to AKT, similar to that seen in SF-295 cells treated with 10 ng/mL of EGF (Fig. 16). Detection of AKT levels with an antibody reveal AKT levels within SF-295 cells treated with 1 ng/mL EGF was less than that seen in vehicle (DMSO) treated SF-295 cells (Fig. 16). Addition of TTI-3066 with 1 ng/mL EGF in SF-295 cells did not return AKT levels back to that seen in vehicle (DMSO) treated cells (Fig. 16). Instead, SF-295 cells co-treated with 1 ng/mL EGF and TTI-3066 displayed similar patterns and levels of AKT to that seen in SF-295 cells treated with 1 ng/mL EGF (Fig. 16).

Detection of AKT activation was monitored at phospho-AKT(S473), one of two sites on AKT needed for full activation of AKT activity (Fig. 16). As expected, and in agreement with findings from detection with an AKT antibody, treatment of SF-295 cells with 10 ng/mL of EGF stimulated higher phospho-AKT levels relative to that seen in vehicle (DMSO) treated SF-295 cells (Fig. 16). This signal was confirmed through use of an antibody against phospho-AKT(S473) (Fig. 16). Relative to this EGF treatment within SF-295 cells, treatment of SF-295 cells with 10 ng/mL of EGF followed by TTI-3066 led to a time-dependent decrease in phospho-AKT(S473) levels, according to signals from a phospho-AKT(S473) antibody (Fig. 16). Results from SF-295 cells treated with 1 ng/mL of EGF also showed an increase in phospho-AKT(S473) levels in two out of three experiments (Fig. 16). However, treatments of

1 ng/mL of EGF alongside TTI-3066 did not show a significant decrease in phospho-AKT(S473) levels when applying an antibody against this site, with the exception of one experiment and at the 24-hour timepoint (Fig. 16). The analyses of this decrease was compared to the relative phospho-AKT(S473) signal seen in vehicle (DMSO) treated SF-295 cells (Fig. 16).

To conclude, in at least one of our two EGF conditions, schweinfurthin was able to diminish activation of AKT induced by EGF and likely decouples EGFR from downstream AKT activation. Tracking of phospho-EGFR(Y1068) levels also suggests that schweinfurthins can impair EGF-induced increases in phospho-EGFR(Y1068) levels on mature species of EGFR.

Similar experiments were also performed in A549 cells to see what EGF stimulation before TTI-3066 addition would do to cells (Fig. 15). Detection of EGFR with an antibody reveals that there are at least three forms of EGFR are present in vehicle (DMSO) treated A549 cells (Fig. 15). Many of the treatments, including stimulation of A549 cells with 1 ng/mL of EGF, did not increase nor decrease total levels or individual levels of different species of EGFR relative to vehicle (DMSO) treated A549 cells (Fig. 15). Treatment of A549 cells with 10 ng/mL of EGF was sometimes able to induce an upward smear in the topmost band of EGFR, believed to be the mature form of the receptor (Fig. 15). Total levels of EGFR, however, was not quantitatively different from that seen in A549 cells treated with vehicle (DMSO) (Fig. 15). This smear also was not seen when EGF at this concentration was combined with TTI-3066 in A549 cells (Fig. 15). Detection of EGFR phosphorylation at Y1068 and Y1173 using two site-specific antibodies indicates that the combination of EGF/TTI-3066 treatment was able to reduce phospho-EGFR levels away from that seen when A549 cells are treated with 10 ng/mL of EGF (Fig. 15). Instead, phospho-EGFR levels moved towards levels seen in A549 cells treated with vehicle (DMSO) (Fig. 15). Phospho-EGFR levels did not respond to treatments with

1 ng/mL of EGF nor did it change with the co-treatment of 1 ng/mL of EGF and TTI-3066 when detected with a specific antibody towards the phospho-Y1068 or phospho-Y1173 site on EGFR (Fig. 15). These levels, as detected by both a phospho-EGFR(Y1068) antibody and a phospho-EGFR(Y1173) antibody were comparable to that seen in vehicle (DMSO) treated A549 cells where all forms of EGFR are phosphorylated (Fig. 15). The most abundant phospho-form of EGFR seen in all treatments was predominantly the topmost band/mature form of the receptor (Fig. 15). Treatments seemed to not appear to change pAKT(S473)/AKT levels, though quantification of the bands did reveal some fluctuation of in both pAKT(S473) levels and AKT levels (Fig. 16). These level changes in pAKT(S473) and AKT expression are not believed to reflect a significant biological phenomenon nor an altered change in the resistance of these cells to schweinfurthin-mediated effects on EGFR-AKT signaling.

Additional experiments were conducted in SF-295 cells to see if different conditions of EGF combined with schweinfurthin treatment would reveal a time-dependent decrease in Ras-mediated activation of phospho-MAPK expression (Fig. 17). Contrary to the above findings on phospho-EGFR(Y1173) levels within schweinfurthin-treated SF-295 cells, phospho-MAPK expression was not reduced or increased by combined EGF/TTI-3066 treatment, despite attempts to elevate phospho-MAPK levels with the two EGF conditions (Fig. 17). In sum, these findings suggest that the K-Ras mutation in A549 cells is unlikely to enhance the survival of these cells via the canonical pathways in which Ras proteins are known to function. The hypothesis that K-Ras has some sort of a protective effect on A549 cells that confers schweinfurthin resistance, not seen in SF-295, we believe, is still valid. However, it may not be within the scope of A549 cells showing enhanced AKT or MAPK activation upon schweinfurthin treatment.

To revisit this hypothesis, other effects were considered in the off-chance that they may be involved in an interaction with an oncogenic K-Ras mutant protein. Due to observations that this protein accumulates loss of prenylation slowly upon schweinfurthin treatment, it is believed

that the K-Ras mutation within cancer cell lines confers resistance against schweinfurthin toxicities [8,22]. One route of investigation was to look into the possibility that the endoplasmic reticulum could be influencing the glycosylation status and the apparent molecular weight of EGFR (Fig. 14). We chose to study the effects of schweinfurthin on low density lipoprotein receptor (LDLR), with a focus on how TTI-3066 treated, EGF/TTI-3066 treated, and tunicamycin treated SF-295 cells alters the apparent molecular weight of LDLR when compared to vehicle (DMSO) treated SF-295 cells (Fig. 14). We chose to investigate LDLR to learn more about EGFR as LDLR is also a glycoprotein, with 11 to 12 O-linked glycans that are different in structure from N-linked glycans [76,77,78,79]. The important exception to this is that these O-linked glycans are also modified with terminal sialyl groups derived from the trans-Golgi/trans-Golgi network [76,77,78,79]. Compared to the fully modified version of LDLR, which has an apparent molecular weight ~150-160 kDa, the precursor form of LDLR is much smaller at 135 KDa [76,77,78,79]. Tunicamycin treatments on transformed HEK293 with LDLR expression shifts the apparent molecular weight of LDLR to 135 kDa, supporting other reports that LDLR also has N-linked glycosylation on at least two asparagine sites [76,77,78,79]. As an aside, we also took note at how LDLR levels would change in response to schweinfurthins for several reasons. First, our group has shown that schweinfurthins can affect cholesterol homeostasis on the transcriptional level in cancer cell lines both sensitive and resistant to the effects of schweinfurthins [8]. Additionally, certain findings suggest that oncogenic EGFR, when stimulated with EGF, activates the transcriptional activity of sterol response element binding proteins that transcribe LDLR and increases its levels upon activation of the
EGFR-AKT pathway [80].

Detection of LDLR with an antibody had been looked at before over a time-course to see if TTI-3066 changes LDLR levels in SF-295 cells. Preliminary findings (not shown) did not appear to indicate any changes in LDLR levels relative to vehicle (DMSO) treated SF-295 cells.

However, while detection of LDLR does not suggest that TTI-3066 or EGF/TTI-3066 treatments in SF-295 cells have an effect on LDLR levels, quantification of western blots suggests an increase in LDLR expression from both treatments relative to vehicle (DMSO) treated SF-295 cells (Fig. 14). In the context of these results, it may be that wild type EGFR and its signaling activity may not overlap with the regulation and expression of LDLR. However, prior work on the effects of lovastatin on LDLR levels indicates that statins can increase LDLR levels, but not its activity in taking up its cholesterol laden ligand, low density lipoprotein (LDL).

In the future, EGF pre-conditioning or other growth factor stimulation may be influential in understanding schweinfurthin-mediated effects on LDLR levels. Treatments with tunicamycin on SF-295 cells also yielded results where the precursor form of LDLR, not seen in vehicle (DMSO) treated SF-295 cells, accumulates, with minimal changes to the mature levels of LDLR (Fig. 14). This confirms that LDLR has N-linked glycan residues, as detected with an antibody against LDLR. Minimal reductions in the levels of mature LDLR upon tunicamycin treatment may be related to the half life of LDLR which is ~12 hours (Fig. 14) [76,77,78,79].

Bao et. al. proposed that schweinfurthins impair the addition of terminal sialylated glycans to EGFR at the trans-Golgi based on two observations, one of which is related to a fluorescent schweinfurthin analog and its co-localization with Golgi markers [7]. Another observation is that one out of three glycan-binding proteins called lectins has a substrate specificity for asialylated proteins and was the only one to detect EGFR after schweinfurthin treatment [7]. An overlooked point in this study is that the other lectins that were specific to core mannose residues and sialyl groups may be limited in their substrate specificity and not cover the range of EGFR glycans that can be present on the receptor [7]. This also lends to other alternative possibilities that schweinfurthin-mediated effects on glycosylation maybe partly, but not completely, related to the process of sialylation at the trans-Golgi. The observation that treatment with TTI-3066 has no effect on the apparent molecular weight of LDLR like it does with EGFR

may suggest that O-linked glycosylation, as a different process of glycosylation, is not involved in schweinfurthin mechanism of action. However, the end stages of O-linked glycosylation for LDLR happens at the trans-golgi/trans-golgi network and sialylation is involved in capping the sugars of LDLR [76,77,78,79]. If schweinfurthins were to target a specific enzyme, for instance a sialyltransferase, involved in terminal sialylation of EGFR, then this would support the idea that schweinfurthins impair terminal sialylation at the trans-Golgi.

To date, no evidence supports enzymes in the glycosylation process as schweinfurthin targets. Furthermore, support that an oxysterol binding protein is responsible for the glycosylation defect via trans-golgi network arrest does not fit with our findings on LDLR. Our observations on LDLR in conjunction with the observation that immature forms of EGFR in schweinfurthin-treated SF-295 cells are present in both tunicamycin- and swainsonine-treated SF-295 cells suggests that Golgi-related dysfunctions can feed back towards ER-related processes. Indeed, research has shown that loss of CMP-sialic acid transporters or GDP-fucose transporters can not only impair glycosylation in the golgi, but also induce ER stress and potential re-glucosylation of proteins [81,82,83,84,85]. On the other hand, little is known about how schweinfurthins affect the levels of nucleosides (e.g. CMP, UMP) in cells, but there is some research linking cancers with K-Ras mutations with a strong dependence on glucose/glutamine levels and the hexosamine biosynthetic pathway [81,82,83,84,85]. This could explain differences in glycosylation and EGFR signaling defects in cancer cell lines with different sensitivities to schweinfurthins and would be very close in line with supporting our hypothesis.

References

1. Shoemaker, R. H. (2006). The NCI60 human tumour cell line anticancer drug screen. *Nature Reviews Cancer*, *6*(10), 813–823. https://doi.org/10.1038/nrc1951

2. Beutler, J. A., Shoemaker, R. H., Johnson, T., & Boyd, M. R. (1998). Cytotoxic geranyl stilbenes from Macaranga schweinfurthii. *Journal of Natural Products*, *61*(12), 1509–1512. https://doi.org/10.1021/np980208m

3. Neighbors, J. D., Beutler, J. A., & Wiemer, D. F. (2005). Synthesis of nonracemic 3-deoxyschweinfurthin B. *Journal of Organic Chemistry*, *70*(3), 925–931. https://doi.org/10.1021/jo048444r

4. Koubek, E. J., Weissenrieder, J. S., Neighbors, J. D., & Hohl, R. J. (2018). Schweinfurthins: Lipid Modulators with Promising Anticancer Activity. *Lipids*, *53*(8), 767–784. https://doi.org/10.1002/lipd.12088

5. Harmalkar, D. S., Mali, J. R., Sivaraman, A., Choi, Y., & Lee, K. (2018). Schweinfurthins A-Q: Isolation, synthesis, and biochemical properties. *RSC Advances*, *8*(38), 21191–21209. https://doi.org/10.1039/c8ra02872a

6. Burgett, A. W. G., Poulsen, T. B., Wangkanont, K., Anderson, D. R., Kikuchi, C., Shimada, K., … Shair, M. D. (2011). Natural products reveal cancer cell dependence on oxysterol-binding proteins. *Nature Chemical Biology*.https://doi.org/10.1038/nchembio.625

7. Bao, X., Zheng, W., Sugi, N. H., Agarwala, K. L., Xu, Q., Wang, Z., … Nomoto, K. (2015). Small molecule schweinfurthins selectively inhibit cancer cell proliferation and mTOR/AKT signaling by interfering with trans-Golgi-network trafficking. *Cancer Biology and Therapy*, *16*(4), 589–601. https://doi.org/10.1080/15384047.2015.1019184

8. Holstein, S. A., Kuder, C. H., Tong, H., & Hohl, R. J. (2011). Pleiotropic effects of a schweinfurthin on isoprenoid homeostasis. *Lipids*, *46*(10), 907–921. https://doi.org/

9. Rajapakse, V. N., Luna, A., Yamade, M., Loman, L., Varma, S., Sunshine, M., … Pommier, Y. (2018). CellMinerCDB for Integrative Cross-Database Genomics and Pharmacogenomics Analyses of Cancer Cell Lines. *IScience*, *10*, 247–264. https://doi.org/10.1016/j.isci.2018.11.029

10. Turbyville, T. J., Gürsel, D. B., Tuskan, R. G., Walrath, J. C., Lipschultz, C. A., Lockett, S. J., … Reilly, K. M. (2010). Schweinfurthin a selectively inhibits proliferation and rho signaling in glioma and neurofibromatosis type 1 tumor cells in a NF1-GRD-dependent manner. *Molecular Cancer Therapeutics*. https://doi.org/10.1158/1535-7163.MCT-09-0834

11. Kuder, C. H., Sheehy, R. M., Neighbors, J. D., Wiemer, D. F., & Hohl, R. J. (2012). Functional evaluation of a fluorescent schweinfurthin: Mechanism of cytotoxicity and intracellular quantification. *Molecular Pharmacology*, *82*(1), 9–16. https://doi.org/10.1124/mol.111.077107

12. Kuder, C. H., Weivoda, M. M., Zhang, Y., Zhu, J., Neighbors, J. D., Wiemer, D. F., & Hohl, R. J. (2015). 3-Deoxyschweinfurthin B Lowers Cholesterol Levels by Decreasing Synthesis and Increasing Export in Cultured Cancer Cell Lines. *Lipids*. https://doi.org/10.1007/s11745-0152-4083-z

13. Ownby, S. E., &Hohl, R. J. (2003). Isoprenoid Alcohols Restore Protein Isoprenylation in a Time-Dependent Manner Independent of Protein Synthesis. *Lipids*.

14. Orzechowski, A., Gajkowska, B., Pajak, B., & Wojewódzka, U. (2008). Lipid rafts in anticancer therapy: Theory and practice (Review). *Molecular Medicine Reports*, 167–172. https://doi.org/10.3892/mmr.1.2.167

15. Mantha, A. J., Hanson, J. E. L., Goss, G., Lagarde, A. E., Lorimer, I. A., & Dimitroulakos, J. (2005). Targeting the mevalonate pathway inhibits the function of the epidermal growth factor receptor. *Clinical Cancer Research*, *11*(6), 2398–2407. 17

16. Cemeus, C., Zhao, T. T., Barrett, G. M., Lorimer, I. A., & Dimitroulakos, J. (2008). Lovastatin enhances gefitinib activity in glioblastoma cells irrespective of EGFRvIII and PTEN status. *Journal of Neuro-Oncology*, *90*(1), 9–17.

17. Zhao, T. T., Le Francois, B. G., Goss, G., Ding, K., Bradbury, P. A., & Dimitroulakos, J. (2010). Lovastatin inhibits EGFR dimerization and AKT activation in squamous cell carcinoma cells: Potential regulation by targeting rho proteins. *Oncogene*, *29*(33), 4682–4692. https://doi.org/10.1038/onc.2010.219

18. Irwin, M. E., Mueller, K. L., Bohin, N., Ge, Y., & Boerner, J. L. (2011). Lipid raft localization of EGFR alters the response of cancer cells to the EGFR tyrosine kinase inhibitor gefitinib. *Journal of Cellular Physiology*. https://doi.org/10.102102/jcp.22570

19. Hamadmad, S. N., Henry, M. K., & Hohl, R. J. (2006). Erythropoietin receptor signal transduction requires protein geranylgeranylation. *Journal of Pharmacology and Experimental Therapeutics*, *316*(1), 403–409. https://doi.org/10.1124/jpet.105.092510

20. Palsuledesai, C. C., & Distefano, M. D. (2015). Protein prenylation: Enzymes, therapeutics, and biotechnology applications. *ACS Chemical Biology*, *10*(1), 51–62. https://doi.org/10.1021/cb500791f

21. Whyte, D. B., Kirschmeier, P., Hockenberry, T. N., Nunez-Oliva, I., James, L., Catino, J. J., … Pai, J. K. (1997). K- and N-Ras are geranylgeranylated in cells treated with farnesyl protein transferase inhibitors. *Journal of Biological Chemistry*, *272*(22), 14459–14464. https://doi.org/10.1074/jbc.272.22.14459

22. Holstein, S. A., Tong, H., &Hohl, R. J. (2010). Differential activities of thalidomide and isoprenoid biosynthetic pathway inhibitors in multiple myeloma cells. *Leukemia Research*. https://doi.org/10.1016/j.leukres.2009.06.035

23. Lodish, H., Berk, A., Kaiser, C. A., Krieger, M., Bretscher, A., Ploegh, H., … Scott, M. P. (2012). Vesicular Traffic, Secretion, and Endocytosis. *Molecular Cell Biology*. https://doi.org/10.1007/978-94-6091-478-2_14

24. Taylor, E. S., Pol-Fachin, L., Lins, R. D., & Lower, S. K. (2017). Conformational stability of the epidermal growth factor (EGF) receptor as influenced by glycosylation, dimerization and EGF hormone binding. *Proteins: Structure, Function and Bioinformatics*, *85*(4), 561–570. https://doi.org/10.1002/prot.25220

25. Huang, Y., & Chang, Y. (2011). Epidermal Growth Factor Receptor (EGFR) Phosphorylation, Signaling and Trafficking in Prostate Cancer. *Prostate Cancer - From Bench to Bedside*. https://doi.org/10.5772/27021

26. Munkley, J., & Elliott, D. J. (2016). Hallmarks of glycosylation in cancer. *Oncotarget*, *7*(23), 35478–35489. https://doi.org/10.18632/oncotarget.8155

27. Soderquist, A. M., & Carpenter, G. (1984). Glycosylation of the epidermal growth factor receptor in A-431 cells. The contribution of carbohydrate to receptor function. *Journal of Biological Chemistry*, *259*(20), 12586–12594.29

28. Whitson, K. B., Whitson, S. R., Red-Brewer, M. L., McCoy, A. J., Vitali, A. A., Walker, F., … Staros, J. V. (2005). Functional effects of glycosylation at Asn-579 of the epidermal growth factor receptor. *Biochemistry*, *44*(45), 14920–14931. https://doi.org/10.1021/bi050751j

29. Azimzadeh Irani, M., Kannan, S., & Verma, C. (2017). Role of N-glycosylation in EGFR ectodomain ligand binding. *Proteins: Structure, Function and Bioinformatics*, *85*(8), 1529–1549. https://doi.org/10.1002/prot.25314

30. Sebti, S. M. (2005). Protein farnesylation: Implications for normal physiology, malignant transformation, and cancer therapy. *Cancer Cell*, *7*(4), 297–300. https://doi.org/10.1016/j.ccr.2005.04.005

31. Holstein, S. A., Wohlford-Lenane, C. L., &Hohl, R. J. (2002). Consequences of mevalonate depletion. Differential transcriptional, translational, and post-translational up-regulation of Ras, Rap1a, RhoA, and RhoB. *Journal of Biological Chemistry*, *277*(12), 10678–10682. https://doi.org/10.1074/jbc.M111369200

32. Hamadmad, S. N., &Hohl, R. J. (2007). Lovastatin suppresses erythropoietin receptor surface expression through dual inhibition of glycosylation and geranylgeranylation. *Biochemical Pharmacology*, *74*(4), 590–600. https://doi.org/10.1016/j.bcp.2007.04.028

33. Holstein, S. A., Wohlford-Lenane, C. L., Wiemer, D. F., & Hohl, R. J. (2003). Isoprenoid pyrophosphate analogues regulate expression of ras-related proteins. *Biochemistry*, *42*(15), 4384–4391. https://doi.org/10.1021/bi027227m

34. Hamadmad, S. N., &Hohl, R. J. (2008). Erythropoietin stimulates cancer cell migration and activates RhoA protein through a mitogen-activated protein kinase/extracellular signal-regulated kinase-dependent mechanism. *Journal of Pharmacology and Experimental Therapeutics*, *324*(3), 1227–1233. https://doi.org/10.1124/jpet.107.129643

35. Dricu, A., Wang, M., Hjertman, M., Malec, M., Blegen, H., Wejde, J., … Larsson, O. (1997). Mevalonate-regulated mechanisms in cell growth control: Role of dolichyl phosphate in expression of the insulin-like growth factor-1 receptor (IGF-1R) in comparison to Ras prenylation and expression of c-myc. *Glycobiology*, *7*(5), 625–633. https://doi.org/10.1093/glycob/7.5.625

36. Vivanco, I., Ian Robins, H., Rohle, D., Campos, C., Grommes, C., Nghiemphu, P. L., … Mellinghoff, I. K. (2012). Differential sensitivity of glioma- versus lung cancer-specific EGFR mutations to EGFR kinase inhibitors. *Cancer Discovery*. https://doi.org/10.1158/2159-8290.CD-11-0284

37. Zhang, F., Wang, S., Yin, L., Yang, Y., Guan, Y., Wang, W., … Tao, N. (2015). Quantification of Epidermal Growth Factor Receptor Expression Level and Binding Kinetics on Cell Surfaces by Surface Plasmon Resonance Imaging. *Analytical Chemistry*. https://doi.org/10.1021/acs.analchem.5b02572

38. Singh, B., Carpenter, G., & Coffey, R. J. (2016). EGF receptor ligands: Recent advances [version 1; referees: 3 approved]. *F1000Research*, *5*(0), 1–11. https://doi.org/10.12688/F1000RESEARCH.9025.1

39. Tao, R. H., & Maruyama, I. N. (2008). All EGF(ErbB) receptors have preformed homo- and heterodimeric structures in living cells. *Journal of Cell Science*, *121*(19), 3207–3217. https://doi.org/10.1242/jcs.033399

40. Aksamitiene, E., Kiyatkin, A., & Kholodenko, B. N. (2012). Cross-talk between mitogenic Ras/MAPK and survival PI3K/Akt pathways: A fine balance. *Biochemical Society Transactions*, *40*(1), 139–146. https://doi.org/10.1042/BST20110609

41. Yamaoka, T., Frey, M. R., Dise, R. S., Bernard, J. K., & Polk, D. B. (2011). Specific epidermal growth factor receptor autophosphorylation sites promote mouse colon epithelial cell chemotaxis and restitution. *American Journal of Physiology - Gastrointestinal and Liver Physiology*, *301*(2), 368–376. https://doi.org/10.1152/ajpgi.00327.2010

42. Lopez-Sambrooks, C., Shrimal, S., Khodier, C., Flaherty, D. P., Rinis, N., Charest, J. C., … Contessa, J. N. (2016). Oligosaccharyltransferase inhibition induces senescence in RTK-driven tumor cells. *Nature Chemical Biology*. https://doi.org/10.1038/nchembio.2194

43. Tsuda, T., Ikeda, Y., & Taniguchi, N. (2000). The Asn-420-linked sugar chain in human epidermal growth factor receptor suppresses ligand-independent spontaneous oligomerization: Possible role of a specific sugar chain in controllable receptor activation. *Journal of Biological Chemistry*, *275*(29), 21988–21994. https://doi.org/10.

44. Liu, Y. C., Yen, H. Y., Chen, C. Y., Chen, C. H., Cheng, P. F., Juan, Y. H., … Wong, C. H. (2011). Sialylation and fucosylation of epidermal growth factor receptor suppress its dimerization and activation in lung cancer cells. *Proceedings of the National Academy of Sciences of the United States of America*, *108*(28), 11332–11337. https://doi.org/10.1073/pnas.1107385108

45. Yen, H. Y., Liu, Y. C., Chen, N. Y., Tsai, C. F., Wang, Y. T., Chen, Y. J., … Wong, C. H. (2015). Effect of on EGFR phosphorylation and resistance to tyrosine kinase inhibition. *Proceedings of the National Academy of Sciences of the United States of America*, *112*(22), 6955–6960.

46. Cummings, R. D., Soderquist, A. M., & Carpenter, G. (1985). The oligosaccharide moieties of the epidermal growth factor receptor in A-431 cells. Presence of complex-type N-linked chains that contain terminal N-acetylgalactosamine residues. *Journal of Biological Chemistry*.

47. Martin-Fernandez, M. L., Clarke, D. T., Roberts, S. K., Zanetti-Domingues, L. C., &Gervasio, F. L. (2019). Structure and Dynamics of the EGF Receptor as Revealed by Experiments and Simulations and Its Relevance to Non-Small Cell Lung Cancer. *Cells*. https://doi.org/10.3390/cells8040316

48. Slieker, L. J. S., Martensen, T. M., &, M. D. (1986). Synthesis of Epidermal Growth Factor Receptor in Human A431 Cells. *Journal of Biological Chemistry*, *261*(32), 15233–15241.

49. Slieker, L. J., & Lane, M. D. (1985). Post-translational Processing of the Epidermal Growth Factor. *Journal of Biological Chemistry*, *260*(2), 687–690.

50. Carlberg, M., Dricu, A., Blegen, H., Wang, M., Hjertman, M., Zickert, P., … Larsson, O. (1996). Mevalonic acid is limiting for N-linked glycosylation and translocation of the insulin-like growth factor-1 receptor to the cell surface. Evidence for a new link between 3-hydroxy-3-methylglutaryl-coenzyme A reductase and cell growth. *Journal of Biological Chemistry*, *271*(29), 17453–17462. https://doi.org/10.1074/jbc.271.29.17453

51. Carlin, C. R., & Knowles, B. B. (1986). Biosynthesis and glycosylation of the epidermal growth factor receptor in human tumor-derived cell lines A431 and Hep 3B. *Molecular and Cellular Biology*, *6*(1), 257–264. https://doi.org/10.1128/mcb.6.1.257

52. Gamou, S., Hirai, M., Shimizu, N., Rikimaru, K., &Enomoto, S. (1988). Biosynthesis of the Epidermal Growth Factor Receptor in Human Squamous Cell Carcinoma Lines: Secretion of the Truncated Receptor is not Common to Epidermal Growth Factor Receptor-Hyperproducing Cells.*Cell Structure and Function*, *13*(1), 25–38.

53. Liu, W., Wu, X., Zhang, W., Montenegro, R. C., Fackenthal, D. L., Spitz, J. A., … Ratain, M. J. (2007). Relationship of EGFR mutations, expression, amplification, and polymorphisms to epidermal growth factor receptor inhibitors in the NCI60 cell lines. *Clinical Cancer Research*, *13*(22), 6788–6795. https://doi.org/10.1158/1078-0432.CCR-07-0547

54. Ikediobi, O. N., Davies, H., Bignell, G., Edkins, S., Stevens, C., O'Meara, S., … Wooster, R. (2006). Mutation analysis of 24 known cancer genes in the NCI-60 cell line set. *Molecular Cancer Therapeutics*, *5*(11), 2606–2612. https://doi.org/10.1158/1535-7163.MCT-06-0433

55. Prior, I, Lewis, P, Mattos, Carlos. (1999). A comprehensive survey of Ras mutations in cancer.*72*(10), 1–24. https://doi.org/10.1158/0008-5472.CAN-11-2612.A

56. Liu, S., Sheng, R., Jung, J. H., Wang, L., Stec, E., Connor, M. J. O., … Cho, W. (2018). Orthogonal lipid sensors identify transbilayer asymmetry of plasma membrane cholesterol.*Nature Chemical Biology*,*13*(3), 268–274. https://doi.org/10.1038/nchembio.2268

57. Roy, S., Luetterforst, R., Harding, A., Apolloni, A., Etheridge, M., Stang, E., … Parton, R. G. (1999). Dominant-negative caveolin inhibits H-Ras function by disrupting cholesterol-rich plasma membrane domains. *Nature Cell Biology*.

58. Kranenburg, O., Verlaan, I., &Moolenaar, W. H. (2001). Regulating c-Ras function: Cholesterol depletion affects caveolin association, GTP loading, and signaling. *Current Biology*, *11*(23), 1880–1884. https://doi.org/10.1016/S0960-9822(01)00582-6

59. Cho, K. J., Park, J. H., Piggott, A. M., Salim, A. A., Gorfe, A. A., Parton, R. G., … Hancock, J. F. (2012). Staurosporines disrupt phosphatidylserine trafficking and mislocalizeras proteins. *Journal of Biological Chemistry*, *287*(52), 43573–43584. https://doi.org/10.1074/jbc.M112.424457

60. Kwang-jin Cho. (2016). Inhibition of Acid Sphingomyelinase Depletes Cellular Phosphatidylserine and Mislocalizes K-Ras from the Plasma Membrane. *Molecular and Cellular Biology*, *36*(2), 363–374. https://doi.org/10.1128/MCB.00719-15.

61. Michaelson, D., Silletti, J., Murphy, G., D'Eustachio, P., Rush, M., & Philips, M. R. (2001). Differential localization of Rho GTPases in live cells: Regulation by hypervariable regions and RhoGDI binding. *Journal of Cell Biology*, *152*(1), 111–126. https://doi.org/10.1083/jcb.152.1.111

62. Heo, W. Do, Inoue, T., Park, W. S., Kim, M. L., Park, B. O., Wandless, T. J., & Meyer, T. (2007). PI(3,4,5)P_3 and PI(4,5)P_2 Lipids Target Proteins with Polybasic Clusters to the Plasma Membrane. *Science*, *1458*(5804), 1458–1461.https://doi.org/10.1126/science.1134389

63. Chen, X., &Resh, M. D. (2002). Cholesterol depletion from the plasma membrane triggers ligand-independent activation of the epidermal growth factor receptor. *Journal of Biological Chemistry*. https://doi.org/10.1074/jbc.M208327200

64. Roschke, A. V.,Tonon, G., Gehlhaus, K. S., McTyre, N., Bussey, K. J., Lababidi, S., … Kirsch, I. R. (2003). Karyotypic Complexity of the NCI-60 Drug-Screening Panel. *Cancer Research*, *63*(24), 8634–8647.

65. Zheng, C (2015). *Molecular Mechanisms of the Anti-Cancer Action of Schweinfurthins.* (THESIS)

66. Sheehy, R. M. (2015). *Mechanisms of the anti-proliferative actions of the schweinfurthins in cancer cells*. (THESIS)

67. Contessa, J. N., Bhojani, M. S., Freeze, H. H., Rehemtulla, A., & Lawrence, T. S. (2008). Inhibition of N-linked glycosylation disrupts receptor tyrosine kinase signaling in tumor cells. *Cancer Research*. https://doi.org/10.1158/0008-5472.CAN-07-6389

68. Kim, Y. H., Kwak, M. S., Park, J. B., Lee, S. A., Choi, J. E., Cho, H. S., & Shin, J. S. (2016). N-linked glycosylation plays a crucial role in the secretion of HMGB1. *Journal of Cell Science*. https://doi.org/10.1242/jcs.176412

69. Richardson, P. G., Eng, C., Kolesar, J., Hideshima, T., & Anderson, K. C. (2012). Perifosine, an oral, anti-cancer agent and inhibitor of the Akt pathway: Mechanistic actions, pharmacodynamics, pharmacokinetics, and clinical activity. *Expert Opinion on Drug Metabolism and Toxicology*. https://doi.org/10.1517/17425255.2012.681376

70. Rush, J. S., Quinalty, L. M., Engelman, L., Sherry, D. M., &Ceresa, B. P. (2012). Endosomal accumulation of the activated epidermal growth factor receptor (EGFR) induces apoptosis. *Journal of Biological Chemistry*. https://doi.org/10.1074/jbc.M111.294470

71. Visser Smit, G. D., Place, T. L., Cole, S. L., Clausen, K. A., Vemugantl, S., Zhang, G., … Lill, N. L. (2009). CBL controls EGFR fate by regulating early endosome fusion. *Science Signaling*. https://doi.org/10.1126/scisignal.2000217

72. Pinilla-Macua, I., Grassart, A., Duvvuri, U., Watkins, S. C., & Sorkin, A. (2017). EGF receptor signaling, phosphorylation, ubiquitylation and endocytosis in tumors in vivo. *ELife*. https://doi.org/10.7554/eLife.31993

73. Alwan, H. A. J., Van Zoelen, E. J. J., & Van Leeuwen, J. E. M. (2003). Ligand-induced lysosomal epidermal growth factor receptor (EGFR) degradation is preceded by proteasome-dependent EGFR de-ubiquitination. *Journal of Biological Chemistry*. https://doi.org/10.1074/jbc.M301326200

74. Wang, Y., Pennock, S., Chen, X., & Wang, Z. (2002). Endosomal Signaling of Epidermal Growth Factor Receptor Stimulates Signal Transduction Pathways Leading to Cell Survival. *Molecular and Cellular Biology*. https://doi.org/10.1128/mcb.22.20.7279-7290.2002

75. Toulany, M., Dittmann, K… Rodemann, P. (2005). Radioresistance of K-Ras Mutated Human Tumor Cells Is Mediated Through EGFR-dependent Activation of PI3K-AKT. *Radiotherapy & Oncology.*

76. Cummings, R. D., Kornfeld, S., Schneider, W. J., Hobgood, K. K., Tolleshaug, H., Brown, M. S., & Goldstein, J. L. (1983). Biosynthesis of N- and O-linked oligosaccharides of the low density lipoprotein receptor. *Journal of Biological Chemistry*.

77. Casciola, L. A. F., Van Der Westhuyzen, D. R., Gevers, W., & Coetzee, G. A. (1988). Low density lipoprotein receptor degradation is influenced by a mediator protein(s) with a rapid turnover rate, but is unaffected by receptor up- or down-regulation. *Journal of Lipid Research*.

78. Wang, S., Mao, Y., Narimatsu, Y., Ye, Z., Tian, W., Goth, C. K., … Clausen, H. (2018). Site-specific O-glycosylation of members of the low-density lipoprotein receptor superfamily enhances ligand interactions. *Journal of Biological Chemistry*. https://doi.org/10.1074/jbc.M117.817981

79. Chan, P. C., Lafrenière, R., & Parsons, H. G. (1997). Lovastatin increases surface low density lipoprotein receptor expression by retarding the receptor internalization rate in proliferating lymphocytes. *Biochemical and Biophysical Research Communications*. https://doi.org/10.1006/bbrc.1997.6736

80. Guo, D., Reinitz, F., Youssef, M., Hong, C.…Mischel, P.S. (2011). An LXR agonist promotes glioblastoma cell death through inhibition of an EGFR/AKT/SREBP-1/LDLR-dependent pathway.*Cancer Discovery.*

81. Shen, Z., Huang, S., Fang, M., & Wang, X. (2011). ENTPD5, an endoplasmic reticulum UDPase, alleviates ER stress induced by protein overloading in AKT-activated cancer cells. *Cold Spring Harbor Symposia on Quantitative Biology*. https://doi.org/10.1101/sqb.2011.76.010876

82. Zhao, W., Chen, T. L. L., Vertel, B. M., & Colley, K. J. (2006). The CMP-sialic acid transporter is localized in the medial-trans Golgi and possesses two specific endoplasmic reticulum export motifs in its carboxyl-terminal cytoplasmic tail. *Journal of Biological Chemistry*. https://doi.org/10.1074/jbc.M605564200

83. Xu, Y. X., Liu, L., Caffaro, C. E., & Hirschberg, C. B. (2010). Inhibition of Golgi apparatus glycosylation causes endoplasmic reticulum stress and decreased protein synthesis. *Journal of Biological Chemistry*. https://doi.org/10.1074/jbc.M110.134544

84. Palorini, R., Cammarata, F., Balestrieri, C., Monestiroli, A., Vasso, M., Gelfi, C., … Chiaradonna, F. (2013). Glucose starvation induces cell death in -transformed cells by interfering with the hexosamine biosynthesis pathway and activating the unfolded protein response. *Cell Death and Disease*. https://doi.org/10.1038/cddis.2013.257

85. Chen, Y., Huang, R., Ding, J., Ji, D., Song, B., Yuan, L., … Chen, G. (2015). Multiple myeloma acquires resistance to EGFR inhibitor via induction of pentose phosphate pathway. *Scientific Reports*. https://doi.org/10.1038/srep09925